TelA Promoted Telomere Resolution Features an Underwound Pre-cleavage Intermediate

A Thesis Submitted to the College of Graduate and Postdoctoral Studies
In Partial Fulfillment of the Requirements
For the Degree of Master of Science
In the Department of Biochemistry, Microbiology and Immunology
University of Saskatchewan
Saskatoon

By

Mahrokh Balouchi

PERMISSION TO USE

In presenting this thesis in partial fulfillment of the requirements for a Postgraduate degree from the University of Saskatchewan, I agree that the Libraries of this University may make it freely available for inspection. I further agree that permission for copying of this thesis in any manner, in whole or in part, for scholarly purposes may be granted by the professor or professors who supervised my thesis/dissertation work or, in their absence, by the Head of the Department or the Dean of the College in which my thesis work was done. It is understood that any copying or publication or use of this thesis/dissertation or parts thereof for financial gain shall not be allowed without my written permission. It is also understood that due recognition shall be given to me and to the University of Saskatchewan in any scholarly use which may be made of any material in my thesis/dissertation.

Requests for permission to copy or to make other uses of materials in this thesis in whole or part should be addressed to:

Head of the Department of Biochemistry, Microbiology and Immunology
GA20.12, Health Sciences
107 Wiggins Road
University of Saskatchewan
Saskatoon, Saskatchewan S7N 5E5
Canada

OR

Dean College of Graduate and Postdoctoral Studies
University of Saskatchewan
116.4a, Thorvaldson Building, 110 Science Place
Saskatoon, Saskatchewan S7N 5C9
Canada

ABSTRACT

Agrobacterium tumefaciens and *Borrelia species* are two examples of prokaryotic organisms that have linear replicons, in contrast to most prokaryotes that have circular genomes. These organisms can replicate the lagging strand end of linear (deoxyribonucleic acid) DNAs without the loss of the DNA's information due to the covalently closed DNA hairpin telomeres at the termini of the DNA. Replication of DNAs with hairpin telomeres produces a circular inverted repeat dimer with replicated telomere junctions. This intermediate cannot be segregated into two daughter cells without a two-step DNA breakage and rejoining process known as telomere resolution. Specialized enzymes known as telomere resolvases create hairpin telomeres from a dimeric replication intermediate through telomere resolution. Telomere resolvases share a similar mechanism to that of topoisomerase-IB and tyrosine recombinase enzymes. The proposed models for telomere resolution include a pre-cleavage intermediate where the base pairing between the scissile phosphates is broken helping to propel the reaction forwards. A class of variants was examined in previous studies on the borrelial telomere resolvase, ResT. These variants were inactive on parental substrates but were rescued by substrate alterations that mimicked DNA unwinding between the cleavage sites. In ResT, the catalytic domain and the hairpin-binding module cooperate to stabilize an underwound pre-cleavage intermediate. The idea that the telomere resolvase from *Agrobacterium tumefaciens,* TelA, and ResT follow the same reaction pathway was generated from the crystal-structure data of TelA, and the homology between ResT and TelA. We generated TelA variants homologous to those in ResT that stabilize the pre-cleavage intermediate. We also generated TelA variants of sidechains that were shown to interact with the hairpin turnarounds in TelA structures. Reaction analysis showed that the central two basepairs of the replicated telomere (*rTel*) junction are likely to be underwound and stabilized by TelA in a pre-cleavage intermediate. We also have evidence that the next two basepairs are also broken and likely have a base flipped out of the helix in the pre and post-cleavage intermediate. It is predicted that an underwound pre-cleavage intermediate drives the reaction forward and ensures reaction completion.

ACKNOWLEDGMENTS

First and foremost, I would like to especially thank my supervisor, Dr. Kerri Kobryn for his constant support throughout my project. I cannot put into words how grateful I am for the opportunity he gave me to work with him and become a scientist. Secondly, I would also thank Ms. Linda Huang for supporting me through the rough time of the Covid-19 pandemic and her efforts to make Saskatoon my second home, in addition to her guidance and technical support during daily laboratory work. Lastly, I am the luckiest to have my mom's and my auntie's unconditional support. I am also so thankful to have such incredible friends, namely Dilraj, Negar, and Sepideh who are my mental support and always encourage me to peruse more and more in life.

PERMISSION TO REPRODUCE

The following figure has been reproduced with permission from the journal in which it was published.

Figure 1.2. Casjens, S. (1999). Evolution of the linear DNA replicons of the Borrelia spirochetes. Curr. Opin. Microbiol. *2*, 529–534.

Figure 1.3. Ravin, N. V. (2011). N15: The linear phage-plasmid. Plasmid *65*, 102–109.

Figure 1.4. Chaconas, G. (2005). Hairpin telomeres and genome plasticity in Borrelia: All mixed up in the end. Mol. Microbiol. *58*, 625–635.

Figure 1.5. Kobryn, K., and Chaconas, G. (2002). ResT, a telomere resolvase encoded by the Lyme disease spirochete. Mol. Cell *9*, 195–201.

Figure 1.6. Kobryn, K., and Chaconas, G. (2014). Hairpin Telomere Resolvases. Microbiol. Spectr. *2*.

Figure 1.7. Chaconas, G. (2005). Hairpin telomeres and genome plasticity in Borrelia: All mixed up in the end. Mol. Microbiol. *58*, 625–635.

Figure 1.8. Kobryn, K., and Chaconas, G. (2005). Fusion of hairpin telomeres by the B. burgdorferi telomere resolvase ResT: Implications for shaping a genome in flux. Mol. Cell *17*, 783–791.

Figure 1.10. Kobryn, K., and Chaconas, G. (2014). Hairpin Telomere Resolvases. Microbiol. Spectr. *2*.

Figures 1.9, 1.11 and 1.12 do not require to obtain permission to reuse from the publisher.

TABLE OF CONTENTS **PAGE**

LIST OF TABLES **PAGE**

LIST OF FIGURES **PAGE**

LIST OF ABBREVIATIONS

BSA	Bovine serum albumin
CD	Circular dichroism
CPs	Cleavage products
DNA	Deoxyribonucleic acid
ds	Double strand
DTT	1,4-dithiothreitol
EDTA	Ethylenediaminetetraacetic acid
EM	Erythema migrans
EMSA	Electrophoretic mobility shift assay
HEPES	4-(2-hydroxyethyl)-1-piperazineethanesulfonic acid
HJ	Holliday junctions
Hp	Hairpin
HS	Heparin-Sepharose column
IDT	Integrated DNA Technologies
IPTG	Isopropyl β-D-1 thiogalatopyranoside
mc	Main chain
MM	Mismatch
nt	nucleotide
OH	Hydroxyl
*ori*C	Origin of replication
PAGE	Polyacrylamide gel electrophoresis
pdb	Protein data bank
PNK	T4 polynucleotide kinase
rTel	Replicated telomere
SDS	Sodium dodecyl sulfate
SH	Sulfhydryl
spp.	Species
ss	Single strand
SSAPs	Single strand annealing proteins
ssDNA	Single-stranded DNA
SSB	Single-stranded DNA binding protein
TAE	Tris Acetate EDTA
TAR	Transactivational response element
Tap	Telomere-associated primase
TBE	Tris Borate EDTA
Ti	Tumor inducing
TopI	Topoisomerase I

TP	Terminal protein
t-loop	Telomeric loop
WT	Wild type

1. Introduction

1.1. Linear replicons in bacteria

1.1.1. The end-replication and end-protection problems

Contrary to eukaryotic systems, only a small number of prokaryotic organisms, such as some species of *Streptomyces* species (spp.), *Borrelia* species, *Agrobacterium* biovar I strains, and various phages, have been characterized to possess a linear configuration of deoxyribonucleic acid (DNA). These prokaryotes have either linear plasmids, linear chromosomes, or mix of the two. Although these organisms achieved some advantages by possessing linear DNAs (discussed in section 1.5) maintaining these genomes requires overcoming two main problems called the end-replication and end-protection problems. The end-replication problem for linear DNAs was first shown in studies of linear phage replication and stated that removing the final primer produces a 3' gap at the end of the replicon with no 3' hydroxyl (-OH) group available for extension by DNA polymerases; this prevents the termini from being fully replicated (Figure 1.1; (Olovnikov, 1973)). This leads to lost genomic information after several rounds of DNA replication (Olovnikov, 1973). Another problem that linear replicons face is the end-protection problem. The end-protection problem refers to the susceptibility of double-stranded ends to degradation by nucleases or to generate improper fusions of different replicons. It is essential to overcome these problems to maintain linear DNAs. Organisms came up with different solutions for the mentioned problems; these solutions are discussed in the following sections.

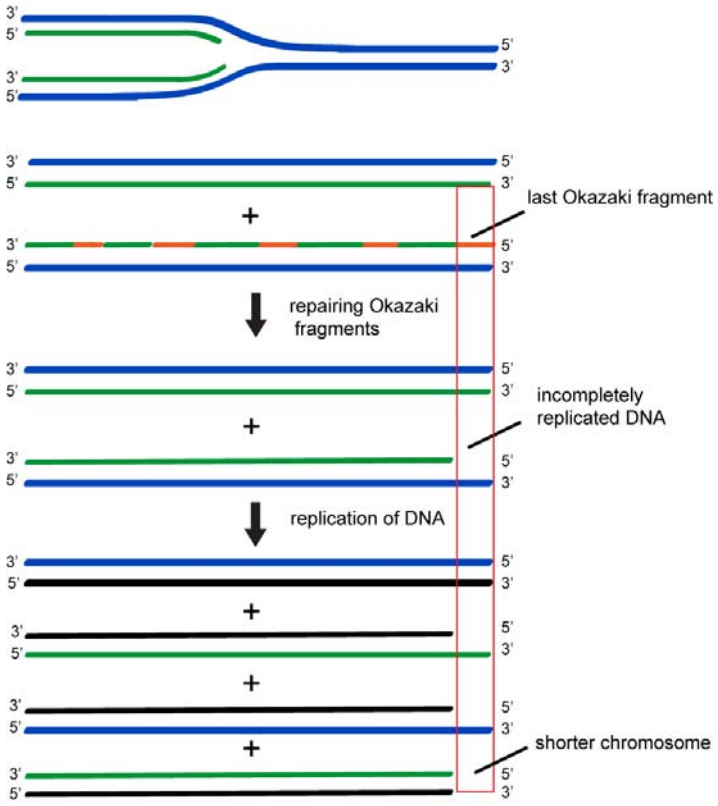

Figure 1.1. Schematic representation of the end replication problem. Short RNA primers are created by RNA primase for lagging-strand DNA replication. DNA polymerase extends the primers to create Okazaki fragments. After removal of the RNA primers, a 3' gap will remain that cannot be replicated; therefore, linear chromosomal ends lose sequence as a result of ongoing cell division. Figure is adapted from (Wynford-Thomas and Kipling, 1997).

1.1.2. Different solutions to the end-replication problem

In eukaryotes, a ribonucleoprotein complex called telomerase contains a telomere reverse transcriptase and an RNA template. Telomerase produces tandem repeats of telomeric DNA to counteract DNA degradation (Lingner et al., 1995). A protein complex known as shelterin, consisting of six different proteins, binds to telomeric DNA to protect chromosomes from end-to-end recombination and degradation. In part, this telomere capping role is played by shelterin forming a telomeric loop (t-loop) (De Lange, 2005). Shelterin also controls how processing enzymes like telomerase and helicases gain access to telomeric DNA (Figure 1.2a; (Erdel et al., 2017)).

Lacking such enzymes and proteins mentioned above, prokaryotes overcome the end-replication and end-protection issues via a variety of different methods. 5' terminal protein-capped telomeres are utilized by *Bacillus subtilis* phage φ29 and *Streptomyces* spp. A terminal

protein (TP) covalently bonded to the 5' end of the DNA is used as a primer for the linear DNA replication's initiation mechanisms, in addition to protecting the ends of linear DNAs (Figure 1.2 b; (Casjens, 1999)). Each terminal end of the linear replicon of the φ29 phage has an origin of replication. The origins are recognized by the TP-DNA polymerase complex through the parental TPs. A TP is placed at either end of the terminus by interaction with the parental TP and a specific sequence at the ends of the DNA. The DNA polymerase adds the first nucleotide to the -OH group of the Ser^{232} residue that acts as the primer within the TP (Blanco et al., 1992; Hermoso et al., 1985). A short product of 10 nucleotides is produced by the polymerase before switching to DNA-primed elongation when the complex moves back one nucleotide to retrieve the template at the 3' terminal end of the DNA (Mendez et al., 1992). The use of this end-to-end replication technique avoids discontinuous synthesis on the lagging strands and the end replication issue.

Streptomyces spp. utilize TPs for their linear plasmids and chromosomes in a different mechanism than the φ29 phage. Replication of both linear plasmids and liner chromosomes is similar to other bacterial replication systems with circular replicons which initiates from an internal origin. Replication proceeds bidirectionally and leaves single-strand overhangs, of about 250–300 nucleotides, at the telomeres. The single-strand gaps at the telomeres are then filled with TP primed DNA synthesis. This process is known as end-patching (Chang and Cohen, 1994; Yang et al., 2017). End-patching involves the terminal protein, Tpg, and a telomere associated primase (Tap). Tpg includes the HIV reverse transcriptase thumb domain, which binds DNA (Tsai et al., 2008). The helix-turn-helix DNA-binding domain in Tap interacts with both the Tpg and the telomere regions (Bao and Cohen, 2003). The terminal protein acts as a protein primer for extension of a short DNA primer. Tap then creates a longer (DNA) primer and then the replisome fills in the rest of the gap (Yang et al., 2015, 2017).

1.2. Replication of linear replicons with hairpin telomeres

Agrobacterium (Goodner et al., 2001), *Borrelia* (Barbour and Garon, 1987; Casjens et al., 1997; Fraser et al., 1997), *Klebsiella oxytoca* phage φKO2 (Stoppel et al., 1995), *Escherichia coli* phage N15 (Rybchin and Svarchevsky, 1999), and some other phages possess covalently closed hairpin loops, also known as hairpin telomeres, at the termini of linear replicons. The hairpin telomere is probably the simplest solution to the end-replication and end-

protection problems. (Figure 1.2c; (Casjens, 1999)). DNA replication in organisms with hairpin (hp) telomeres results in daughter replicons that are covalently linked at their telomere ends through replicated telomere (*rTel*) junctions. These replicons need further processing by specific enzymes to segregate the products into daughter cells. This processing involves a strand breakage and rejoining reaction known as telomere resolution (Figure 1.2c). Therefore, these structures cause a different problem when trying to solve the end replication problem. The *E. coli* phage N15 and *B. burgdorferi* have been the subject of the most in-depth research into the mechanics of linear DNA replication in organisms with hairpin telomeres (Barbour and Garon, 1987; Casjens et al., 1997; Ravin, 2015; Ravin et al., 2003).

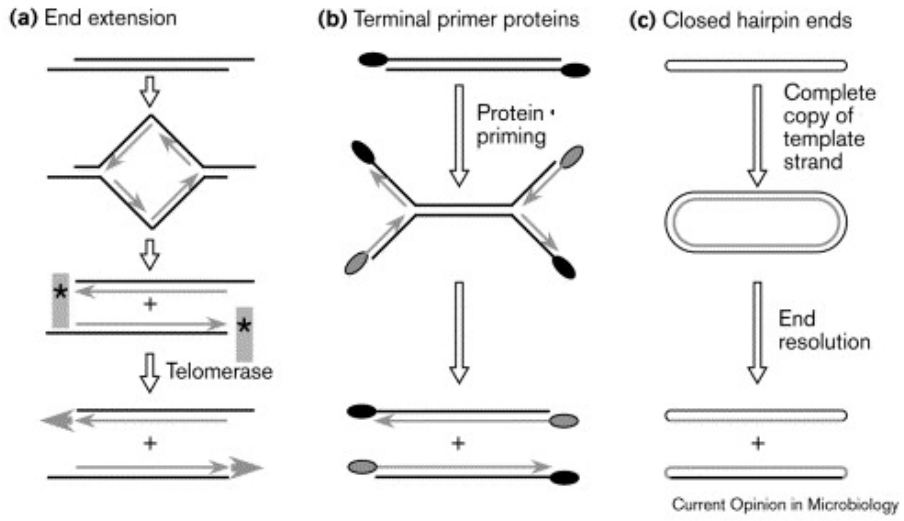

Figure 1.2. Different approaches to solving the end replication problem. **A)** In eukaryotes the 3' overhangs resulting from replication linear replicons are needed to be extended by telomerase. DNA information in the areas shown by asterisks were not replicated by the DNA polymerase. **B)** DNA polymerases utilize the terminal proteins, shown as black and grey ovals, as primers at the 3' ends of the linear replicon. **C)** Replication of linear DNA with closed hairpin ends results in a dimer of replicon which is resolved into two daughter linear replicons with closed hairpin ends. Figure is reused with permission of (Casjens, 1999).

1.2.1. The N15 phage paradigm

N15 phage of *E. coli* is a member of the lambdoid phage family, which was identified through the cross-hybridization of their DNAs. It was shown that N15 shares many characteristics with λ phage. However, it was demonstrated that phage N15's prophage replicates extrachromosomally (Ravin et al., 2000; Rybchin and Svarchevsky, 1999). The identification of closed linear DNA with covalent hairpin loops in the N15 phage was the next

critical stage of studies on this phage. A few years later, the same structure was discovered in the plasmids of the spirochete genus *Borrelia* (Ravin et al., 2000; Rybchin and Svarchevsky, 1999). In the mature N15 phage, the double-stranded DNA chromosome has 12 base pairs single-stranded cohesive endpoints called *cos*L and *cos*R. When it infects *E. coli*, these cohesive termini cause the chromosome to circularize by its cohesive termini (Ravin et al., 2000; Rybchin and Svarchevsky, 1999). The product of the phage gene *telN,* TelN, is a specialized enzyme called a telomere resolvase or protelomerase which cuts the *tel*RL sequence and makes the hairpin telomeres, referred to as *tel*L and *tel*R, through the cleavage and refolding the strands into a hp conformation followed by rejoining the strands (Deneke et al., 2000). The resulting linear plasmid is used as a template for lysogenic replication.

Visualization of multiple replication intermediates by electron microscopy supported a model of asymmetric linear replication and telomere resolution (Ravin et al., 2003). The *repA* gene of the linear plasmid contains an origin from which bidirectional replication of the plasmid begins. The left telomere's replication is finished first, then TelN promotes telomere resolution of the *tel*L/L' replicated junction, resulting in a Y-shaped molecule. The longer right arm of the phage is then fully replicated without telomere resolution would, and TelN resolves the *tel*R/R' junction and produces two linear daughter plasmids with hairpin telomeres (Figure 1.3 pathway A1; (Ravin et al., 2003)). As an alternative, full replication without telomere resolution would result in a full head-to-head circular dimer form before the resolution of the ends of the replicon (Figure 1.3 pathway A2; (Ravin et al., 2003)). The minimum complement of genes to replicate the N15 prophage was identified by mini plasmids containing various N15 DNA fragments and an antibiotic resistance gene (Ravin et al., 2003). It was shown that *repA* was both required and sufficient to replicate the circular plasmid. RepA is a multi-domain protein with primase, helicase with origin binding activities (Ziegelin et al., 1993). RepA with *telN* gene and *tel*RL site was the minimum requirement to produce linear plasmid in N15 phage system (Mardanov and Ravin, 2006).

The mechanism of N15 lytic replication was explained using the model mentioned above. TelN resolves the head-to-head circular dimer replication intermediate into two circular monomers, instead of two linear plasmids (Figure 1.3 pathway B). The processing of these circular monomers then resembles lambda phage's late lytic replication since the N15's

morphogenetic genes resemble genes of phage λ (Ravin, 2015). The transition to circular plasmid formation may be caused by TelN depletion or by a phage-encoded protein that alters either the telomere resolvase or its target site (Mardanov and Ravin, 2009). Later findings from other phage systems with linear plasmid prophages, such as *K. oxytoca* phage φKO2 (Casjens et al., 2004) and *Yersinia enterocolitica* phage PY54 (Hertwig et al., 2003), suggest the replication of N15 prophage can serve as a generic paradigm.

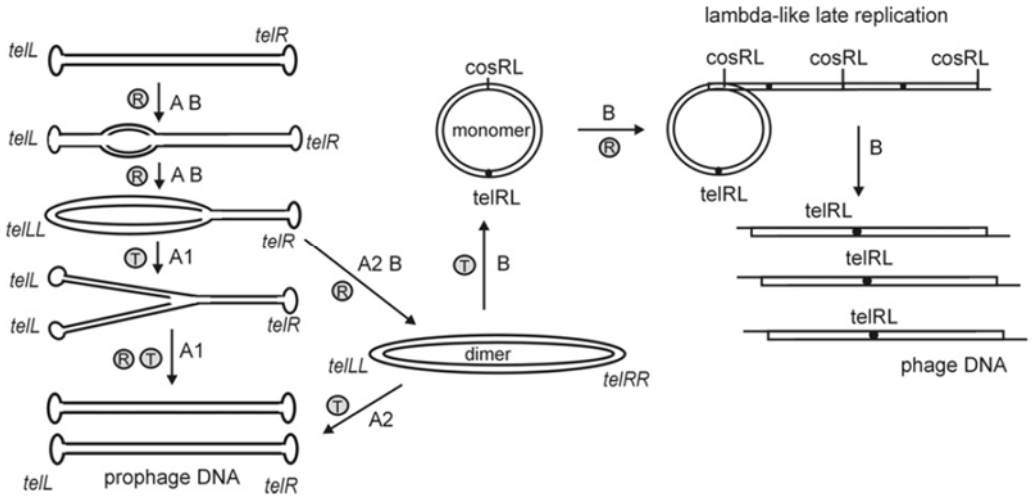

Figure 1.3. Schematic representation of lysogenic *vs.* lytic modes of replication of phage N15. A) In N15 plasmid prophage replication, Y-like structures are formed by protelomerase cutting before replication is finished (A1). In the alternative pathway, circular head-to-head dimer are formed after replication but before protelomerase cleavage (A2). **B)** During of lytic replication in the lysogen, the circular head-to-head dimer is divided into two circular monomers. The N15 genes TelN (T) and RepA (R) are known in the phases they have a potential role in each phase. The figure is captured from (Ravin, 2011).

1.2.2. The *Borrelia* paradigm

Linear bacterial chromosomes with hairpin telomeres were found in a small number of bacterial systems. Studies on *B. burgdorferi* revealed a distinctive, highly segmented genomic structure, including a linear chromosome and >20 circular and linear plasmids (Barbour and Garon, 1987; Fraser et al., 1997). This was discovered at the same time as the discovery that N15 prophage DNA was maintained as a linear plasmid with covalently closed hairpin ends. In contrast to N15 phage, the linear chromosome's origin of replication (*oriC*) was not found close to the hairpin telomeres (Picardeau et al., 1999). Replication initiation from *ori*C was discovered in a 240 bp sequence between *dna*A and *dna*N for *B. burgdorferi* placing the origin almost in the center of the chromosome (Fraser et al., 1997; Picardeau et al., 1999). The

discovery of a central origin was supported by demonstration of the nucleoid-associated protein, Hbb, binding site close to *ori*C, (a family of DNA-bending proteins, some members of which facilitate origin DNA melting by DnaA), transcriptional directionality, and a change in the polarity of the GC skew close to the chromosome's center (Casjens et al., 2000; Fraser et al., 1997; Kobryn et al., 2000; Mouw and Rice, 2007; Tilly et al., 1996). The chromosome of *B. burgdorferi* can be split into two halves from the middle of the genome to termini, based on GC skew (Picardeau et al., 1999). Compared to *E. coli, B. burgdorferi*'s linear chromosome replication uses a smaller set of replication proteins, a simpler, single-subunit replicative polymerase, and no clearly identifiable helicase loader (Fraser et al., 1997). The bidirectional and symmetric replication initiates from *ori*C and proceeds through the hairpin telomeres (Picardeau et al., 1999). The result of the replication is a replication intermediate containing a DNA dimer fused at replicated telomere junctions (*rTel*) head-to-head and tail-to-tail. The linear replicons and the whole replicated intermediate possess inverted repeat symmetry (Figure 1.4; (Kobryn and Chaconas, 2002)). The specialized telomere resolvase, ResT, resolves the replicated telomere junction into two linear daughter replicons with hairpin telomeres using a two-step cleavage and rejoining reaction known as telomere resolution, as was previously mentioned (Kobryn and Chaconas, 2002).

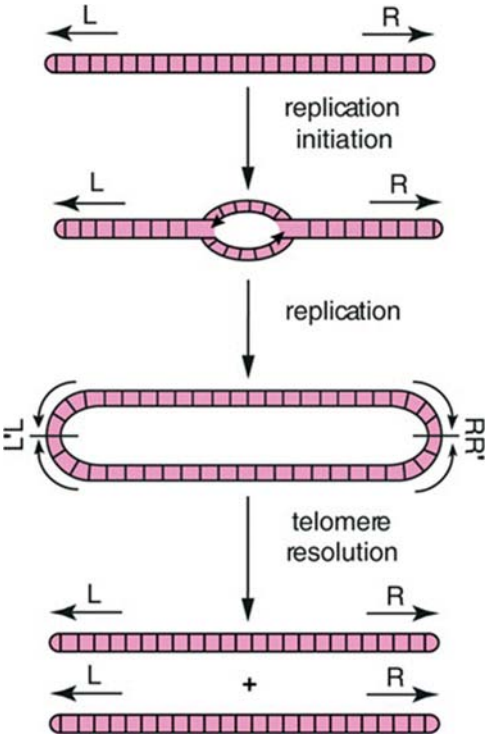

Figure 1.4 Schematic representation of replication of linear DNA with hairpin telomeres. Bidirectional replication begins from an internal origin and continues through the hairpin telomeres. The result is a dimer of replicons that are covalently linked at the replicated telomere junctions, *rTel*, (labeled as L'/L and R/R'). *rTel*s contain inverted repeat symmetry. Then, by a procedure known as telomere resolution, this dimer is resolved into two linear replicons with hairpin ends. The figure is captured from (Chaconas, 2005)**.**

1.3. Telomere Resolvases

1.3.1. A brief overview

Hairpin telomere resolvases or protelomerases are essential in organisms that use hairpin telomeres to overcome the end replication and end protection issues. They are involved in a DNA breakage and rejoining reaction called telomere resolution that results in formation of closed hairpin telomere ends (Chaconas, 2005). Telomere resolvases have been identified and characterized in bacterial species and phages such as *A. tumefaciens* (Huang et al., 2012), the Lyme disease spirochete *B. burgdorferi* (Kobryn and Chaconas, 2002), the relapsing fever borreliae *B. hermsii, B. parkeri, B. recurrentis, B. turicatae*, and the avian spirochete *B. anserine* (Moriarty and Chaconas, 2009), *E. coli* phage N15 (Deneke et al., 2000), *K. oxytoca* phage φKO2 (Casjens et al., 2004), *Y. enterocolitica* phage PY54 (Hertwig et al., 2003), The agrobacterial enzyme, TelA, and the klebsiellal enzyme, TelK, have both been crystallized (Aihara et al., 2007; Shi et al., 2013). ResT from *B. burgdorferi* has undergone the most biochemical research of all the resolvases but has not yet been characterized structurally (Bankhead and Chaconas, 2004; Bankhead et al., 2006; Briffotaux and Kobryn, 2010; Chaconas et al., 2001; Huang and Kobryn, 2016; Mir et al., 2013; Tourand et al., 2009a; Yang et al., 2017). More biochemical investigations have been conducted on TelA in recent years to understand its features (McGrath et al., 2021, 2022).

1.3.2. The mechanism of the telomere resolvase reaction

The new family of DNA cleavage and rejoining enzymes is known as telomere resolvases. These enzymes act on a replication intermediate to produce linear replicons terminated by hairpin telomeres. These enzymes form six nucleotide 5'-overhangs by concurrently cleaving DNA six base pairs apart on opposing strands at the center of *rTel* junctions (previously depicted in Figure 1.4 as L/L' or R/R'). Covalently closed hairpins are created when these overhangs fold back on themselves and reseal the DNA backbone (Figure 1.5; (Huang et al., 2004a; Kobryn and Chaconas, 2002)). These enzymes share a tyrosine recombinase-like active site with type IB topoisomerases and have a similar reaction mechanism. Type IB topoisomerases function as monomers to cleave and rejoin a single DNA strand while the tyrosine recombinases form a tetramer to make a synaptic complex and ultimately cleave and exchange 4 strands of DNA (Grindley et al., 2006; Woodfield et al.,

2000). Telomere resolvases, by contrast, work in the middle of this range. Telomere resolvases act as a coordinated dimer on a single *rTel* to cleave and rejoin two DNA strands (Aihara et al., 2007; Briffotaux and Kobryn, 2010). Telomere resolvases use a two-step transesterification reaction mechanism. The reaction mechanism is isoenergetic and doesn't employ a divalent metal ion or any high energy cofactors. The DNA bond energy of the cleaved and rejoined strands is stored in the protein-DNA complex between the scissile phosphate and the active site tyrosine nucleophile. It has been demonstrated that ResT, the borrelial telomere resolvase, needs interprotomer communication to start reaction. ResT creates a 'cross-axis' complex to promote strand breakage. In the cross-axis complex, a dimer of ResT has assembled into a configuration competent to initiate telomere resolution. Surprisingly, positive supercoiling seemed to aid the development of these active dimers (Bankhead et al., 2006).

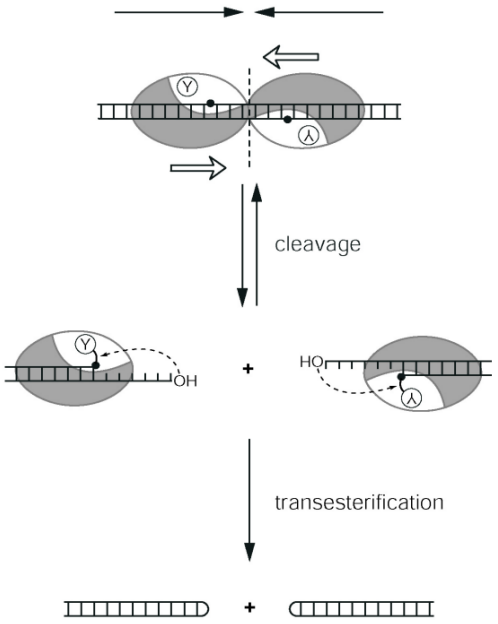

Figure 1.5. Conserved general mechanism of telomere resolution. Telomere resolvase dimerizes at the replicated telomere junction (*rTel*). Inverted repeat symmetry of *rTel* is shown by the dotted line. On opposing strands of the DNA, the tyrosine nucleophile cleaves the DNA six base pairs apart (the scissile phosphates are indicated by black dots). A phosphortyrosine complex and six nucleotide 5'-overhangs are the products of this transesterification. The overhangs fold back on themselves to produces two hairpin telomeres. The 5'-OH works as a nucleophile in a second transesterification event that reseals the DNA to the backbone and releases the tyrosine residue. The figure is captured from (Kobryn and Chaconas, 2002).

1.3.3. Active site of telomere resolvases

Several studies were conducted to determine the crucial catalytic residues needed for telomere resolution (Deneke et al., 2004; Moriarty and Chaconas, 2009). The N15 phage telomere resolvase (TelN) was first aligned against enzymes like phage integrases. The telomere resolvases showed a weak similarity to phage integrases and other tyrosine recombinases (Rybchin and Svarchevsky, 1999). Subsequently, telomere resolvases were discovered to have a conserved tyrosine residue that acted as the active site nucleophile, related

to that used by the tyrosine recombinases and type IB topoisomerases. To determine the tyrosine active site nucleophile of ResT, a DNA substrate modified to become a suicide cleavage substrate was employed. The cleavage complexes were followed by affinity purification of tryptic peptides attached to the DNA was used. The modified substrate contained a change in DNA's scissile phosphate into a 5'-bridging phosphorothiolate. The phosphorothiolate modification still permits DNA cleavage but prevents the second transesterification since the freed sulfhydryl (-SH) is a poor nucleophile (sulfhydryl has a lower pKa than hydroxyl). ResT remained covalently linked to the DNA allowing identification of the active site nucleophile using tandem mass spectrometry (Deneke et al., 2004). Y335 was discovered as the active nucleophile of ResT. ResT was also shown to be intolerant to changes of the Y335 residue (Kobryn and Chaconas, 2002). Both TelA Y405 (Huang et al., 2012) and TelK Y425 (Huang et al., 2004a) are active site nucleophiles that show a comparable intolerance to mutation. A group of additional conserved active site residues (RKHRH/W) are utilized by tyrosine recombinases for the protonation/deprotonation of leaving groups and nucleophiles, respectively. These residues are also thought to be involved in transition state stabilization in addition to roles in general acid/base chemistry to promote the transesterifications of DNA cleavage and rejoining (Chen and Rice, 2003; Grindley et al., 2006; Whiteson et al., 2007). TelA and ResT have conserved catalytic residues, RKYRH, which are similar to the typical RKHRH pentad of tyrosine recombinases, in addition to the active site nucleophile (Deneke et al., 2004; Huang et al., 2012; Nunes-Düby et al., 1998). According to an analysis of ResT variants with substitution of these residues result in a resolvase that can still bind DNA with normal affinity but has significantly decreased telomere resolution proficiency (Deneke et al., 2004). The results of the substitution of histidine with alanine of the active site in ResT showed that this residue might have a structural function as it was dispensable for telomere resolution (Chen and Rice, 2003; Deneke et al., 2004). TelA's Y363 was found out to be replaceable with either lysine or histidine (Huang et al., 2012). Y363 was suggested to be involved in the protonation of the leaving group based on the crystal structure of TelA (Shi et al., 2013). The tolerance for lysine or histidine replacement at TelA Y363 is explained by the fact that this protonation is less dependent on enzyme mediation than the deprotonation of the nucleophile. This is also consistent with the less deficient (2% of activity seen with wild type (WT)) phenotype observed for ResT (Y293F) with mutation in a catalytic residue (Deneke et

al., 2004). In addition, structural analysis was in agreement with the active site architectures in TelK and TelA (Aihara et al., 2007., Shi et al., 2013). TelK was shown to possess a hybrid active site of what is found in type IB topoisomerases and tyrosine recombinases with a lysine residue at the third position, RKKRH instead of RKHRH (Huang et al., 2004a).

1.4. Previous characterization of telomere resolvases

1.4.1. ResT from *Borrelia burgdorferi*

1.4.1.1. Domain structure

Telomere resolvases have a multidomain structure. The highly conserved catalytic domain in all telomere resolvases is surrounded by different N- and C-terminal domains (Figure 1.6). The DNA cleavage and rejoining activities of telomere resolution are provided by the catalytic domain; it contains the active site for telomere resolution. The N- and C-terminal domains might be unrelated to each other in the different resolvases and may have distinct functions. ResT can be proteolytically divided into two fragments: ResT (1-163) and ResT (164-449) which are called N-terminal domain and C-terminal domain, respectively (Tourand et al., 2007). By partial chymotrypsin cleavage, domain boundary mapping by mass spectroscopy, and independent expression of the discovered domains, it was shown that ResT contains two proteolytic domains (Tourand et al., 2007). It was also shown that ResT has an extended N-terminal domain that has general DNA binding abilities and a single-strand annealing activity (Huang and Kobryn, 2016). ResT has a centrally located conserved catalytic domain but it also has an extra C-terminal extension that most likely plays a role in recognition of the telomere sequence (Bankhead and Chaconas, 2004; Tourand et al., 2007; and data not shown). The telomere recognition sites in ResT's C-terminal end seem to be hidden in the full-length protein. This indicates that ResT is susceptible to autoinhibition by its N-terminal end (Tourand et al., 2007). It was proposed that since the C-terminal domain of ResT contains the elements necessary for telomere recognition, which is carried out through the distal box 3 to 5 sequences of the *rTel* (discussed in section 1.4.1.2), and the genome contains thousands of copies of the conserved box 3 sequence that ResT recognizes in the *rTel*; the autoinhibition of telomere binding may function to restrict ResT binding and activity until a *bona fide* cross-axis complex can be generated at legitimate replicated telomere substrates (Tourand et al., 2007).

Figure 1.6. The domain structure of ResT. The N-terminal domain, catalytic domain, and the C-terminal domain of ResT is shown with the amino acid numbers of the proteins above each domain. Precise domain boundaries have been adjusted from those previously reported based upon structural alignments. The catalytic domain of structure has a representation of the nucleophilic tyrosine (Y). This graphic is modified from (Kobryn and Chaconas, 2014).

1.4.1.2. Substrate promiscuity

The segmented genomes of *Borrelia* species contain a linear chromosome and multiple linear and circular plasmids. The *B. burgdorferi* strain B31 genome has almost 1 Mb in over 12 linear replicons that possess 19 distinct but related hairpin telomeres (Casjens et al., 2000). Based on the mechanism proposed for telomere resolution activity of ResT, the first step is the recognition of the telomere by ResT. The substantial sequence variability calls for ResT to have more flexibility to use multiple related substrates. However, other described hairpin telomere resolvases do not need to have this flexibility as they recognize unique *rTel* sequences (Tourand et al., 2009). There are five sequence-homologous regions known as 'boxes' among these telomeres. The conserved boxes 3-5 sequences are responsible for telomere recognition (Figure 1.7; (Tourand et al., 2003)). Based on the sequence insertions and deletions of box 1, the hairpin telomeres have been categorized into three groups (Type 1, 2, and 3). Compared to Type 1 telomeres with no insertions or deletions to the left of box one in type 1 (0/0), Type 2 telomeres (+3/-3) feature a box 1 that is 3 nucleotides away from the axis of symmetry and features a 3 base pair deletion between box 2 and 3 (Figure 1.7; (Huang et al., 2004b; Tourand et al., 2003)). On the other hand, a box 1 which is present in Type 1 and Type 2 telomeres, is absent in Type 3 telomeres. Heterogeneity in box 1 regions and overall telomere sequence is made possible by the fact that cleavage is position-specific rather than sequence-specific; cleavage always occurs 6 bp apart centered around the axis of symmetry of the *rTel* (Tourand et al., 2003). Studies have shown that ResT N-terminal domain contributes to telomere recognition and processing. The N-terminal domain was shown to have non-specific DNA binding activity (Tourand et al., 2007). Compared to Type 1 and 2 telomeres, Type 3 telomeres are unreactive *in vitro*, despite being active *in vivo*, as they lack a box 1. It was inferred that box 1 is crucial for telomere sequence activity *in vitro*. The activity of ResT was demonstrated to be

increased by positive supercoiling of DNA that overcome the autoinhibition of *rTel* binding imposed by the N-terminal domain, suggesting that either the stimulatory proteins are present *in vivo*, or the DNA topology is different (Bankhead et al., 2006; Tourand et al., 2009).

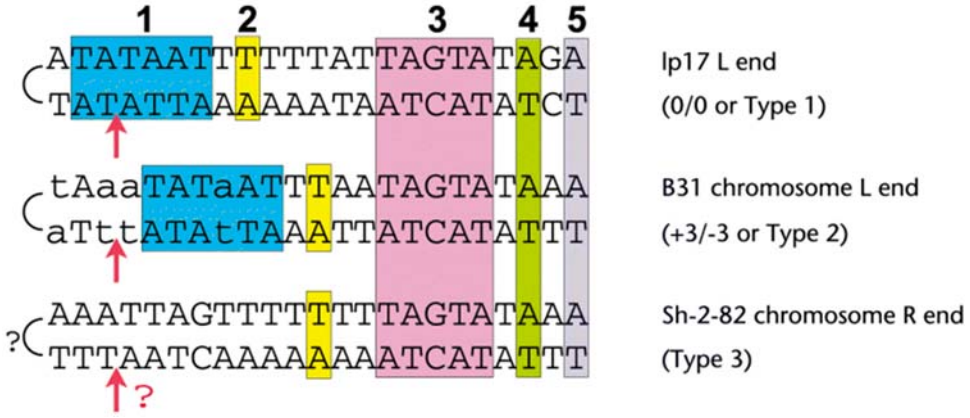

Figure 1.7. *Borrelia* telomeres of Types 1, 2, and 3. Each of the three telomere types that *B. burgdorferi* has is represented by one exemplar. Telomeres with the hairpin ends are aligned. Each conserved sequence or 'box' is shown with a distinct color and number. Known variations in Type 2 telomere sequence are shown by lowercase letters. The cleavage site of ResT is shown by red arrows. The uncertain cleavage site and the nucleotide around the hairpin are shown by question mark. The figure is captured from (Chaconas, 2005).

1.4.1.3. Reaction reversal

The continuing genome instability among the linear chromosome and plasmids of *B. burgdorferi* is another distinctive characteristic of its telomeric and sub-telomeric regions. A patchwork of duplicated sequences from different linear plasmids are found in the subterminal regions of several linear plasmids. On certain chromosomal ends and other linear plasmids, there are also extensions of other plasmid sequences. (Casjens et al., 2000). Although no suggested molecular mechanism has been definitively identified, rearrangement events occur like nonhomologous recombination events (Casjens et al., 2000, 2012; Huang et al., 2004b). However, a study on ResT demonstrated the potential chemical mechanism and the evolutionary benefits of such occurrences (Kobryn and Chaconas, 2005). They explained that ResT can covalently join two hairpin telomeres on distinct DNA molecules to create a replicated telomere structure, which is called a telomere fusion reaction (Kobryn and Chaconas, 2005). Therefore, ResT could not only bind to already-formed hairpin telomeres but also carry out the telomere fusion reaction, the opposite of telomere resolution (Kobryn and Chaconas, 2005). On the other hand, it is possible for DNA molecules from entirely different replicons to

merge to form chimeric plasmids or chromosomes with plasmid extensions (Kobryn and Chaconas, 2005; Tourand et al., 2003). Most of the time, fused telomeres would simply be resolved back into hairpins separating the fused replicons. A mutation, however rare, that could block resolution of the fused telomeres would lead to a chimeric plasmid or an extension on the linear chromosome. To eliminate one or two of the telomere resolution sites and produce a stable fusion, a later, somewhat substantial deletion would need to take place (Figure 1.8). Such deletions might be extremely extensive and eliminate significant amounts of plasmid DNA. The stabilized fusions would be available to take part in subsequent recombination events. These fusion products and the patchwork of repetitive sequences could potentially be result of these processes (Kobryn and Chaconas, 2005).

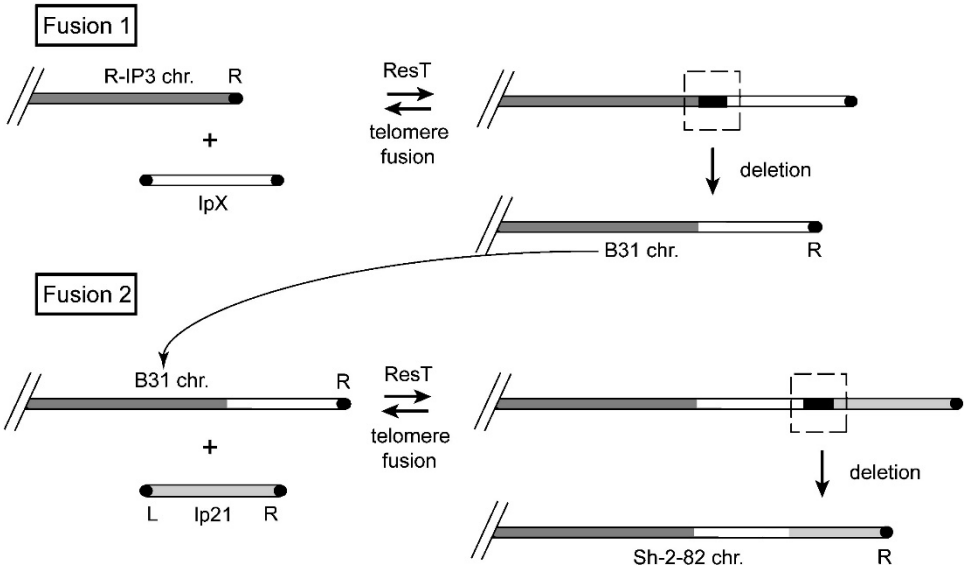

Figure 1.8. Proposed mechanism of telomere exchange by ResT-mediated telomere fusion. In the fusion 1, lpX plasmid and R-IP3 chromosome are fused together by the homologous hairpin ends represented by black tips. This would generate the structure of the right end telomere found in the B31 chromosome (Casjens et al., 1997, 2000). One telomere resolution site would remain after a subsequent large deletion. In the second fusion, telomere exchange converts the right end of B31 to the right end observed for the Sh-2-82 chromosome through fusion with lp21 (see Casjens et al., 1997; Huang et al., 2004b). The following deletion would result in chimeric end points. The chimeric endpoints seen on many *B. burgdorferi* linear plasmids could be explained by many rounds of fusion and deletion. The figure is captured from (Kobryn and Chaconas, 2005).

1.4.1.4. The importance of ResT's hairpin binding module in DNA cleavage

ResT employs a unique region of the protein at the end of the N-terminal domain (139-159) known as the hairpin-binding module to allow DNA cleavage by the catalytic domain. This ResT component resembles the hairpin-binding module found in the cut-and-paste

transposases of Tn10 and Tn5 (Bankhead and Chaconas, 2004; Rice and Baker, 2001). These transposases have a hydrophobic pocket and an α-helix with charged residues as the hairpin-binding module. The conserved YKEK motif is found in ResT's hairpin binding module, which is a derivative of the YREK motif commonly found in transposons' hairpin binding modules. YREK motifs in transposases have been demonstrated to enhance transposon excision by stabilizing the temporary hairpin intermediate that forms during transposon excision. The hydrophobic residues in the hairpin binding module stack against the flipped-out base and charged residues stabilize the cleaved strand for hairpin formation via series of electrostatic interactions (Ason and Reznikoff, 2002; Bischerour and Chalmers, 2007; Davies et al., 2000). Previous studies showed a strong telomere resolution defect was caused by a mutation of residues in ResT's hypothesized hydrophobic binding pocket. When charged residues in ResT were altered, the variants produced were cold-sensitive showing defects in DNA cleavage during telomere resolution at low reaction temperature (10°C). This defect could be rescued by inserting heteroduplex DNA at the middle two base pairs of the *rTel*. The authors concluded that the distortion of the DNA caused by the hairpin binding module appears to be crucial for both DNA cleavage and subsequent hairpin formation, as these rescued mutants complete telomere resolution rather than simply stalling after the DNA cleavage step (Bankhead and Chaconas, 2004).

1.4.1.5. Strand foldback/hairpin formation

The TelK-cleaved *rTel* complex provided the first model for the hairpin formation step promoted by telomere resolvases. Dramatic and out-of-plane bending of the DNA by TelK was hypothesized to provide the energy to promote enzyme dimer dissolution after DNA cleavage to allow and subsequent spontaneous strand foldback (Figure 1.9a; (Aihara et al., 2007)). This dimer dissolution model was proposed since the structure of the TelK dimer suggested steric conflict during hairpin refolding within the highly interlocked dimer. The TelK-DNA structure suggested that the stirrup domain of TelK stabilized the dramatic bend induced in the substrate DNA. Experiments have demonstrated the importance of the stirrup subdomain in the formation and maintenance of the bent DNA substrate. Mutants lacking the stirrup were cleavage competent but deficient in hairpin formation (Aihara et al., 2007).

Research on ResT's biochemistry revealed a different method of enzyme-mediated hairpin formation/strand foldback that diverged from the TelK concept. In contrast to TelK, hairpin telomere formation must take place in the presence of ResT's dimer bound to the *rTel* (Briffotaux and Kobryn, 2010). The model for ResT is called the 'spring-loaded pre-cleavage model'. In this model, DNA cleavage only occurs after ResT induces an underwound conformation in the *rTel* between the scissile phosphates. This allows the catalytic residues of the telomere resolution active site to engage the scissile phosphates and induce DNA cleavage. Studies showed that the hairpin binding module and sidechains from ResT's catalytic domain work together to produce and stabilize an underwound pre-cleavage intermediate. This intermediate promotes ejection of the cleaved strands. Consequently, ejecting the strands promotes the resolution reaction going forward to completion in preference to simply rejoining the cleaved strands to regenerate the substrate *rTel* (Lucyshyn et al., 2015). Most mutants in that study were unable to initiate DNA cleavage due to the inability to unwind the DNA between the scissile phosphates. A couple of cleavage competent mutants were also characterized in the same study. These mutants go through cycles of cleavage and rejoining reaction without generating hp products. The reactions of both classes of mutants could be rescued by employing missing base substrates, mismatches, or nicks that disrupt the base pairing between the scissile phosphates. After both hairpin products are formed, ResT could release the products (Figure 1.9b; (Bankhead and Chaconas, 2004; Briffotaux and Kobryn, 2010; Lucyshyn et al., 2015)).

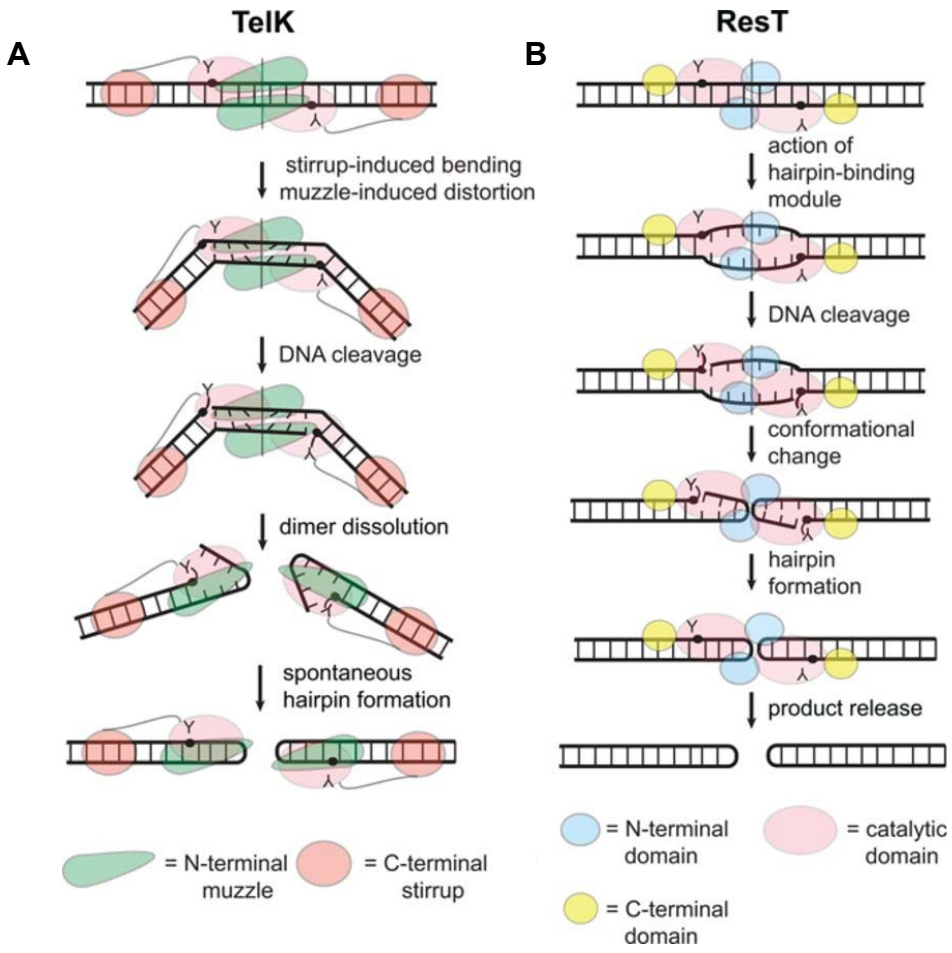

Figure 1.9. Models of telomere resolution in TelK and ResT systems. The main processes of TelK, and ResT promoted telomere resolution are represented in a diagram. Black dots represent the scissile phosphates, and the tyrosine nucleophiles are represented by Y. **TelK**) When TelK binds to substrate DNA, it causes a significant bend in the DNA and severely disrupts the base pairing close to the scissile phosphate. The energy needed to propel the reaction forward is stored in a 'pre-cleavage intermediate' that is produced by this distortion. The DNA cleavage is followed by dimer dissolution and spontaneous hairpin formation. The deletion of TelK's stirrup, which bend the DNA substrate, supports to this model (Aihara et al., 2007). **ResT**) The reaction happens in the context of a dimer. The hairpin binding module of the N-terminal domain in ResT has been characterized for DNA binding and dimerization. An underwound conformation is created and stabilized by hairpin binding module to promote DNA cleavage by catalytic domain (Lucyshyn et al., 2015). The two hairpins are released after completion of formation of both (Briffotaux and Kobryn, 2010). This image is reproduced from (Lucyshyn et al., 2015).

1.4.1.6. Potential multifunctionality: annealing and unwinding activities

Studies on ResT have raised the possibility that the enzyme is multifunctional. First, ResT was shown to possess a single-stranded DNA (ssDNA) annealing and strand exchange activity (Mir et al., 2013). The ResT (1- 163), N-terminal domain, was shown to have annealing activity (Mir et al., 2013). The N-terminal domain was sufficient on its own to anneal naked

ssDNA, however, 8-fold more N-terminal domain was required to achieve 50% of maximum annealing rate compared to full-length ResT (Mir et al., 2013). The N-terminal domain by itself was not enough to promote the annealing of ssDNA associated with cognate single-stranded DNA binding protein (SSB). It was shown that ResT (163-449) interacts with the C-terminal tail of SSB (Huang and Kobryn, 2016). This function of ResT is similar to the RecO protein from *E. coli*, which is a recombinational mediator for RecA in the RecF pathway (Kantake et al., 2002). The annealing activity is also related to the activity of single-strand annealing proteins (SSAPs) characterized from phage λ Beta of the λ Red recombination system and Rad52, and the eukaryotic SSAP which participates in RecA/Rad51-dependent and independent homologous recombination events (Kuzminov, 1999; Mir et al., 2013; Pâques and Haber, 1999). Studies showed that ResT promotes strand exchange across duplex DNA up to 63 bp in length and facilitates single-strand annealing between complementary strands of up to 106 nucleotides in length using synthetic oligonucleotides. Later, it was also shown that ResT's annealing activity could extend to plasmid-length DNA, especially when acting in concert with SSB (Huang and Kobryn, 2016). It can be inferred that ResT might be involved in generating short-patch recombinants (Kobryn, 2021; Kobryn and Chaconas, 2014).

Despite the lack of homology to ATP-binding domains or common helicase motifs, DNA-dependent ATPase activity and ATP-dependent 3'-5' unwinding activity of ResT were demonstrated *in vitro* (Huang et al., 2017). Huang et al showed that ResT could unwind a wide range of branched DNAs, including replication forks and recombination intermediates such as D-loops. Although hyper- or hypoactive ResT mutants with telomere resolution activity have been demonstrated, the same study showed that ResT could only bind ATP when the full-length protein was present and not restricted to a specific domain region. It was inferred that these activities have a different role from telomere resolution. ResT showed activity in a fork regression assay on a partially mobile synthetic replication fork mimic (Huang et al., 2017). Additionally, TelN and TelK showed weak homology to P-loop NTPase and UvrD helicase conserved domains, suggesting other telomere resolvases could possibly have DNA helicase activity or at least be modulated by nucleotide binding. It can be inferred from the complex character of ResT that it may have a function in replication completion at the hp telomeres in addition to its well-known telomere resolution (Huang et al., 2017).

1.4.1.7. Conditional expression of *resT in vivo*

For a deeper knowledge of the telomere resolution mechanism, ResT has been studied through biochemical experiments using *in vitro* assays. However, the first evidence of telomere resolution function was demonstrated *in vivo* (Chaconas et al., 2001). The conditions used *in vitro* most likely are not an ideal mimic for *in vivo* conditions. For instance, Type 3 *rTels* cannot be processed *in vitro* but they are effectively used by ResT *in vivo* (Tourand et al., 2006). This indicates that additional conditions such as positive supercoiling in the substrate or accessory proteins help driving the reaction *in vivo* (Kobryn and Chaconas, 2014).

Attempts to knock out *B. burgdorferi resT* resulted in merodiploid transformants carrying both WT and mutant copy of *resT* (Byram et al., 2004). This suggested that the *B. burgdorferi resT* gene is essential. Therefore, a *resT* knockout strain was generated in a background that allowed conditional expression of *resT* to learn more about its *in vivo* functions (Bandy et al., 2014). Expression of ResT under the control of an IPTG-inducible expression system resulted in high expression of the ResT comparable to that seen for endogenous expression (15,000 monomers per cell). It was inferred from the phenotype observed that ResT might have other functions as well as telomere resolution. Disruption of proteins involved in resolving chromosome dimers would result in dimers of the DNA that cannot be segregated to daughter cells. Dimers would continue to be replicated but they are unable to segregate into daughter cells, resulting in elongation and filamentation of the bacterial cells (Barre et al., 2000; Draper et al., 1998; Wang and Lutkenhaus, 1998). After ResT depletion, unresolved dimeric replication intermediates accumulated as expected between 24 to 48 hours but then changed into complex, high molecular weight forms. This highlights ResT's essential role in telomere resolution (Bandy et al., 2014). However, ResT depletion beyond 48 hours, the *Borrelia*'s replication was stopped without any filamentation of the cells. This suggests that the telomere resolvase interacted either directly or indirectly with *Borrelia*'s replication machinery because cellular depletion of ResT caused growth arrest and the bacterial cells subsequently stopped DNA replication. (Bandy et al., 2014).

1.4.2. TelA from *Agrobacterium tumefaciens*

1.4.2.1. The TelA substrate

Species of *Agrobacterium* genus contains both circular and linear chromosomes and a plasmid known as a tumor inducing (Ti) plasmid (Goodner et al., 1999). Several of these bacteria cause tumorous crown gall disease on a range of plants (Smith, E.F., and Townsend, 1907). *Agrobacterium tumefaciens* has been modified to become a crucial tool for plant genetic engineering. The focus of most investigations on *A. tumefaciens* were on the tumor inducing (Ti) plasmid (Newell, 2000). Studies on the linear chromosome-generating machinery in *A. tumefaciens* was the first initiated with the work of Huang et al., 2012. In this study, the mapping of the linear chromosome's sequences to its telomeres was completed. The authors presented biochemical evidence that the protein encoded by Atu2523 is the agrobacterial telomere resolvase, TelA (Huang et al., 2012). The previous attempts to fully sequence the *A. tumefaciens* chromosome were not successful in reaching the telomeric ends of the linear chromosome. This was because during the building of the library, the closed ends at the termini were not free to ligate to the vector; therefore, these sequences were omitted from the typical genomic sequence (Goodner et al., 2001). Huang et al, discovered specifically the terminal sequences of the linear chromosome with a different approach than what have been used in previous studies. They identified the two terminal pieces of the linear chromosome and then utilized single strand-specific nucleases to open the closed ends. The same method had been used to successfully identify the telomeres of the linear chromosome of *B. burgdorferi* and some its linear plasmids (Casjens et al., 1997). Their results were in perfect agreement with previously published sequences where they overlapped and were followed by the extending new sequences. Inverted repeats starting 25 bp from the ends were formed after combining and aligning the left and right telomeres in the context of the linear chromosome.

The investigation of TelA followed by cloning the Atu2523 gene into an expression vector and purifying the generated recombinant protein. The mass of resulting protein was determined to be ~ 51 kDa by sodium dodecyl sulfate (SDS)-gel electrophoresis and mass spectrometry analysis which was consistent with the estimation from the open reading frame. In addition, incubation of the protein encoded by the gene Atu2523 with plasmid substrate containing the target 50-bp inverted sequence, resulted in the products with hairpin ends. Consequently, the conclusion was drawn that the protein encoded by the gene Atu2523 creates

closed hairpin ends in the cloned target sequence (Huang et al., 2012). The same study determined the exact nucleotide location of cleavage-and-ligation in TelA reaction by utilizing a panel of labelled substrates. The results showed that cleavage occurs between nucleotides 22 and 23 on the top strand and between nucleotides 28 and 29 on the bottom strand, resulting in two halves with 6-base 5-overhangs as the intermediate of reaction. However, the minimal target site of TelA to produce the hairpin ends was shown to be the central 26 base pairs (bps) which includes the internal inverted repeat and 10 bp flanking either side of the central 6-bp cleavage regions (Huang et al., 2012).

1.4.2.2. The structure of TelA

Similar to other telomere resolvases, TelA consists of a conserved catalytic domain flanked by N and C-terminal domains. Compared to other enzymes of this class, TelA has a relatively small C-terminal extension that helps with dimerization interactions during telomere resolution (Kobryn and Chaconas, 2014; Shi et al., 2013). In TelK, a special insert on its C-terminal end known as the 'stirrup', causes a significant bend in the DNA by making distal interactions with the DNA substrate (shown in figure 1.9). Bending the DNA in this system promotes the hairpin formation. The stirrup extension is unique for TelK, and it is absent in both TelA and ResT (Figure 1.10a; (Aihara et al., 2007)). The sub-domain region of TelA and TelK's N-terminal ends known as the N-core domain show strong structural homology. However, in TelK the N-core domain also has a large insertion of a 'muzzle' domain that contributes to DNA distortions between the scissile phosphates (Aihara et al., 2007). It has been shown that the N-terminal domain of TelA has an active role in other activities of TelA which is discussed in section 1.4.2.4 (McGrath et al., 2021). A study with several crystal structures of TelA with DNA revealed more details about TelA interaction with the hairpin products and even on how the cleaved strands are refolded into hairpins in the TelA system (Shi et al., 2013). TelA-DNA complexes in which the dimer of TelA bound to telomere sequence were shown by crystallization of full-length TelA with different DNA substrates (Figure 1.10b). Results showed that two structural domains in the TelA monomer, the catalytic domain and the hairpin binding module, work together to distort the DNA substrate. The crystal structures suggested that TelA stabilizes the tight di-nucleotide hairpin products by a variety of interactions (Shi et al., 2013). In the hairpin binding module within the N-core domain, TelA (A198- G217), Y201

and R205 showed a crucial role in refolding of the duplex DNA substrate into hairpin products which is discussed more in section 1.4.2.3 (Shi et al., 2013).

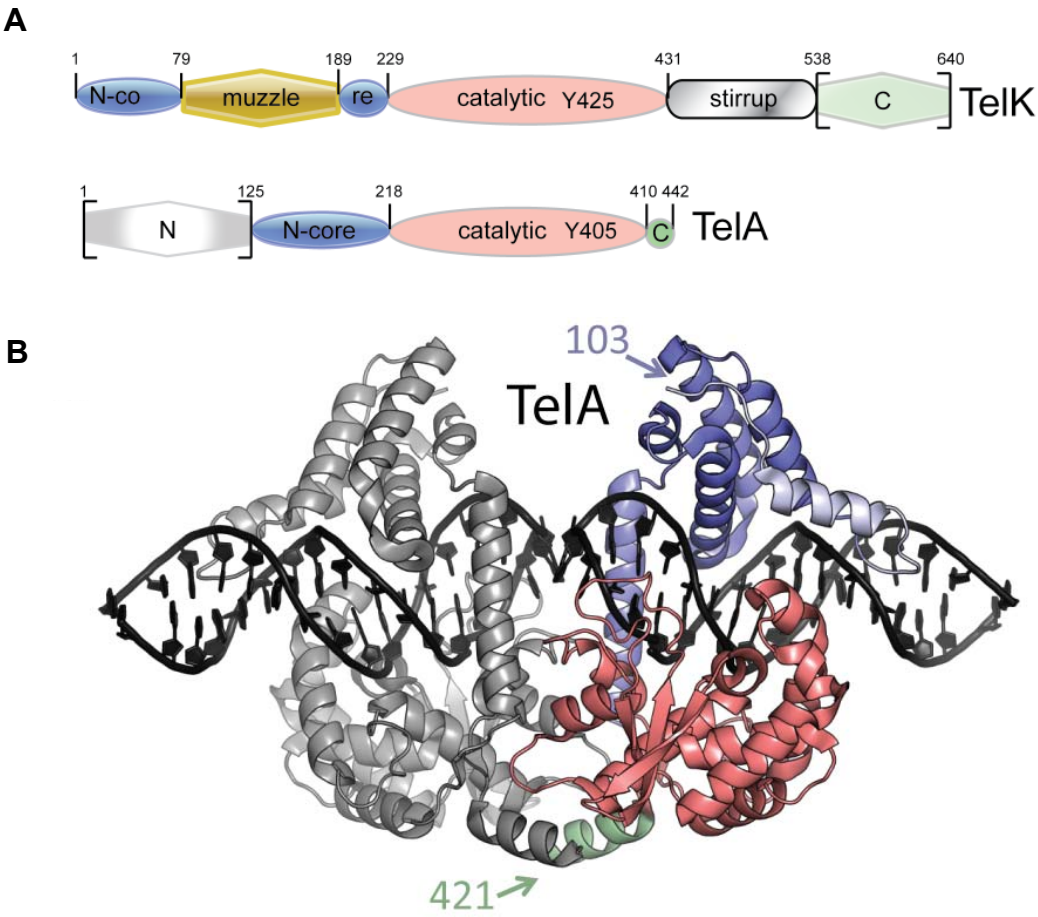

Figure 1.10. The schematic representation of TelA and TelK structure. A) The homologous domains are shown in same colors. These domains in TelA and TelK has been identified by BLAST or by structural analysis. Square brackets show the domains that have been shown to be dispensable for telomere resolution. Y represents the nucleophilic tyrosine within the catalytic domain. **B)** The crystallography of TelA dimer bond to the hp telomere products. The hairpin binding module and catalytic domain make interactions with the hairpin product. TelA domains of one monomer are color coded according to part A. This graphic is modified from (Kobryn and Chaconas, 2014).

1.4.2.3. Hairpin binding module of TelA

Formation of hairpin products in the TelA system was shown in a crystallography study. TelA dimers severely distort the DNA into a stable conformation which is thermodynamically more favorable for hairpin formation (Shi et al., 2013). It was also shown that TelA residues in the α-helix linker in the N-core domain, known as the hairpin binding module, interact with the hairpin refolding strand to stabilize a 'refolding intermediate'. Using suicide substrates that block hp formation, a TelA-DNA refolding intermediate was trapped and

crystalized. The resulting structures supported the hypothesis that a set of protein-DNA and DNA-DNA interactions direct the refolding of DNA strands into hairpins. The A6 nucleotides in the refolding intermediate lie flipped out of the helix with Y201 stacked against them. The G5 nucleotides were also out of the helix and stacked on A6. Non-canonical base pairing was seen between G5 and T4 from opposing sides of the substrate in the refolding strands (Figure 1.11; (Shi et al., 2013)). The authors explained that R205 played an active role in hairpin loop formation by ejecting the refolding strand with its positive charge. The TelA (Y201A) and (R205A) were reported to be cleavage competent but deficient for hp formation. The role of Y201 and R205 can be related to the Y319 and R322 in 'YREK' conserved sequence of hairpin binding module of transposases which are involved in stabilizing the hairpin DNA shape and base out of helix, as mentioned before. The authors concluded that the refolding intermediate allows the telomere resolution activity of TelA to go forward to completion (Shi et al., 2013).

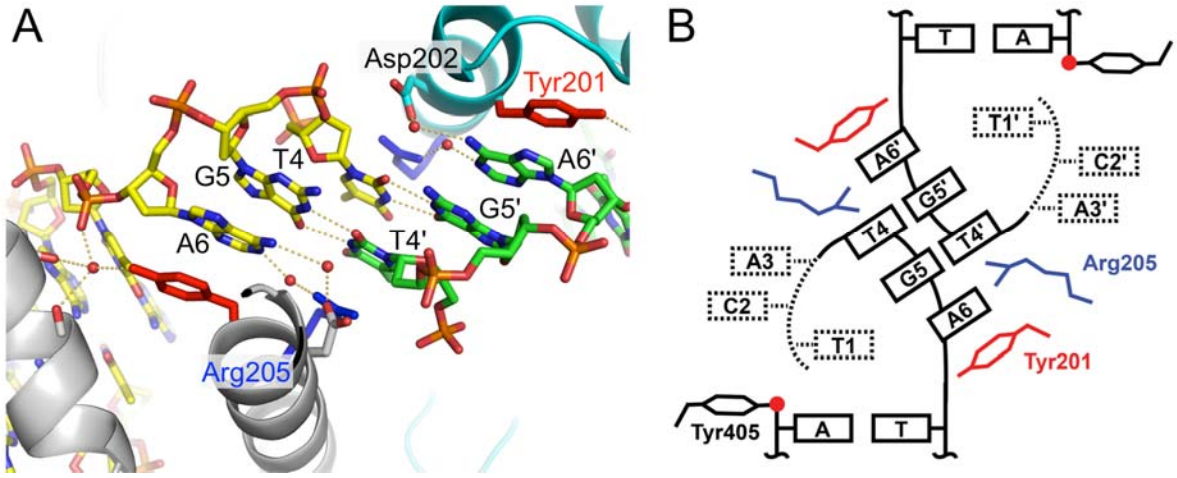

Figure 1.11. The refolding intermediate in TelA system. A) The crystalized structure of refolding strands. The dimer of TelA is shown in gray and blue. The refolding strands are shown green and blue *vs*. yellow and red. Y201 and R205 are shown in red and blue, respectively. **B)** The schematic representations of the refolding strands with the residues involve in stabilizing refolding intermediate in TelA. Y201 stacks against the A6, flipped out of helix base. R205 is in contact with T4 and helps ejecting the refolding strand. T4 and G5 make non-canonical base pairing. This graphic is modified from (Shi et al., 2013). The model is derived from the 4e0p pdb.

1.4.2.4. Multifunctionality of TelA

As mentioned in section 1.4.1.7, conditional expression of ResT resulted in stalled DNA replication, suggesting a direct or indirect interaction with the replication machinery (Bandy et al., 2014). In addition, ResT exhibited ssDNA annealing activity with naked DNA and DNA complexed with its corresponding SSB (Huang and Kobryn, 2016; Mir et al., 2013).

A recent study on TelA showed that both naked ssDNA and ssDNA complexed with its cognate SSB can be annealed by TelA, as well (McGrath et al., 2021). Biochemical studies showed that TelA was able to anneal DNA at a rate significantly above that of spontaneous annealing. It was discovered that TelA's annealing activity was less effective than ResT's necessitating use of a higher protein concentration (around 10-fold higher) for half-maximal annealing rate (Huang and Kobryn, 2016). Nonetheless, TelA is a potent ssDNA annealing activity that appears to be combined with a modest ability to remove complex secondary structure from DNA. The HIV transactivational response (TAR) element forms a complicated hairpin with several bulges. It was shown that TelA can also remove these complicated secondary structures and anneal the oligo that mimics the TAR element to its complementary strand (McGrath et al., 2021).

The TelA (Y405F) variant is defective in telomere resolution due to mutation of the active site nucleophile. It was used to evaluate if the annealing activity of TelA was separate from its telomere resolution activity. TelA (Y405F) showed annealing abilities comparable to the WT enzyme, suggesting separate functional determinants for these processes in TelA. The crystal structure study showed that the structure starts to resolve from residue 102, leaving the entire N-terminal domain absent from the structures (Shi et al., 2013). According to a prior study, TelA's N-terminal domain is not necessary for telomere resolution activity (Huang et al., 2012). As the evidence suggests, the N-terminal domain of TelA may have annealing activity. To determine if the deletion of TelA's N-terminal domain affected annealing activity, an N-terminal truncation variant was used. Despite the telomere resolution activity of TelA (107-442), it was unable to anneal complementary ssDNA faster than the spontaneous rate (McGrath et al., 2021). The findings implied that TelA's N-terminal domain is crucial for the annealing activity but dispensable for telomere resolution. With higher concentration of protein, the N-terminal domain of TelA, TelA (1-106), showed ssDNA annealing activity, with naked ssDNA and ssDNA complexed with its cognate SSB (McGrath et al., 2021).

1.4.2.5. Autoinhibition of TelA

A very recent study on TelA demonstrated that the N-terminal domain of TelA has an active role in regulation of TelA’s DNA cleavage and rejoining activities (McGrath et al., 2022). The study showed that the addition of a divalent metal ion significantly increased telomere resolution activity, with calcium preferred over magnesium. The N-terminal domain

truncation variant of TelA, TelA (107–442), showed hyper activity in telomere resolution than WT TelA (McGrath et al., 2022). Also, deletion of the N-terminal domain eliminated the need for a divalent metal ion to promote telomere resolution. Addition of N-terminal domain (1-106) *in trans* to TelA (107-442) restored the phenotype of WT TelA with its marked divalent metal ion dependency; therefore, it was concluded that the N-terminal domain is responsible of TelA's autoinhibitory regulation (McGrath et al., 2022).

On the other hand, TelA (D202A) was characterized to be hyperactive and semi-metal independent, suggesting that this residue might be part of autoinhibitory interactions regulating telomere resolution activity (McGrath., 2022). The N-terminal domain deletion combined with the D202A mutation resulted in a hyperactivated, metal-independent form of TelA. Adding the N-terminal domain *in trans* to TelA (107-442; D202A) re-established the semi-metal independence noted for TelA (D202A). It was inferred from the pattern of reactivity that TelA has at least two sites for binding divalent metal ions, one of which is in the N-terminal domain and the other of which is located someplace else in the protein and has a lower affinity (McGrath et al., 2022). Telomere resolution is inhibited when calcium is present in this second site. The D202A mutation either directly or indirectly disrupts this second location. This suggests that an autoinhibitory relationship between the N-terminal domain and the rest of the protein is relieved by the binding of divalent metal ions (Figure 1.12; (McGrath et al., 2022)). The authors hypothesized that D202 in the hairpin-binding module may physically interact with the N-terminal domain. The interaction of TelA N-terminal domain (1-106) and TelA (107-442) was shown using protein-protein cross-linking investigations and the addition of divalent metal ions interferes with this interaction (McGrath et al., 2022).

ResT can promote reactions that compete with telomere resolution; hp telomere fusion (a reversal of telomere resolution) and site-specific recombination between *rTels* to produce Holliday junctions (HJ; an intermediate of recombination promoted by tyrosine recombinases; (Kobryn and Chaconas, 2005; Kobryn et al., 2009)). In contrast to ResT, investigation of hp telomere fusion or HJ formation by WT TelA showed that TelA does not promote these reactions unless TelA is hyperactivated by mutation and highly artificial reaction conditions are employed (McGrath et al., 2022). With the N-terminal domain deletion and hyperactive TelA (107-442; D202A) variants, HJ can form. With such hyperactivated versions of TelA and

divalent metal ions, hairpin telomere fusion was possible after adding the N-terminal domain added *in trans* to N-terminal truncation mutants. Alongside of the ssDNA annealing reaction of N-terminal domain, the N-terminal domain of TelA is involved in regulation of TelA's telomere resolving activity to make it responsive to divalent metal ions and to limit reaction reversal and the side reaction of strand exchange between *rTels* to form HJs that could cause genomic instability (McGrath et al., 2022).

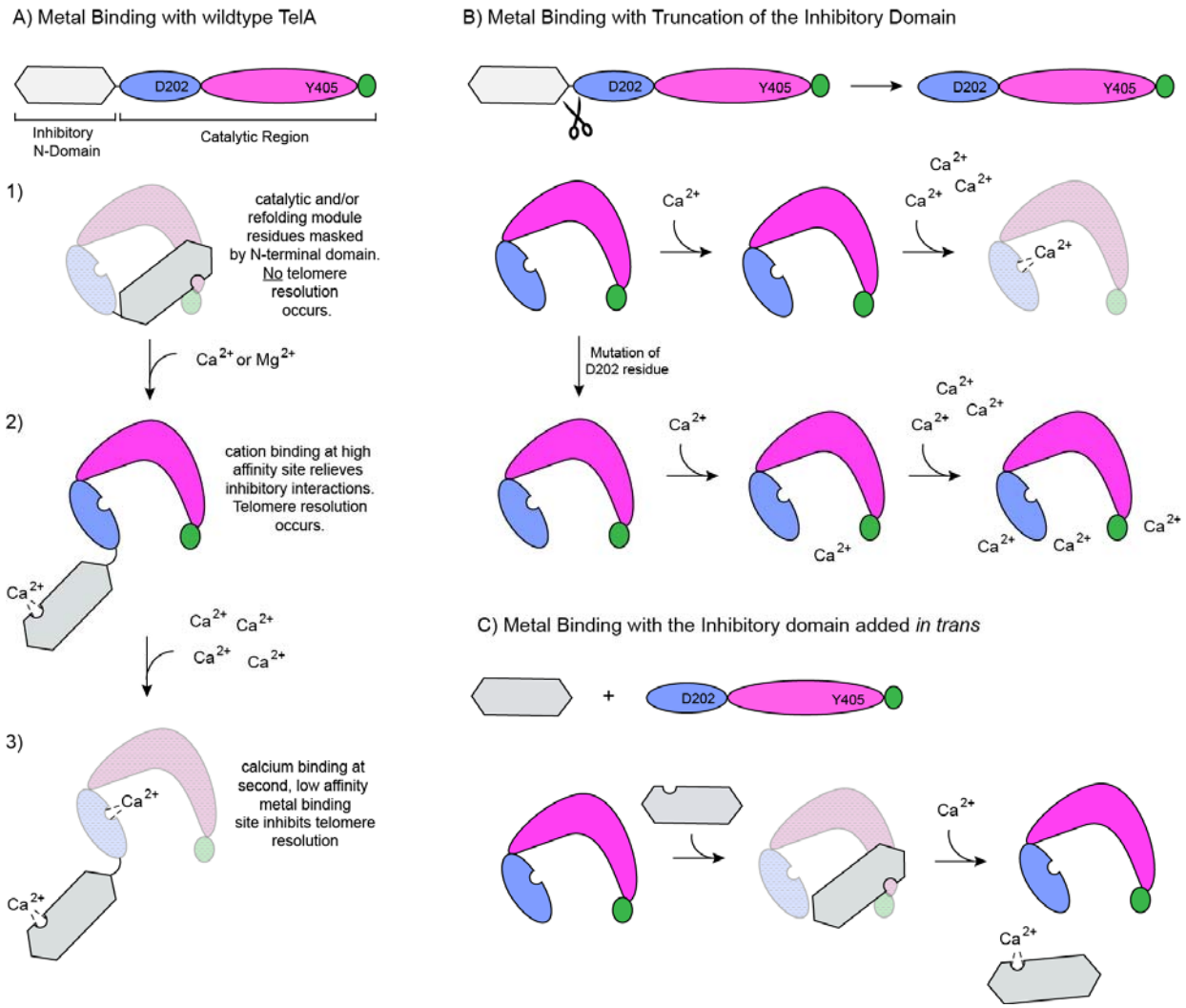

Figure 1.12. Schematic representation of TelA regulation by metal binding. A: The regulation of WT TelA. The N-terminal domain covers the rest of TelA and interact with it to inhibit the activity of enzyme in absent of divalent metal ion (shown with half opacity). In the present of low concentration of calcium, the N-terminal domain relieves the inhibitory effect as the metal ion binds to a high-affinity site resulting in activation of TelA. Stimulation of the low-affinity metal-binding site located in D202 results in inactivation of telomere resolution of TelA. B: N-terminal truncation mutant of TelA is active without divalent metal ion. Mutation of D202 results in disruption of the low-affinity metal-binding site; therefore, TelA remain active even with the present of high calcium concentrations. C: By adding the N-

terminal domain *in trans*, the phenotype of WT TelA was restored. The figure is captured from (McGrath et al., 2022).

1.5. Are there any advantages to genome linearity?

Despite the challenges of maintaining linear chromosomes, studies have shown that there are a number of potential advantages for organisms by possessing a linear configuration of DNA. DNA processes such as conjugation, replication termination, replicative transposition and genome stability have been affected greatly by a linear configuration (Wang et al., 1999). The linear plasmids of *B. burgdorferi* undergo rapid rearrangement so that each strain has a linear plasmid complement with differing structures but similar gene content (Casjens et al., 2000, 2012). Notable homology of the right terminal sequence of the *B. burgdorferi* chromosome and a linear plasmid in some strains suggests that *B. burgdorferi*'s chromosome and linear plasmids can undergo fusion events (Casjens et al., 1997, 2000; Fraser et al., 1997). The comparisons of the plasmids component in the different strains showed mosaic sequences and the authors concluded that non-homologous recombination was most likely the cause of such rearrangements (Casjens et al., 2000, 2012). Gene duplication and genetic redundancy resulting from recombination events are crucial for the development of new gene functions amongst the paralogous gene families in the *B. burgdorferi* genome. There are many examples amongst of the various linear and circular plasmids of *B. burgdorferi*; some of which have been implicated in virulence and infectivity (Casjens et al., 2000; Fraser et al., 1997). For instance, the surface-exposed lipoprotein of *B. burgdorferi*, VlsE, was found on a linear plasmid called lp28-1 using subtractive hybridization. lp28-1 contains fifteen tandem repeats that are unexpressed *vls* cassettes and an expressed *vls*E locus (Zhang et al., 1997). Previous attempts to sequence the *B. burgdorferi* failed to detect this locus as the tandem repeats of *vls* cassettes make secondary structures and will be deleted in the cloning process. Loss of lp28-1 significantly lowers the infectivity and resulting lipoproteins of these genes are crucial for surviving from immune system attacks of the various mammalian and avian hosts (Anguita et al., 2000). During a mouse infection, genetic material is copied from the tandem repeats of the silent *vls* cassettes into the *vls*E expression locus. In theory, this could result in millions of different amino acid sequences for the expressed VlsE. These rearrangements make new and unique expressed lipoproteins to present the host immune system (Gu et al., 2003; Zhang et al.,

1997). Thus, the linearity of the *Borrelia* genome has become essential for the maintenance of an antigenic variation system required for persistent infections in mammalian hosts.

The existence of some examples of genome linearity in bacteria begs the question of how the chromosomes/plasmids of *Agrobacterium* and *Borrelia* originated. One possible explanation is ancestral circular chromosomes have been linearized independently in bacterial evolution, even though circular chromosomes have been selected as the primary configuration for prokaryotes (Volff and Altenbuchner, 2000). The results of a study have shown that the similarity of ResT with tyrosine recombinases, enables the ResT to synapse *rTels* and form HJ (Kobryn et al., 2009). The authors explained that the λ integrase and/or Xer-like were the ancestors of the telomere resolvases that obtained or became converted to the novel activity (Kobryn et al., 2009). Studies have also shown that for the related tyrosine recombinase, Cre, self-complementary sequences at the *lox*P recombination sites results in accumulation of the HJ intermediate of recombination. This significantly lowers the recombination efficiency (Ghosh et al., 2005; Hoess et al., 1986; Lee et al., 2003; Senecoff and Cox, 1986). Additionally, under unusual conditions and modified substrate, λ integrase and Flp can make hairpins instead of promoting recombination (Lee and Landy, 2004; Lee et al., 1997; Nash and Robertson, 1989).

Studies argued for the reversibility of the linearity of chromosomes in *Streptomyces. lividans* (Lin et al., 1993; Volff and Altenbuchner, 2000; Volff et al., 1997). Deletion of the inverted repeats at terminal of the linear chromosomes showed that *S. lividans* with such circular chromosome mutations were viable with little to no growth disadvantage in comparison to the WT (Lin et al., 1993; Volff and Altenbuchner, 2000; Volff et al., 1997). In contrast, a recombinant linear genome of *E. coli* containing palindromic sequence called *tel*LR, the reaction site of TelN, and the telomere resolvase TelN, showed viability over 170 generations with its genome linearized by TelN (Cui et al., 2007). The authors concluded that *E. coli* linear chromosomes acted normally. It can be inferred that linear DNA might have limited drawbacks for the organisms (Cui at el., 2007). With the discovery of the ease with which *E. coli* can propagate linear DNA it was not long until this discovery was applied to develop a linear cloning vector. With the use of phage N15 genetic elements, such as *tel*N, *tel*LR site, *sop*AB, and *ant*A, the pJAZZ vector was constructed (Godiska et al., 2009). pJAZZ is suitable for cloning the sequences with tandem repeats and genomes with a high A-T content. Cloning

these sequences in *E. coli* using supercoiled plasmids results in gaps as these sequences induce secondary structures such as intrastrand hairpins and cruciforms that are highly susceptible to deletions or rearrangements (Leach and Lindsey, 1986). Therefore, linear plasmid is the only suitable tool to maintain or clone these sequences (Godiska et al., 2009).

1.6. Are telomere resolvases a 'druggable' target?

Lyme disease is a multi-stage infection that affects many organ systems such as the joints, nervous system, or skin. The symptoms may arise in different steps of infection, making diagnosis and treatment challenging. The most common method for diagnosing Lyme disease is the observation of an active erythema migrans (EM) skin lesion in conjunction with other recognizable symptoms (Aguero-Rosenfeld et al., 2005). Other methods for diagnosing Lyme disease such as culturing the skin biopsies of EM lesions in the early stages and positive antibody response for all stages of infection are also being used (Aguero-Rosenfeld., 2005). Doxycycline is most frequently administered for a period of 14 to 21 days to treat early localized or widespread illnesses with a high rate of well-response (Steere et al., 2004). Two 4-week regimens of doxycycline are used to treat late-stage infections that have become widely disseminated. In case of treatment failure, a 2 to 4-week course of intravenous ceftriaxone is recommended treatment (Wormser et al., 2000). Despite the availability of relatively effective antibiotic treatments for Lyme disease, the necessity and uniqueness of ResT to *B. burgdorferi* makes ResT a possible specific antiborrelial drug target as an alternative of current treatment to prevent spreading antibiotic resistance (Hunfeld and Brade, 2006)

A study developed a fluorescence-based high-throughput screen for ResT based on its telomere resolution activity to check the inhibitory activity of a library of small-molecule drug-like compounds (Lefas and Chaconas, 2009). Inhibition of telomere resolution by 6 compounds of interest on the oligonucleotide substrates was at least 70%. The inhibitory impact of these compounds was more significant on telomere resolution rather than on cleavage (Lefas and Chaconas, 2009). The authors concluded that an inhibitory compound might either bind to the active site directly or affects other steps in the reaction pathway. The compounds were classified by the DNA-binding results. In Class I, the amount of DNA cleavage corresponds with the amount of sequence-specific DNA binding by ResT (164-449) in the presence of the compounds in this class. It can be inferred that ResT's failure to bind DNA may be the cause of the degree of inhibition of telomere cleavage. Class II are the compounds that target the steps

after DNA cleavage. Lastly, Class III compounds severely affected the telomere binding activity of ResT (Lefas and Chaconas, 2009). It can be concluded that due to the importance for survival and the unique reaction promoted by telomere resolvases that these preliminary results on small molecule inhibitors suggest that telomere resolvases could be a druggable target.

2. Rationale, Hypotheses and Objectives

2.1. Rationale and Hypotheses

Overall, we hypothesized that ResT and TelA participate in a similar reaction pathway for telomere resolution, based on the results of the biochemical and crystallography information on these two enzymes' pre- and post-cleavage steps. For instance, by creating an underwound pre-cleavage intermediate that enables DNA cleavage, both enzymes ensure the reaction proceeds in a forward direction. DNA cleavage from this underwound intermediate ensures strand ejection and prevents the reformation of the substrate DNA. The refolding hairpin is stabilized by cross-axis DNA contacts and protein-DNA contacts. Finally, the refolding hairpin is tested for proper base pairing to ensure hairpins are only formed from *bona fide* replicated telomeres (*rTels*). In this study we characterize a series of TelA variants expected to play a role in forming/stabilizing a pre-cleavage intermediate, similar to that seen for ResT. To do this we characterized these variants using missing base and mismatch modified substrates that mimic the hypothesized substrate DNA unwinding. Mismatches break base pairing without removing bases from the duplex DNA and aid DNA melting, bending and other deformations of the double helix. Missing base modifications have the effects of removing base pairing and stacking partners, which causes the double helix to become unstable to promote the flexibility of DNA for unwinding, twisting and bending. Additionally, missing base changes can eliminate crucial interactions between an enzyme and a substrate that are necessary for the reaction. The expectation was that if a pre-cleavage intermediate features DNA unwinding between the scissile phosphates that the mismatch and missing base substrates would rescue the activity of the variants to allow DNA cleavage and hairpin telomere formation.

Specifically, we hypothesize that:

1) Telomere resolution by TelA progresses forwards via a pre-cleavage unwinding of the DNA between the scissile phosphates.

2) That this underwound pre-cleavage intermediate is promoted/stabilized by interactions with conserved TelA residues similar to those found in ResT used for this role.

2.2. Objectives

1. To mutate residues in TelA homologous in ResT implicated in creating/stabilizing the underwound pre-cleavage intermediate.
2. To mutate residues in TelA shown in the TelA-hp structure that interact with bases in the hp turnaround.
3. To test these TelA variants for a defect in telomere resolution.
4. To verify that these variants are otherwise functional for their other expected activities (test for *rTel* binding and annealing activities).
5. To rescue the telomere resolution defect of these variants with substrate modifications that mimic substrate unwinding between the scissile phosphates of the *rTel* substrate (mismatches, missing bases).

3. Materials and Methods

3.1 DNA cloning and assembly

3.1.1. A synthetic TelA gene codon optimized for expression in *E. coli* and construction of the TelA variants

The plasmid, pEKK394 (Figure 3.1), was constructed previously in the Kobryn's lab by obtaining a codon-optimized synthetic gene bounded by NdeI and BamHI sites for TelA from Integrated DNA Technologies (IDT). The codon optimized synthetic gene was cloned into the NdeI/BamHI digested pET15b vector by excising the gene with NdeI/BamHI. This allowed for the overexpression of a 6X His-tagged TelA in *E. coli*. Using the primers listed in Table 1 all TelA variants were produced by site-directed mutagenesis using pEKK394 as the template DNA. The parental DNA was then digested with DpnI. The remaining, mutagenized DNA was transformed into the NEB5α strain of *E. coli*. After DNA sequencing verification, each plasmid was transferred into the Rosetta (DE3) pLysS expression strain. Names were given to each plasmid; the resulting plasmid strains archived in NEB5α and the expression strains are listed in Table 2.

```
   1 catatgctggcggccaagcgtaagacaaaaacgccagtgttagtggaacgtatcgaccaattcgtcggtcaaattaaagaa 81
   1    M  L  A  A  K  R  K  T  K  T  P  V  L  V  E  R  I  D  Q  F  V  G  Q  I  K  E   27

  82 gccatgaaatcggacgatgctagtcgcaatcgcaaaatccgtgatctgtgggatgcggaggtgcgctatcatttcgacaac 162
  28 A  M  K  S  D  D  A  S  R  N  R  K  I  R  D  L  W  D  A  E  V  R  Y  H  F  D  N   54

 163 ggtcgtactgaaaagaccttggagttatacattatgaaatatcgtaatgcattaaaagccgaatttggacccaagtcaaca 243
  55 G  R  T  E  K  T  L  E  L  Y  I  M  K  Y  R  N  A  L  K  A  E  F  G  P  K  S  T   81

 244 ccgctggctatctgtaatatgaagaagttgcgcgagcgcctgaacacatatattgcacgtggcgattatcccaaaaccgga 324
  82 P  L  A  I  C  N  M  K  K  L  R  E  R  L  N  T  Y  I  A  R  G  D  Y  P  K  T  G   108

 325 gtggcgacctctatcgttgaaaagatcgagcgtgccgagttcaataccgcgggccgtaaacctacagttttattgcgtatc 405
 109 V  A  T  S  I  V  E  K  I  E  R  A  E  F  N  T  A  G  R  K  P  T  V  L  L  R  I   135

 406 gcagacttcattgctgcaatgaacggtatggatgctaaacaagacatgcaggccctttgggacgccgaaattgctattatg 486
 136 A  D  F  I  A  A  M  N  G  M  D  A  K  Q  D  M  Q  A  L  W  D  A  E  I  A  I  M   162

 487 aacggccgtgctcagacaactatcatctcctacattacaaaataccgcaatgcgattcgcgaagcttttggggacgaccac 567
 163 N  G  R  A  Q  T  T  I  I  S  Y  I  T  K  Y  R  N  A  I  R  E  A  F  G  D  D  H   189

 568 ccaatgttgaaaattgccactggcgacgctgctatgtacgacgaagctcgtcgtgttaagatggaaaaaatcgcgaataaa 648
 190 P  M  L  K  I  A  T  G  D  A  A  M  Y  D  E  A  R  R  V  K  M  E  K  I  A  N  K   216

 649 cacggtgcacttatcacgtttgaaaattatcgccaggtcctgaaaatctgcgaggattgcttgaaaagctccgacccactt 729
 217 H  G  A  L  I  T  F  E  N  Y  R  Q  V  L  K  I  C  E  D  C  L  K  S  S  D  P  L   243

 730 atgatcgggattggccttattgggatgacggggcgtcgcccctacgaagtctttactcaagctgagtttagtccagctccg 810
 244 M  I  G  I  G  L  I  G  M  T  G  R  R  P  Y  E  V  F  T  Q  A  E  F  S  P  A  P   270

 811 tacggaaaaggggtatcgaagtggtcgatccttttaacggacaggccaagactaagcaaggtgagggaacgaagtttggg 891
 271 Y  G  K  G  V  S  K  W  S  I  L  F  N  G  Q  A  K  T  K  Q  G  E  G  T  K  F  G   297

 892 atcacgtacgaaatccctgtcttgacccgctcagaaactgtccttgccgcctacaagcgcctgcgtgaaagtggccaaggc 972
 298 I  T  Y  E  I  P  V  L  T  R  S  E  T  V  L  A  A  Y  K  R  L  R  E  S  G  Q  G   324

 973 aagttgtggcatggcatgtcgatcgacgacttctcgtccgagacacgtctgctgttacgcgatacggtctttaacttgttt 1053
 325 K  L  W  H  G  M  S  I  D  D  F  S  S  E  T  R  L  L  L  R  D  T  V  F  N  L  F   351

1054 gaggatgtttggccgaaggaagagcttccgaaaccgtacggtcttcgccacttgtacgctgaagtggcataccataatttt 1134
 352 E  D  V  W  P  K  E  E  L  P  K  P  Y  G  L  R  H  L  Y  A  E  V  A  Y  H  N  F   378

1135 gcacctccgcacgtcactaaaaacagttatttcgcagccatcctgggccacaacaataatgacttagaaacaagtctttct 1215
 379 A  P  P  H  V  T  K  N  S  Y  F  A  A  I  L  G  H  N  N  N  D  L  E  T  S  L  S   405

1216 tacatgacttatacgctgcctgaggaccgtgataacgcactggcgcgcctgaagcgcaccaacgaacgcacattgcaacag 1296
 406 Y  M  T  Y  T  L  P  E  D  R  D  N  A  L  A  R  L  K  R  T  N  E  R  T  L  Q  Q   432

1297 atggccaccattgcgcccgtaagtcgtaaggggtaaggatcc 1338
```

Figure 3.1. The sequence of a synthetic TelA gene. The synthetic TelA gene sequence and related amino acid sequence are displayed and numbered, respectively. The stop codon inserted into the synthetic gene is indicated in red, and the restriction sites for NdeI and BamHI are bolded. IDT's blunt-end cloning of the artificial gene into pUCIDT followed by DNA sequencing gave confirmation of its validity. The figure was generated using https://www.bioinformatics.nl/cgibin/emboss/prettyseq

Table 3.1. Oligonucleotide primers for the construction of variants in TelA were used in this study.

Mutation	Oligo Number[1]	Primers Used for Mutagenesis[2]
Y201A	OGCB900	5′-GGCGACGCTGCTATGGCCGACGAAGCTCGTCGT-3′
	OGCB901	5'-ACGACGAGCTTCGTCGGCCATAGCAGCGTCGCC-3'
R205A	OGCB780	5′-TACGACGAAGCTGCGCGTGTTAAGATG-3′
	OGCB781	5′-CATCTTAACACGCGCAGCTTCGTCGTA-3′
K208A	OGCB839	5′-GAAGCTCGTCGTGTTGCGATGGAAAAAATCGCG-3′

	OGCB840	5'-CGCGATTTTTTCCATCGCAACACGACGAGCTTC-3'
K211A	OGCB915 OGCB 916	5'-CGTCGTGTTAAGATGGAAGCAATCGCGAATAAACACGGT-3' 5'-ACCGTGTTTATTCGCGATTGCTTCCATCTTAACACGACG-3'
K288A	OGCB 917 OGCB918	5'-GACAGGCCAAGACTGCGCAAGGTGAGGGAAC-3' 5′-CTGTCCGGTTCTGACGCGTTCCACTCCCTTG-3′
I297A	OGCB 910 OGCB 911	5′-GGAACGAAGTTTGGGGCCACGTACGAAATCCCT-3′ 5'-AGGGATTTCGTACGTGGCCCCAAACTTCGTTCC-3'
D398A	OGCB 878 OGCB 879	5′-CTGGGCCACAACAATAATGCGTTAGAAACAAGTCTTTCT-3′ 5'-AGAAAGACTTGTTTCTAACGCATTATTGTTGTGGCCCAG-3'
E400A	OGCB972 OGCB973	5′-GGCCACAACAATAATGACTTAGCAACAAGTCTTTCTTACATGGCC-3′ 5'-GGCCATGTAAGAAAGACTTGTTGCTAAGTCATTATTGTTGTGGCC-3'
T401A	OGCB841 OGCB842	5′-GGCCACAACAATAATGACTTAGAAGCGAGTCTTTCTTACATGA CTTATACG-3′ 5'-CGTATAAGTCATGTAAGAAAGACTCGCTTCTAAGTCATTATTG TTGTGGCC-3'
S404A	OGCB882 OGCB 883	5′-TGACTTAGAAACAAGTCTTGCGTACATGACTTATACGCTG-3′ 5'-GCAGCGTATAAGTCATGTACGCAAGACTTGTTTCTAAGTC-3'

[1]Top strand are shown on top. Bottom strands are shown on the bottom.
[2]The modified codons to obtain mutant protein are shown in red.

Table 3.2. Expression strain numbers for TelA and mutations.

TelA Variants	Archival Strain	Expression Strain
WT TelA	EKK394	EKK395
Y201A	EKK398	EKK455
R205A	EKK397	EKK403
K208A	EKK440	EKK442
K211A	EKK460	EKK464
K288A	EKK461	EKK465
I297A	EKK459	EKK463
D398A	EKK447	EKK452
E400A	EKK472	EKK480
T401A	EKK441	EKK443
S404A	EKK448	EKK453

3.2. TelA expression and purification

WT TelA, TelA (Y201A), TelA (R205A), TelA (K208A), and TelA (T401A) were previously overexpressed and purified in the lab. 500 mL of LB broth with 100 μg/mL ampicillin and 30 μg/mL chloramphenicol were used to express other TelAs. A seed culture of the expression strain was grown overnight at 37°C with 100 μg/mL ampicillin, 30 μg/mL chloramphenicol, and 1% glucose. 5 mL of the expression strain's overnight culture was used to seed the 500 mL culture, which was then grown at 37°C to an A_{600nm} of 0.4. After cooling the

temperature to 24°C for 20 minutes, 250 μM of isopropyl β-D-1-thiogalactopyranoside (IPTG) was added to induce the reaction for TelA (K288A), (D398A), and (S404A). 500 μM of IPTG was added for induction of strains TelA (I297A), (K211A), and (E400A). All the cultures were induced overnight at 24°C. Using the Bankhead and Chaconas freeze-thaw technique, a lysate of soluble proteins was made from the pelleted cells (Bankhead and Chaconas, 2004). The salt content of the lysate was reduced to 0.5 M by addition of Ni-load buffer lacking salt (50 mM NaH_2PO_4, 10 mM imidazole, 10% glycerol). The lysate was then loaded in a 10 mL Ni-NTA affinity column. 10 column volumes of 0.5 M NaCl Ni-wash buffer (50 mM NaH_2PO_4, 20 mM imidazole, and 10% glycerol) were used to wash the column. To elute TelA, 15 mL of 0.5 M NaCl Ni-elution buffer (50 mM NaH_2PO_4, 400 mM imidazole, and 10% glycerol) were divided to 1 mL aliquots. 15% SDS polyacrylamide gel electrophoresis (PAGE) with a 5% stacking gel was used to identify the peak fractions, and the results were pooled together. The combined Ni-elutions were diluted to a salt concentration of 0.25 M NaCl in HG buffer with no salt (25 mM 4-(2-hydroxyethyl)-1-piperazineethanesulfonic acid (HEPES) [pH 7.6], 0.2 mM EDTA, and 10% glycerol), and then loaded to a 6 mL Heparin-Sepharose (HS) CL6B column. 10 column volumes of 0.25 M NaCl HG and 2 column volumes of 0.35 M NaCl HG were used to wash the HS column. With 5 mL of 0.5 M NaCl HG and 10 mL of 1.5 M NaCl HG in 1.5 mL fractions, TelA was eluted from the HS column. The fractions were tested for nuclease activity assay with 25 mM HEPES, 1 mM Dithiothreitol (DTT), 2 mM $MgCl_2$, 100 μg/mL bovine serum albumin (BSA), 50 mM NaCl, 15 nM of radiolabelled ssDNA and 0.5 μL of each fraction incubated at 37°C for 1 hour. 8 μL of SDS loading dye to a 1X final concentration (1X SDS load dye includes 20 mM EDTA, 3.2% glycerol, 0.1% SDS, and 0.0024% bromophenol blue) added/ tube. 12 μL of samples were loaded to 8% PAGE, 1X Tris-acetate EDTA (TAE), and 0.1% SDS gels, they were all electrophoresed at 13 V/cm for 1 hour. Gels were dried and exposed to phosphor-imaging screens for visualization with phosphor-imager ‘Typhoon FLA 7000’. Nuclease-free peak fractions from 0.5 M and 1.5 M NaCl HG fractions were pooled separately to produce 2 versions of each prep stored in different buffers. Where possible, preps stored in HG 0.5M NaCl were used. To determine the concentration of each purified protein, Bio-Rad's protein assay dye reagent was used (Bradford assay).

3.3. Substrate assembly

3.3.1. Oligonucleotide substrate assembly

3 μM of substrate oligonucleotides were 5'- ^{32}P endlabeled with 4 units of T4 polynucleotide kinase (PNK) and 66 nM [γ-^{32}P] ATP at 37°C for 1 hour to produce the substrates. The oligonucleotides were then annealed by putting reactions into a boiling water bath and allowed to slowly cool to room temperature overnight in a buffer containing 25 mM (HEPES) pH 7.6, 0.1 mM EDTA, and 50 mM NaCl. The oligonucleotides employed for the various substrates are listed in Table 3 in detail.

Table 3.3. Oligonucleotides were employed to produce the substrate in this study.

Oligo number	Oligo Sequence[1, 2]	Use
OGCB664	5′-GGAAGCGATAAAACTCTGCAGGTTGGATACGCCAA-3′	35 nt; for nuclease assay
OGCB763	5′-gatcCATAATAACAATAT-3′	18 nt top strand; for TelA half-site cleavage substrate, annealed with 865, 979, 980 and 981
OGCB827	5′-gatcCCTCTAACCATTGCGCGATCGATCATAATA ACAATATCATGATATTGTTATTGTAATCGATCGCGGATC CCGGGCGTAGCCACGTAGGTA-3′	94 nt top strand of asymmetric TelA; annealed with 828
OGCB828	5′-gatcTACCTACGTGGCTACGCCCGGGATCCGCGA TCGATTACAATAACAATATCATGATATTGTTATTATGAT CGATCGCGCAATGGTTAGAGG-3′	94 nt bottom strand of asymmetric TelA; annealed with 827
OGCB865	5′-TCATGATATTGTTATTATG-3′	19 nt top strand; for TelA half-site cleavage substrate, annealed with 763
OGCB886	5′-gatcCCTCTAACCATTGCGCGATCGATCATAATA ACAATA-3′	40 nt, left top strand +0N of TelA *rTel*; annealed with 887 and 828
OGCB887	5′-TCATGATATTGTTATTGTAATCGATCGCGGATCC CGGGCGTAGCCACGTAGGTA-3′	54 nt, right top strand +0N of TelA *rTel*; annealed with 886 and 828
OGCB888	5′-gatcCCTCTAACCATTGCGCGATCGATCATAATA ACAATAT-3′	41 nt, left top strand +1N of TelA *rTel*; annealed with 889 and 828
OGCB889	5′-CATGATATTGTTATTGTAATCGATCGCGGATCCC GGGCGTAGCCACGTAGGTA-3′	53 nt, right top strand +1N of TelA *rTel*; annealed with 888 and 828
OGCB890	5′-gatcCCTCTAACCATTGCGCGATCGATCATAATA ACAATATC-3′	42 nt, left top strand +2N of TelA *rTel*; use with 891 and 828

OGCB891	5′-ATGATATTGTTATTGTAATCGATCGCGGATCCCG GGCGTAGCCACGTAGGTA-3′	52 nt, right top strand +2N of TelA *rTel*; use with 890 and 828
OGCB892	5′-gatcCCTCTAACCATTGCGCGATCGATCATAATA ACAATATCA-3′	43 nt, left top strand +3N of TelA *rTel*; use with 893 and 828
OGCB893	5′-TGATATTGTTATTGTAATCGATCGCGGATCCCGG GCGTAGCCACGTAGGTA-3′	51 nt, right top strand+ +3N of TelA *rTel*; use with 892 and 828
OGCB894	5′-gatcCCTCTAACCATTGCGCGATCGATCATAATA ACAATATCAT-3′	44 nt, left top strand +4N of TelA *rTel*; use with 895 and 828
OGCB895	5′-GATATTGTTATTGTAATCGATCGCGGATCCCGGG CGTAGCCACGTAGGTA-3′	50 nt, right top strand +4N of TelA *rTel*; use with 894 and 828
OGCB896	5′-gatcCCTCTAACCATTGCGCGATCGATCATAATA ACAATATCATG-3′	45 nt, left top strand +5N of TelA *rTel*; use with 897 and 828
OGCB897	5′-ATATTGTTATTGTAATCGATCGCGGATCCCGGGC GTAGCCACGTAGGTA-3′	49 nt, right top strand +5N of TelA *rTel*; use with 896 and 828
OGCB898	5′-GGTCTCTCTTGTTAGACCAGGTCGAGCCCGGGAG CTCTCTGGCTAGCAAGGAACCC-3′	HIV TAR sense TAR (+); use with 899 for annealing structured DNA positive control
OGCB899	5′-GGGTTCCTTGCTAGCCAGAGAGCTCCCGGGCTCG ACCTGGTCTAACAAGAGAGACC-3′	HIV TAR sense TAR (-); use with 898 for annealing structured DNA positive control
OGCB919	5′-gatcCCTCTAACCATTGCGCGATCGATCATAATA ACAATACCATGATATTGTTATTGTAATCGATCGCGGATC CCGGGCGTAGCCACGTAGGTA-3′	1 mismatch top strand; annealed with 920; based on 827/828 *rTel*
OGCB920	5′-gatcTACCTACGTGGCTACGCCCGGGATCCGCGA TCGATTACAATAACAATACCATGATATTGTTATTATGAT CGATCGCGCAATGGTTAGAGG-3′	1 mismatch bottom strand; annealed with 919; based on 827/828 *rTel*
OGCB921	5′-gatcCCTCTAACCATTGCGCGATCGATCATAATA ACAATACCATGGTATTGTTATTGTAATCGATCGCGGATC CCGGGCGTAGCCACGTAGGTA-3′	1 mutant top strand; annealed with 922; based on 827/828 *rTel*
OGCB922	5′-gatcTACCTACGTGGCTACGCCCGGGATCCGCGA TCGATTACAATAACAATACCATGGTATTGTTATTATGAT CGATCGCGCAATGGTTAGAGG-3′	1 mutant bottom strand; annealed with 921; based on 827/828 *rTel*
OGCB923	5′-gatcCCTCTAACCATTGCGCGATCGATCATAATA ACAATATTATGATATTGTTATTGTAATCGATCGCGGATC CCGGGCGTAGCCACGTAGGTA-3′	2 mismatch top strand; annealed with 924; based on 827/828 *rTel*
OGCB924	5′-gatcTACCTACGTGGCTACGCCCGGGATCCGCGA TCGATTACAATAACAATATTATGATATTGTTATTATGAT CGATCGCGCAATGGTTAGAGG-3′	2 mismatch bs; annealed with 923; based on 827/828 *rTel*

OGCB925	5′-gatcCCTCTAACCATTGCGCGATCGATCATAATA ACAATATTATAATATTGTTATTGTAATCGATCGCGGATC CCGGGCGTAGCCACGTAGGTA-3′	2 mutant top strand; annealed with 926; based on 827/828 *rTel*
OGCB926	5′-gatcTACCTACGTGGCTACGCCCGGGATCCGCGA TCGATTACAATAACAATATTATAATATTGTTATTATGAT CGATCGCGCAATGGTTAGAGG-3′	2 mutant top strand; annealed with 925; based on 827/828 *rTel*
OGCB927	5′-gatcCCTCTAACCATTGCGCGATCGATCATAATA ACAATATCTTGATATTGTTATTGTAATCGATCGCGGATC CCGGGCGTAGCCACGTAGGTA-3′	3 mismatch top strand; annealed with 928; based on 827/828 *rTel*
OGCB928	5′-gatcTACCTACGTGGCTACGCCCGGGATCCGCGA TCGATTACAATAACAATATCTTGATATTGTTATTATGAT CGATCGCGCAATGGTTAGAGG-3′	3 mismatch bottom strand; annealed with 927; based on 827/828 *rTel*
OGCB929	5′-gatcCCTCTAACCATTGCGCGATCGATCATAATA ACAATATCTAGATATTGTTATTGTAATCGATCGCGGATC CCGGGCGTAGCCACGTAGGTA-3′	3 mutant top strand; annealed with 930; based on 827/828 *rTel*
OGCB930	5′-gatcTACCTACGTGGCTACGCCCGGGATCCGCGA TCGATTACAATAACAATATCTAGATATTGTTATTATGAT CGATCGCGCAATGGTTAGAGG-3′	3 mutant top strand; annealed with 929; based on 827/828 *rTel*
OGCB931	5′-gatcCCTCTAACCATTGCGCGATCGATCATAATA ACAATATCACGATATTGTTATTGTAATCGATCGCGGATC CCGGGCGTAGCCACGTAGGTA-3′	4 mismatch top strand; annealed with 932; based on 827/828 *rTel*
OGCB932	5′-gatcTACCTACGTGGCTACGCCCGGGATCCGCGA TCGATTACAATAACAATATCACGATATTGTTATTATGAT CGATCGCGCAATGGTTAGAGG-3′	4 mismatch bottom strand; annealed with 931; based on 827/828 *rTel*
OGCB933	5′-gatcCCTCTAACCATTGCGCGATCGATCATAATA ACAATATCGCGATATTGTTATTGTAATCGATCGCGGATC CCGGGCGTAGCCACGTAGGTA-3′	4 mutant top strand; annealed with 934; based on 827/828 *rTel*
OGCB934	5′-gatcTACCTACGTGGCTACGCCCGGGATCCGCGA TCGATTACAATAACAATATCGCGATATTGTTATTATGAT CGATCGCGCAATGGTTAGAGG-3′	4 mutant bottom strand; annealed with 935; based on 827/828 *rTel*
OGCB935	5′-gatcCCTCTAACCATTGCGCGATCGATCATAATA ACAATATCATCATATTGTTATTGTAATCGATCGCGGATC CCGGGCGTAGCCACGTAGGTA-3′	5 mismatch top strand; annealed with 936; based on 827/828 *rTel*
OGCB936	5′-gatcTACCTACGTGGCTACGCCCGGGATCCGCGA TCGATTACAATAACAATATCATCATATTGTTATTATGAT CGATCGCGCAATGGTTAGAGG-3′	5 mismatch bottom strand; annealed with 935; based on 827/828 *rTel*
OGCB937	5′-gatcCCTCTAACCATTGCGCGATCGATCATAATA ACAATATGATCATATTGTTATTGTAATCGATCGCGGATC CCGGGCGTAGCCACGTAGGTA-3′	5 mutant top strand; annealed with 938; based on 827/828 *rTel*
OGCB938	5′-gatcTACCTACGTGGCTACGCCCGGGATCCGCGA TCGATTACAATAACAATATGATCATATTGTTATTATGAT CGATCGCGCAATGGTTAGAGG-3′	5 mutant bottom strand; annealed with 937; based on 827/828 *rTel*
OGCB939	5′-gatcCCTCTAACCATTGCGCGATCGATCATAATA ACAATATCATGTTATTGTTATTGTAATCGATCGCGGATC CCGGGCGTAGCCACGTAGGTA-3′	6 mismatch top strand; annealed with 940; based on 827/828 *rTel*

OGCB940	5′-gatcTACCTACGTGGCTACGCCCGGGATCCGCGA TCGATTACAATAACAATATCATGTTATTGTTATTATGAT CGATCGCGCAATGGTTAGAGG-3′	6 mismatch bottom strand; annealed with 939; based on 827/828 *rTel*
OGCB941	5′-gatcCCTCTAACCATTGCGCGATCGATCATAATA ACAATAACATGTTATTGTTATTGTAATCGATCGCGGATC CCGGGCGTAGCCACGTAGGTA-3	6 mutant top strand; annealed with 942; based on 827/828 *rTel*
OGCB942	5′-gatcTACCTACGTGGCTACGCCCGGGATCCGCGA TCGATTACAATAACAATAACATGTTATTGTTATTATGAT CGATCGCGCAATGGTTAGAGG-3′	6 mutant top strand; annealed with 941; based on 827/828 *rTel*
OGCB945	5′-gatcCCTCTAACCATTGCGCGATCGATCATAATA ACAATATCAGGATATTGTTATTGTAATCGATCGCGGATC CCGGGCGTAGCCACGTAGGTA-3′	4 mismatch G top strand; annealed with 946; based on 827/828 *rTel*
OGCB946	5′-gatcTACCTACGTGGCTACGCCCGGGATCCGCGA TCGATTACAATAACAATATCACGATATTGTTATTATGAT CGATCGCGCAATGGTTAGAGG-3′	4 mismatch G bottom strand; annealed with 945; based on 827/828 *rTel*
OGCB947	5′-gatcCCTCTAACCATTGCGCGATCGATCATAATA ACAATATCCGGATATTGTTATTGTAATCGATCGCGGATC CCGGGCGTAGCCACGTAGGTA-3′	4 mutant G top strand; annealed with 948; based on 827/828 *rTel*
OGCB948	5′-gatcTACCTACGTGGCTACGCCCGGGATCCGCGA TCGATTACAATAACAATATCCGGATATTGTTATTATGAT CGATCGCGCAATGGTTAGAGG-3′	4 mutant G bottom strand; use with 947; based on 827/828 *rTel*
OGCB951	5′-gaCTCTAACCATTGCGCGATCGATCATAATAACA ATATCATGATATTGTTATTGTAATCGATCGCGGATCCCG GGCGTAGCCACGTAGGT-3′	Top strand, 90 nt version of 827/828 *rTel* parental for abasic *rTel*s; use with 952
OGCB952	5′-gaACCTACGTGGCTACGCCCGGGATCCGCGATCG ATTACAATAACAATATCATGATATTGTTATTATGATCGA TCGCGCAATGGTTAGAG-3′	ts 90 nt version of 827/828 *rTel* parental for abasic *rTel*s; use with 951
OGCB953	5′-gaCTCTAACCATTGCGCGATCGATCATAATAACA ATATCXTGATATTGTTATTGTAATCGATCGCGGATCCCG GGCGTAGCCACGTAGGT-3′	abasic 3 top strand; annealed with 954, based on 951/952 *rTel*
OGCB954	5′-gaACCTACGTGGCTACGCCCGGGATCCGCGATCG ATTACAATAACAATATCXTGATATTGTTATTATGATCGA TCGCGCAATGGTTAGAG-3′	abasic 3 bottom strand; annealed with 953, based on 951/952 *rTel*
OGCB955	5′-gaCTCTAACCATTGCGCGATCGATCATAATAACA ATATCAXGATATTGTTATTGTAATCGATCGCGGATCCCG GGCGTAGCCACGTAGGT-3′	abasic 4 top strand; annealed with 956, based on 951/952 *rTel*
OGCB956	5′-gaACCTACGTGGCTACGCCCGGGATCCGCGATCG ATTACAATAACAATATCAXGATATTGTTATTATGATCGA TCGCGCAATGGTTAGAG-3′	abasic 4 bottom strand; annealed with 955, based on 951/952 *rTel*
OGCB957	5′-gaCTCTAACCATTGCGCGATCGATCATAATAACA ATATCATGXTATTGTTATTGTAATCGATCGCGGATCCCG GGCGTAGCCACGTAGGT-3′	abasic 6 top strand; annealed with 958, based on 951/952 *rTel*
OGCB958	5′-gaACCTACGTGGCTACGCCCGGGATCCGCGATCG ATTACAATAACAATATCATGXTATTGTTATTATGATCGA TCGCGCAATGGTTAGAG-3′	abasic 6 bottom strand; use with 957, based on 951/952 *rTel*
OGCB966	5′-gaCTCTAACCATTGCGCGATCGATCATAATAACA ATATXATGATATTGTTATTGTAATCGATCGCGGATCCCG GGCGTAGCCACGTAGGT-3′	abasic 2 top strand; annealed with 967; based on 951/952 *rTel*

OGCB967	5′-gaACCTACGTGGCTACGCCCGGGATCCGCGATCG ATTACAATAACAATATXATGATATTGTTATTATGATCGA TCGCGCAATGGTTAGAG-3′	abasic 2 bottom strand; annealed with 967; based on 951/952 *rTel*
OGCB968	5′-gaCTCTAACCATTGCGCGATCGATCATAATAACA ATATCATXATATTGTTATTGTAATCGATCGCGGATCCCG GGCGTAGCCACGTAGGT-3′	abasic 5 top strand; use with 969, based on 951/952 *rTel*
OGCB969	5′-gaACCTACGTGGCTACGCCCGGGATCCGCGATCG ATTACAATAACAATATCATXATATTGTTATTATGATCGA TCGCGCAATGGTTAGAG-3′	abasic 5 bottom strand; annealed with 969, based on 951/952 *rTel*
OGCB979	5′-TCATXATATTGTTATTATG-3′	abasic 5 bottom strand for half site to make hp; annealed with 763 top strand
OGCB980	5′-TCATGXTATTGTTATTATG-3′	abasic 6 bottom strand for half site to make hp; annealed with 763 top strand
OGCB981	5′-CCATGATATTGTTATTATG-3′	1 mismatch C bottom strand for half site with; annealed with 763
OGCB982	5'-gatcCTCTAACCATTGCGCGATCGATCATAATAA CAATATCATGATATTGTTATTGTAATCGATCGCGGATCC CGGGCGTAGCCACGTAG-3′	Top strand *rTel* based on 951 for directional cloning with BamHI and HindIII, used with 983
OGCB983	5'-agctCTACGTGGCTACGCCCGGGATCCGCGATCG ATTACAATAACAATATCATGATATTGTTATTATGATCGA TCGCGCAATGGTTAGAG-3′	bottom strand *rTel* based on 952 for directional cloning with BamHI and HindIII, used with 982
OGCB984	5′-gatcCTCTAACCATTGCGCGATCGATCATAATAA CAATACCATGATATTGTTATTGTAATCGATCGCGGATCC CGGGCGTAGCCACGTAG-3′	top strand of *rTel* with CCATGA overlap sequence and ends for BamHI-HindIII directional cloning; use with 985
OGCB985	5′-gatcCTACGTGGCTACGCCCGGGATCCGCGATCG ATTACAATAACAATATCATGGTATTGTTATTATGATCGA TCGCGCAATGGTTAGAG-3′	bottom strand of *rTel* with CCATGA overlap sequence and ends for BamHI-HindIII directional cloning; use with 984

[1] overhangs are shown in lowercase [2] X indicates an abasic site

3.3.2. Plasmid substrate for telomere resolution

Oligonucleotides OGCB982/983 with a parental *rTel* (5'-TCATGA-3') and OGCB984/985 with a mutant 1C *rTel* (5'-CCATGA-3') overlap (the sequence between the scissile phosphates) were used as a synthetic *rTels* to make plasmid substrates. The oligonucleotide *rTel*s were designed with overhangs compatible with directional BamHI/HindIII cloning. The assembled *rTel* was cloned into BamHI/ HindIII-digested pUC19.

After being validated by DNA sequencing, they were given the designations pEKK494 (parental) and pEKK495 (mutant 1C). pEKK494 and 495 were linearized by SspI so that they may be used in telomere resolution experiments.

3.4. Telomere resolution assays

3.4.1. Telomere resolution assays using oligonucleotide substrates

All oligonucleotide telomere resolution reactions were carried out in a buffer containing 25 mM HEPES (pH 7.6), 1 mM DTT, 4 mM $CaCl_2$, 100 μg/mL BSA, and 50 mM potassium glutamate. At 30°C or 12°C, 76 nM of TelA was incubated with 5 nM of the 5' radiolabelled substrate. Timecourse reactions were used to monitor the transformation of the substrate into two radiolabelled hairpins and/or cleavage products to obtain initial rates. A 60 μL and 120 μL reaction volume was used to set up the endpoint and timecourse reactions, respectively. 18 μL aliquots were taken out at the designated timepoints and mixed with SDS loading dye to a 1X final concentration. After loading all reaction aliquots onto 8% PAGE, 1X TAE, and 0.1% SDS gels, they were all electrophoresed at 13 V/cm for 2 hours. After drying, the gels were exposed to phosphor-imaging screens for documentation.

The results were analyzed using 'Quantity One software Bio-Rad'. Local background removal was used by boxing a region of the gel lacking bands as 'background'. The intensities of cleavage intermediate bands were added together as 'cleavage product' and hairpin and cleavage products were added together as 'total reaction'. The proportion of cleavage product and total reaction were calculated. To obtain the initial rate, the slope of the first plot points on graphs before it becomes non-linear were calculated and reaction statistics were generated with Prism's GraphPad.

3.4.2. Telomere resolution assays using plasmid substrates

All plasmid telomere resolution tests were carried out in a buffer containing 25 mM HEPES (pH 7.6), 1 mM DTT, 4 mM $CaCl_2$, 100 μg/mL BSA, and 50 mM potassium glutamate. At 30°C and 12°C, 1.75 μg/mL (1nM) of pEKK494 or pEKK495 linearized with SspI was incubated with 2 nM of TelA. Timecourse reactions were used to monitor the transformation of the substrate into two hairpins. A 100 μL reaction volume was used to set up the timecourses, and 18 μL aliquots were taken out at the designated timepoints and mixed with SDS loading

dye to a 1X final concentration. Samples were loaded to 0.8% agarose/ 1X TAE and run at 3.75 V/cm for 2 hours. The gels were visualized by 'Bio-Rad ChemiDoc System'. When the ability of TelA to act as a topoisomerase was tested supercoiled pEKK494 and pEKK495 were reacted as indicated above.

3.5. Electrophoretic mobility shift assays

To conduct binding reactions, TelA was incubated at 0°C for 20 minutes with 1 nM of its assembled and radiolabeled *rTel*. The binding buffer contained 25 mM HEPES (pH 7.6), 1 mM DTT, 4 mM $CaCl_2$, 100 μg/mL BSA, 50 mM potassium glutamate, 0.8 μg/mL of competitor DNA (pUC19), and 76 ng/mL heparin sulphate. After the loading dye (- SDS) was added at a final concentration of 1X, samples were loaded onto 6% PAGE/0.5X Tris Borate EDTA (TBE) gels and electrophoresed at 15 V/cm until the dye is around 1 cm from the bottom of the gel at 4°C. The gels were dried and exposed to phosphor-imaging screens for documentation.

3.6. ssDNA annealing assays

Annealing assays were performed in a solution consisting of 25 mM HEPES (pH 7.6), 1 mM DTT, 2 mM $CaCl_2$, 100 μg/mL BSA, and 50 mM potassium glutamate and 15 nM of the labeled reporter oligonucleotide (OGCB898*). To lower the spontaneous rate of annealing, reactions were put on ice for two minutes before adding 15 nM of the corresponding unlabeled complementary oligonucleotide (OGCB899) and 154 nM of TelA. Following the addition of TelA, the reactions were incubated at 30°C and 18 μL aliquots were taken at the indicated timepoints. To stop further annealing, these aliquots were then combined with SDS loading dye that had 0.3 μM of the unlabeled reporter oligonucleotide (OGCB898). After loading all annealing reactions to 8% PAGE, 1X TAE, and 0.1% SDS gels, they were all electrophoresed at 15 V/cm for 2 hours and 30 minutes. Gels were dried and exposed to phosphor-imaging screens for documentation.

3.7. Half-site hairpinning assays

Half-site hairpinning assays were performed in a buffer containing 25 mM HEPES (pH 7.6), 1 mM DTT, 4 mM $CaCl_2$, 100 μg/mL BSA, and 50 mM potassium glutamate. 5 nM

of the 5' radiolabelled substrate and 76 nM of TelA were incubated at 30 °C or 12 °C. The reactions were observed by timecourse reactions. The timecourses were set up in a 60 µL reaction volume, and at the specified timepoints, 18 µL aliquots were removed and mixed with 21 µL of Formamide dye (containing 80% Formamide, 10 mM EDTA, and 0.0024% bromophenol blue) and then with SDS loading dye to a 1X final concentration. The samples were boiled at 95°C for 5 minutes followed by 10 seconds of snap cooling on ice. This treatment denatures duplex DNA not containing a hairpin. All aliquots were loaded onto 8% PAGE, 1X TBE, 6 M Urea, and 0.1% SDS gels before being electrophoresed at 15 V/cm for 1 hour and 12 minutes. Gels were exposed to phosphor-imaging screens for documentation.

3.8. Telomere resolution assays visualized on alkaline agarose gels

Telomere resolution assays visualized on alkaline agarose gels were done in a buffer containing 25 mM HEPES (pH 7.6), 1 mM DTT, 4 mM $CaCl_2$, 100 µg/mL BSA, and 50 mM potassium glutamate. 8.3 µg/mL (4.7 nM) of the SspI linearized pEKK494 and 115 nM of TelA were incubated at 30 °C for the time specified in the figure. The endpoint reactions were set up in a 60 µL volume, and at the end of timepoints, 10 µL of alkaline dye (containing 300 mM NaOH, 6 mM EDTA, 18% (w/v) Ficoll, and 0.25% (w/v) xylene cyanol) were added to reaction tubes. Samples were loaded to 0.8% agarose/ 1X TAE gel/1x alkaline gel electrophoresis buffer (500 mM NaOH, 19 mM EDTA). Gels were run at 1.25 V/cm for 24 hours. Gels were neutralized by soaking in neutralizing buffer (1 mM Tris-Cl, 1.5 M NaCl) for 1 hour and 30 minutes prior to staining with 0.5 µg/mL ethidium bromide (30 minutes). The gels were visualized by 'Bio-Rad ChemiDoc System'.

3.9. CD spectroscopy

Circular dichroism (CD) spectroscopy is a rapid method for characterization of secondary structure of proteins. CD is described as the unequal absorption of left-handed and right-handed circularly polarized light between 190-250 nm. The asymmetric molecules and structural elements, absorb and reflect right- and left-handed circularly polarized light differently. The result of these differences makes CD spectroscopy a rapid method to evaluate the secondary structure and folding of proteins (Greenfield, 2007). The ideal buffer for CD spectroscopy should be transparent and without optically active material. The buffer we used

for protein purification contains high concentrations of salt and ring structures which have absorbance in the range of wavelength used in CD spectroscopy. To cutoff the buffer absorbance and the baseline of high-transparency quartz cuvettes (cells), 400µL of degassed 1.5 M NaCl HG buffer was used. In the 1.5 M NaCl HG buffer, 400 µL of 250 µg/mL of the TelAs CD spectra was measured with 'Applied Photophysics Chirascan CD Spectrometer'. Measurement was between 208 nm to 280 nm at 20°C.

4. Results

4.1. The rationale for the selection of TelA variants to examine

4.1.1. Performing an alignment to identify homologous residues to ResT

To characterize the residues hypothesized to be involved in stabilizing the pre-cleavage intermediate, we started with the homology of residues in TelA with the previous result of ResT's study (Figure 4.1). The previous studies on ResT have shown that the residues in the hairpin binding module and the catalytic domain, including Q161, V231, D328, and H334 are involved in stabilizing the pre-cleavage intermediate (Bankhead and Chaconas, 2004; Lucyshyn et al., 2015). TelA I297, D398, T401, and S404 align with the residues mentioned above. The homologous residues were identified in both the hairpin binding module and the catalytic domain.

Figure 4.1. The alignment of TelA and ResT sequences. The residues of interest are boxed in red and green. The green and red boxes indicate the residues in the hairpin binding module and catalytic domain, respectively. The black boxes indicate the identity, and the grey boxes indicate similarity.

4.1.2. Identifying residues based on base-specific interactions with the hp DNA

As mentioned before, the crystallography of TelA showed that TelA makes several interactions with the hairpin products and the refolding intermediate. We selected Y201, R205, K208, K211, K288, E400, and T401 for mutagenesis based on the interactions they make with the nucleotides or the backbone of the DNA between the scissile phosphates by direct or water-mediated interactions (Figure 4.2.; (Shi et al., 2013)). The 3D visualization of selected residues is shown in (Figure 4.3).

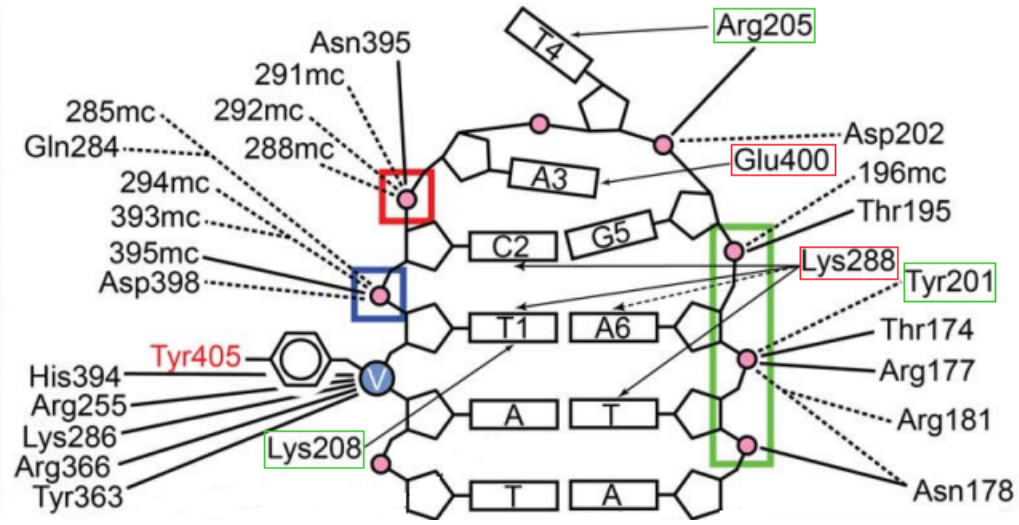

Figure 4.2. The schematic representation of the interaction between the amino acid residues of TelA and the hairpin products. Solid lines represent the direct interaction and dashed lines represent the indirect (water-mediated) interactions. mc stands for main chain (rather than the R group of the amino acid). The backbone of the residues makes the interaction with the base in those cases. The blue, green, and green boxes were to indicate the close-up views in the original figure (Shi et al., 2013). The thinner green and red boxes indicate the residues in the hairpin binding module and catalytic domain, respectively.

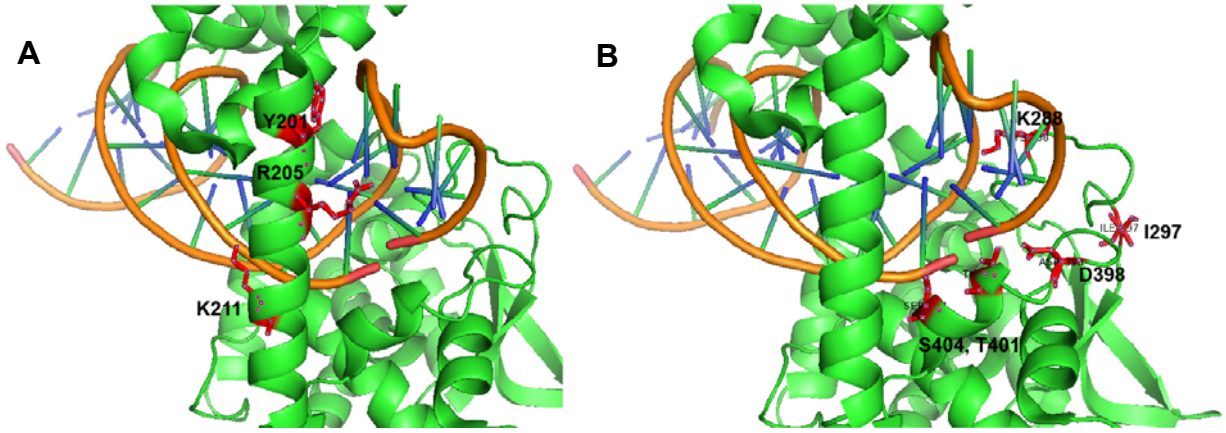

Figure 4.3. Structural view of residues of interest in TelA with the hp products. A) The interaction and the location of hp binding module with hp product. Selected residues are shown in red. **B)** The interaction and the location of catalytic domain with hp product. Selected residues are shown in red. Pymol software was used to generate the highlighted and labelled sidechains.

4.2. Results with WT TelA

4.2.1. Assays with substrates with mismatches between the scissile phosphates

As the first step to characterize the hypothesized pre-cleavage intermediate, we designed and used mismatch (MM) modifications between the scissile phosphates of the *rTel* substrate. MMs induce deformations and alterations in the structure and stability of the DNA helix (Rossetti et al., 2015). The hydrogen bonds between basepairs are disrupted in the MM sites; this helps the protein to melt and unwind the target site. MMs were symmetrically positioned on the top and bottom strands between the scissile phosphates and were named according to the changed position. A further set of control substrates was generated that restored base complementarity by introducing compensatory sequence changes on the opposing strand from the bases that introduced the mismatches. This set of substrates was called 'mutant *rTels* control'. By using the mutant *rTel* control, we could indicate whether any observed reaction stimulation or rescue of TelA variants was from the sequence change or the presence of the MM itself (Figure 4.4). We investigated TelA's telomere resolution activity with these substrates.

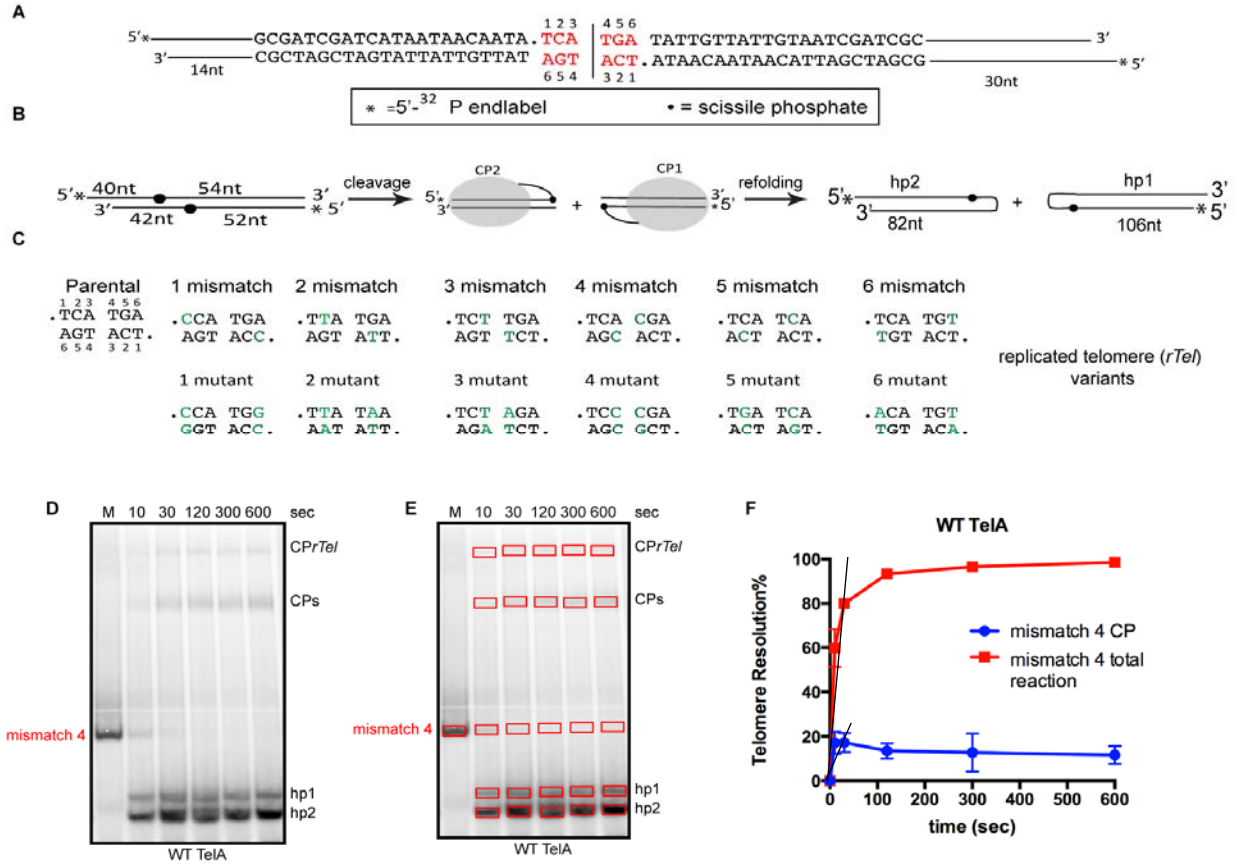

Figure 4.4. A representative example of the use of *rTels* with mismatch modifications between the scissile phosphates. A) The model *rTel* sequence used in this study. To facilitate the annealing rate of oligonucleotides into an *rTel* in preference to forming hairpins, asymmetric sequences were introduced on the left and right sides of *rTel.* Additionally, the asymmetry helps to differentiate between the two hairpin products (hp1 and hp2). The scissile phosphates are represented by dots. The red letters indicate the sequence of *rTel* between the scissile phosphates with nucleotide numbering indicated **B)** The schematic representation of different steps of telomere resolution reaction. CP and hp stand for cleavage product and hairpin, respectively. **C)** The sequence of mismatch modification between the scissile phosphates. The dots represent the position of scissile phosphate. The green letters represent the mismatch modification. **D)** A representative 8% PAGE, 1X TAE/0.1% SDS gel panel of a timecourse reaction of WT TelA with MM4 incubated at 30°C. The mobility of the substrate in the gel is represented by mismatch4; CP*rTel* marks the migration of a product that TelA has cleaved only one strand; CPs is gel migration of the cleavage products; hp1 and hp2 are the positions of the hairpin telomere products on the gel; M stands for mock protein-free reaction. **E)** Representative example of gel boxing for band intensity analysis to obtain the timecourse graphs and the initial rates derived from those timecourses. CP*rTel* and CPs were added together as the cleavage product and cleavage product with hp1 and hp2 as the total reaction. **F)** The % of cleavage products and total reaction *vs*. reaction time plot of telomere resolution reaction with WT TelA and MM4 at 30°C. The black lines represent the slope used to obtain the initial rate.

The reaction of WT TelA with parental *rTel* went straight to hairpin products and the cleavage products (CPs), the transient intermediate products where TelA cleaved the substrate and is covalently linked to the cleaved *rTel,* were not observed. However, WT TelA had

difficulties making hairpins with MMs without accumulation of CPs. On the other hand, the MM4 *rTel* greatly stimulated the reaction rate over that observed with the parental *rTel* (Figure 4.5). MM1 and mutant 1 were poor substrates for WT TelA indicating the importance of the identity of the base (T1) at this position.

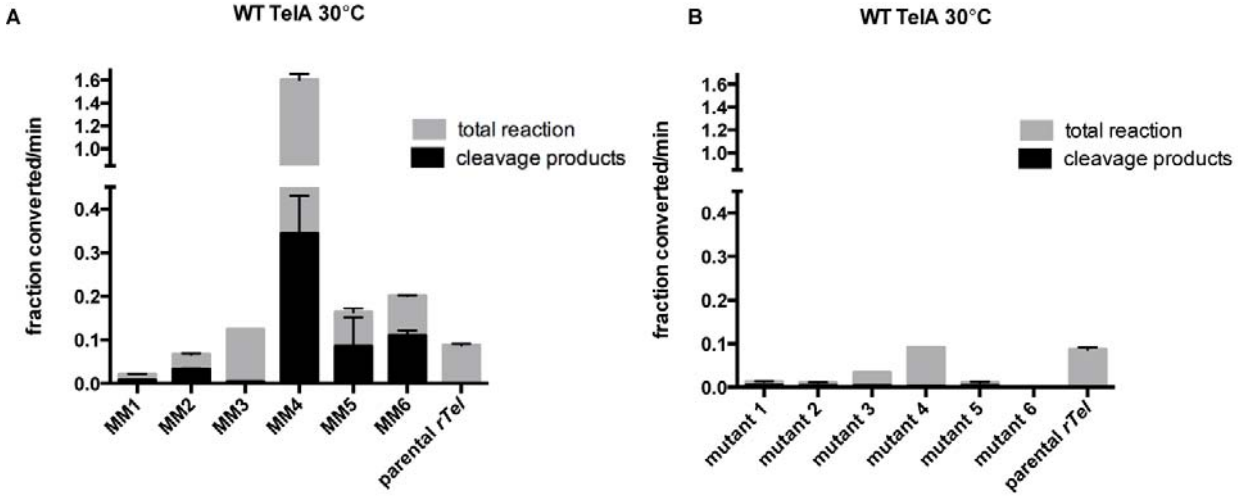

Figure 4.5. The summary of assays performed with WT TelA and mismatch substrate at 30°C. A) Comparison of the initial rates of cleavage product formation and the rate of the total reaction of the parental *rTel* and the substrates with mismatches. The initial rates are demonstrated as the fraction substrate converted/min (1.0 being 100% conversion). The mean and standard deviation of at least three separate replicates are displayed. The gray bars indicate the total reaction, and the black bars indicate the cleavage products. The discontinuous y-axis emphasizes that activity occurred from MM1 to 6, not only with MM4. **B)** The initial rates of mutant control *rTels* with WT TelA.

4.2.2. Assays with substrates with missing bases between the scissile phosphates

Another type of DNA distortion is often involved in reactions where DNA is melted; flipping bases out of the DNA double helix. Here the base is rotated toward an extra-helical location and may require stabilization by interaction with protein. A key example of enzyme stabilized baseflipping in the service of DNA hairpin formation is found in the case of DNA transposition by the Tn5 and Tn10 transposable elements. The crystal structure of the Tn5 transposition post-cleavage intermediate indicated that on the top strand of the transposon, a nucleotide is flipped out of the double helix and is stabilized by the transposase by a stacking interaction between the flipped base and aromatic enzyme sidechains (Ason and Reznikoff, 2002; Bhasin et al., 1999; Davies et al., 2000). The stacking interaction might also be involved in holding the melted strand of DNA during the reaction (Bischerour and Chalmers, 2007). By removing base pairing and base stacking partners, missing base modifications cause the double

helix to become destabilized (Vesnaver et al., 1989). Missing base modifications might also eliminate the crucial specific interactions between the DNA and the protein. Therefore, if the stabilized bases are present in an extrahelical conformation, missing base modifications might be able to partially substitute the unwinding/stabilizing role proposed for the considered residues when those residues are mutated. This approach was used to validate the base stacking interactions present in the Tn5 transpososome crystal structures (Bischerour and Chalmers, 2007; Kennedy et al., 1998; Pribil and Haniford, 2000). We designed the missing base (abasic) modifications in different positions of the *rTel* between the scissile phosphates (Figure 4.6). Results of assays with WT TelA and missing bases showed that the reaction was stimulated with abasic 5 with cleaved products accumulation, but WT TelA failed to make hairpins with abasic 2 and 6 (Figure 4.7). Contrary to the results obtained with the mismatch substrates, the abasic 3 and 4 were poor substrates indicating the importance of the presence of bases at these positions, notwithstanding the apparent need for these sequences to be melted for optimal rates of reaction.

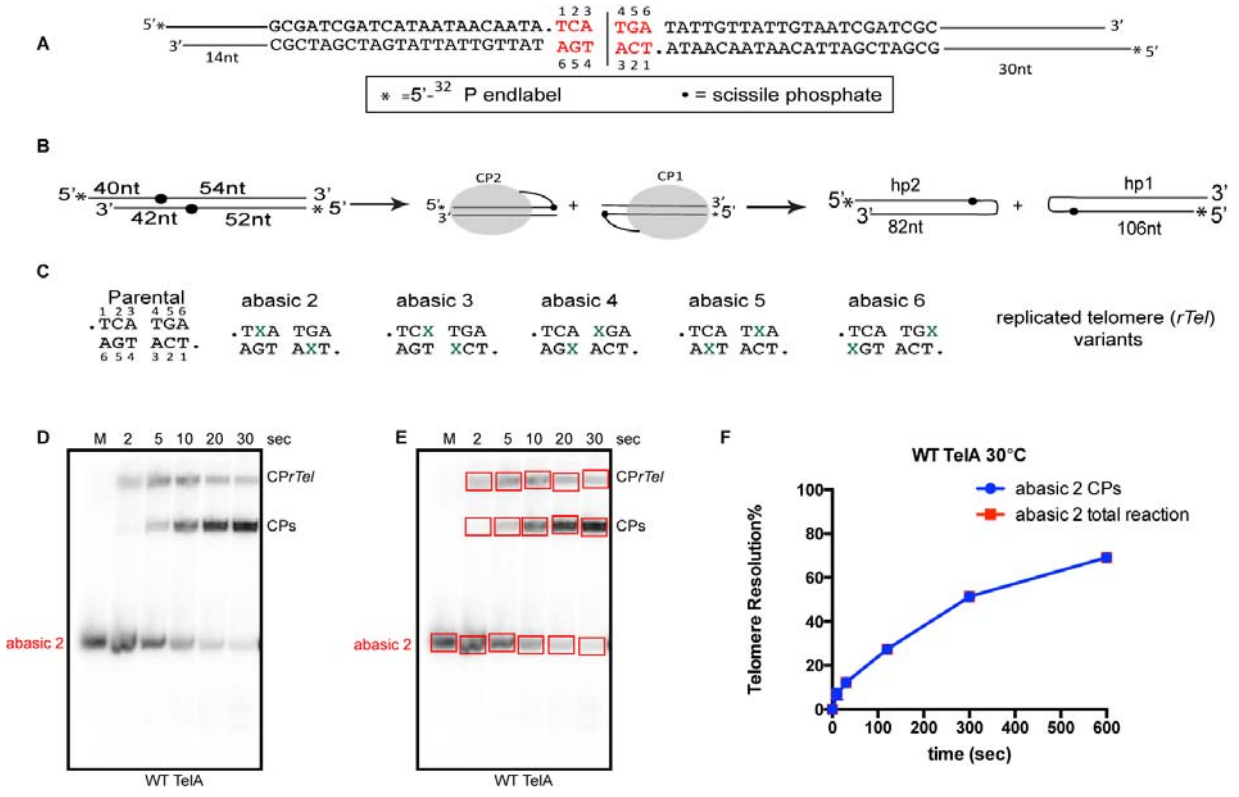

Figure 4.6. A representative example of the use of missing base modifications between the scissile phosphates. A) The model *rTel* sequence used in this study. **B)** The schematic representation of different steps of the telomere resolution reaction. CP and hp stand for cleavage products and hairpins,

respectively. **C)** The sequence of abasic modifications between the scissile phosphates. The dots represent the position of the scissile phosphates. The green X's represent the missing base modifications. **D)** A representative 8% PAGE/ 1X TAE/0.1% SDS gel panel of a timecourse reaction of WT TelA with abasic 2 incubated at 30°C. The mobility of the substrate in the gel is represented by abasic 2; the mobility of CP*rTel* and CPs are shown on the gel; M stands for mock protein-free reaction. **E)** A representative example of gel boxing for band intensity analysis to obtain the timecourse graphs and the initial rates derived from those timecourses. CP*rTel* and CPs were added together as the cleavage product, and since the reaction stuck as the cleavage product, the total reaction and cleavage product would be equal. **F)** The % of cleavage products and total reaction *vs.* reaction time plot of telomere resolution reaction with WT TelA and abasic 2 and 4 at 30°C. The black lines represent the slope used to obtain the initial rate.

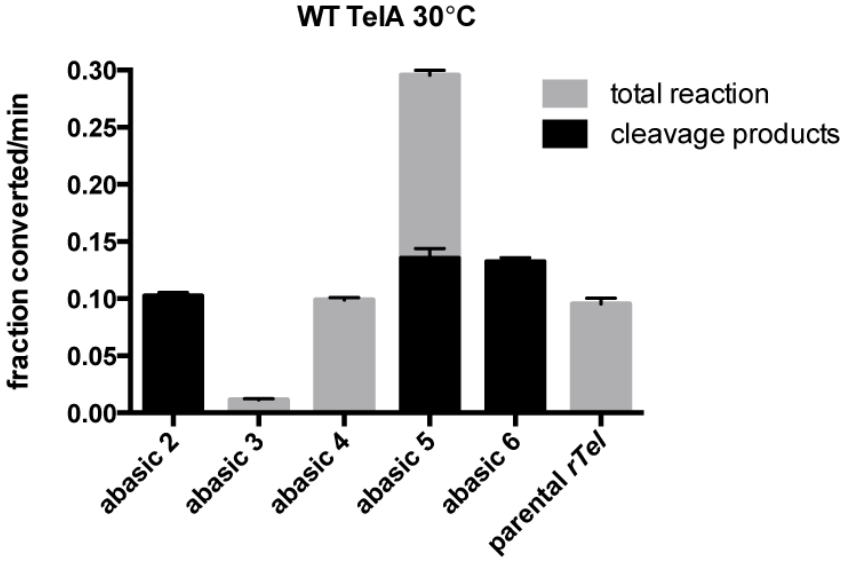

Figure 4.7. Summary of assays performed with WT TelA and the *rTels* with missing base modifications. Comparison of the initial rates of cleavage product formation and the rate of the total reaction of the parental *rTel* and the substrates with missing bases. The initial rates are demonstrated as the fraction substrate converted/min (1.0 being 100% conversion). The mean and standard deviation of at least three separate replicates are displayed. The gray bars indicate the total reaction and the black bars indicate cleavage product production.

4.2.3. Assays with *rTel* substrates with nicks between the scissile phosphates

Studies have shown that nick modifications increase DNA structural flexibility and can facilitate DNA bending (Koudelka et al., 1988; Li and McClure, 1998). Additionally, nick modifications promote base flipping and DNA unwinding at or near the nick site without removing the base. The use of the *rTel*s nicked at different positions between the scissile phosphates was hoped to add extra information on possible melting and base flipping. In addition, because nicks facilitate DNA bending, nicked *rTels* may also provide information on the degree to which DNA bending facilitates telomere resolution. To assess the reaction of nick modified substrates with WT TelA, we introduced the nick modifications on the top strand

between the scissile phosphates of the *rTel* (Figure 4.8b). After cleaving the nick *rTel*, CP1 would be stuck at this level and cannot go forward as the nicked part diffuses away (Figure 4.8a). We observed that WT TelA tolerated the nicked *rTel*s with the production of the expected CP*rTel*, CP1, and hp2 products.

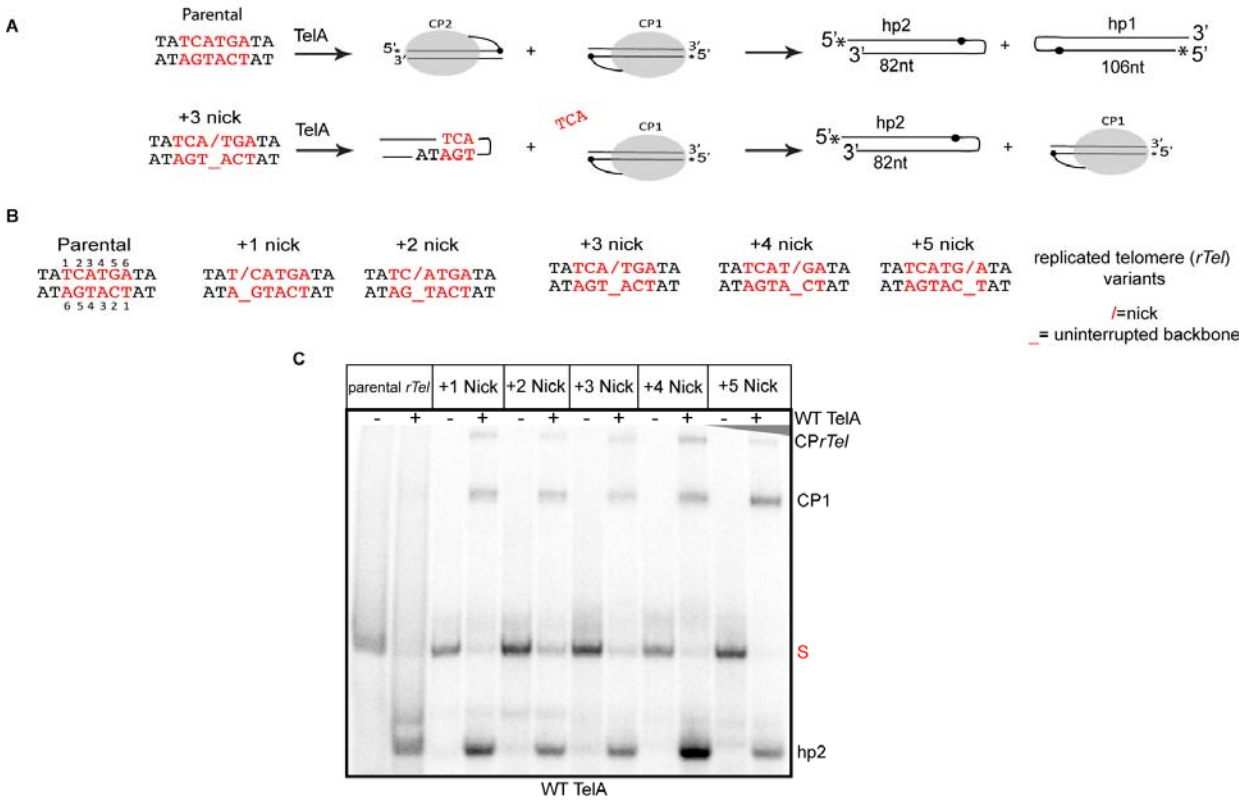

Figure 4.8. Summary of assays performed with WT TelA and *rTel* substrates with nick modifications. A) The schematic representation of different steps of telomere resolution with parental *rTel* and the +3 nick modification used as an example. CP and hp stand for cleavage products and hairpins, respectively. TelA monomer is stuck at the cleavage step and cannot go forward as the nick part of *rTel* diffuses away after the cleavage of the strands. The strand refolding step for hairpin formation can take place for the CP2 and produces hp2. **B)** The sequence of nick modifications between the scissile phosphate of *rTel*. The dots represent the position of scissile phosphates. The red color / indicates the nick on the top strand and the red color _ indicates the uninterrupted DNA backbone on the opposing strand. **C)** A representative 8% PAGE/ 1X TAE/0.1% SDS gel panel of the endpoint reactions of WT TelA with nick modification substrates incubated at 30°C for 10 minutes. The mobility of the substrate in the gel is represented by mismatch4; CP*rTel* marks the migration of a product that TelA has cleaved only the nicked strand; CP1 is gel migration of the cleavage product; hp2 is the position of the hairpin telomere product on the gel. + indicates the reactions incubated with protein; - indicates protein-free mock reactions.

4.2.4. Annealing assays

As mentioned before, a previous study on TelA showed that the TelA promotes annealing of ssDNA possessing complicated secondary structure and that the full-length enzyme is needed for optimal annealing rates (McGrath et al., 2021). We used an

oligonucleotide that mimics the positive sense strand of the HIV transactivational response element (TAR) for our annealing assays. The single-strand form of HIV TAR consists of a stem-loop structure with several bulges. Therefore, TelA would need to remove these structures to promote ssDNA annealing of this element to its complement (Figure 4.9a and b; (Lapadat-tapolsky et al., 1995)). We utilized this characteristic of TelA as one of the parameters to check our purified protein variants for relevant biochemical activities that require properly folded protein (Figure 4.9c).

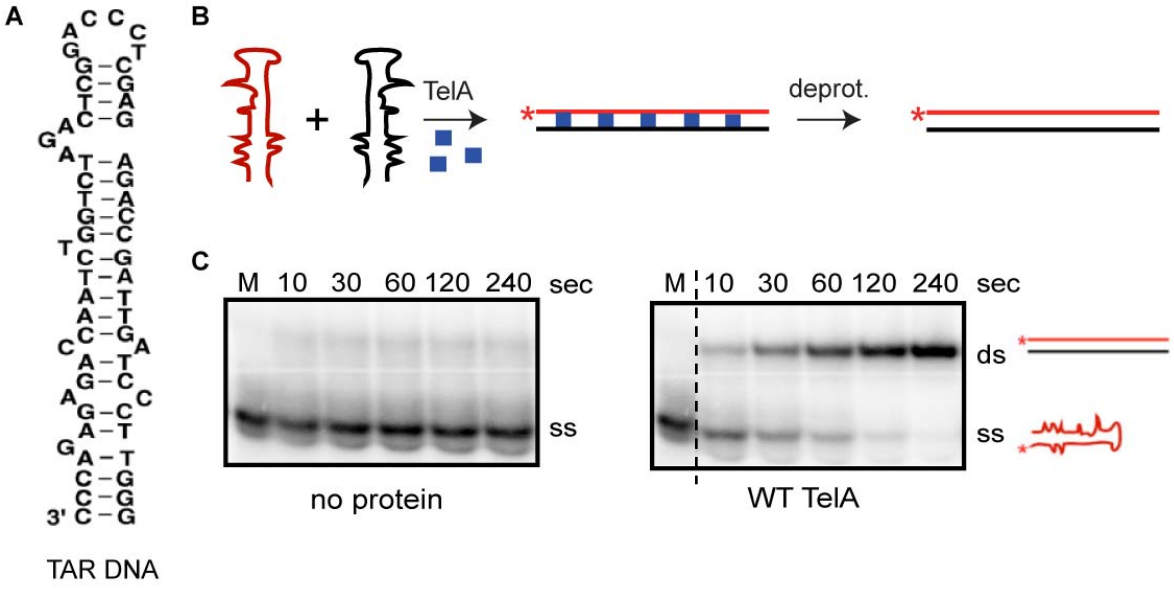

Figure 4.9. Annealing activity of WT TelA. A) A schematic model of the positive sense strand of the HIV transactivational response element (TAR) with its secondary structure. **B)** The schematic of the single-strand annealing activity of TelA with TAR oligonucleotides. The complementary strands are shown in red and black; the asterisk on the red strand indicates the 5'-endlabel on this strand. The blue squares indicate TelA (the schematic of the annealing reaction is from (McGrath et al., 2021). **C)** A representative 8% PAGE/ 1X TAE/ 0.1% SDS gel panels of timecourse reactions with the TAR oligonucleotides. The left panel is the assay without addition of TelA; the right panel is the assay with the addition of 154 nM of TelA. The gel mobility of 5'-^{32}P endlabeled TAR oligonucleotide is shown as ss, and the double-strand product is shown as ds. M stands for mock protein-free reaction. Irrelevant samples are removed. Displacement is indicated by dash line.

4.2.5. *rTel* binding assays

The electrophoretic mobility shift assay (EMSA) or band shift is an affinity assay used to investigate the ability of the proteins to bind to specific DNA sites. TelA's binding to the *rTel* sequence requires the participation of amino acid sidechains scattered throughout TelA (Shi et al., 2013). Therefore, EMSAs of TelA binding to an *rTel* substrate can be used as another indicator of proper folding of the TelA variants purified for this study (Figure 4.10).

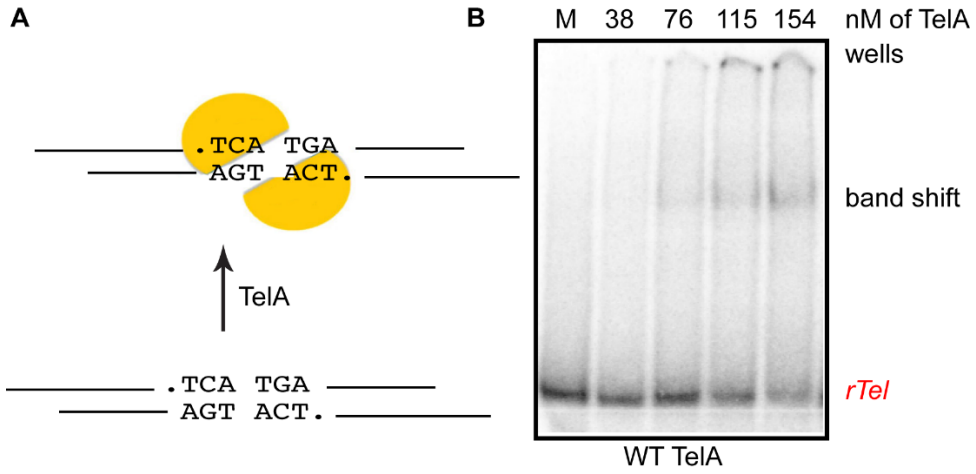

Figure 4.10. The EMSA assay of TelA binding to an *rTel*. A) The schematic representation of TelA binding to an *rTel* which causes the shift in gel mobility. **B)** A representative example of a 6% PAGE/ 0.5X TBE gel panel of endpoint reactions with titration of WT TelA and *rTel* incubated at 0°C for 20 minutes. Low incubation temperature prevented the conversion of the substrate into products. Band shift indicates gel mobility of the TelA bound to *rTel*; *rTel* in red color indicates the *rTel* substrate; M stands for mock protein-free reaction. Irrelevant samples are removed. Displacement is indicated by dash line.

4.3. Telomere resolution is cold-sensitive

At low temperatures, the efficiency of a DNA unwinding process is typically considerably reduced. Cold-sensitivity results from the reaction's reduced ability to provide energy for the DNA unwinding process. Mismatches and missing base modifications should reduce the cold-sensitivity of telomere resolution if it has an underwound but not yet cleaved intermediate as the base pairing between the cleavage sites is disrupted (Lucyshyn et al., 2015). Previous results with ResT showed a significant reduction of the cold-sensitivity of telomere resolution by the use of substrates with mismatches and missing bases (Lucyshyn et al., 2015). We tested the modified substrates with WT TelA at 30ºC *vs.* 12°C to assess the degree of cold-sensitivity of TelA promoted telomere resolution (Figure 4.11).

4.3.1. Attempt to rescue the cold-sensitivity of telomere resolution with mismatch substrates

The results with mismatch substrates showed that MM4 stimulated the reaction at 30°C but also rescued the cold-sensitivity of WT TelA, compared to the parental *rTel*. However, at 12°C WT TelA was inactive with MM1, almost inactive with MM6, and had a lower reaction rate with MM3 than with parental substrate. In addition, the reactions with MM5 and 6 stalled at the cleavage step (Figure 4.11). This represents a significant departure from the results with ResT. ResT showed significant rescue with MM4 and 5 (Lucyshyn et al., 2015). We inferred

that the hairpin formation step of telomere resolution in TelA may possess significant cold-sensitivity when substrates other than MM4 are employed. WT TelA was inactive with all mutant *rTel* substrates at 12°C, in contrast to 30°C.

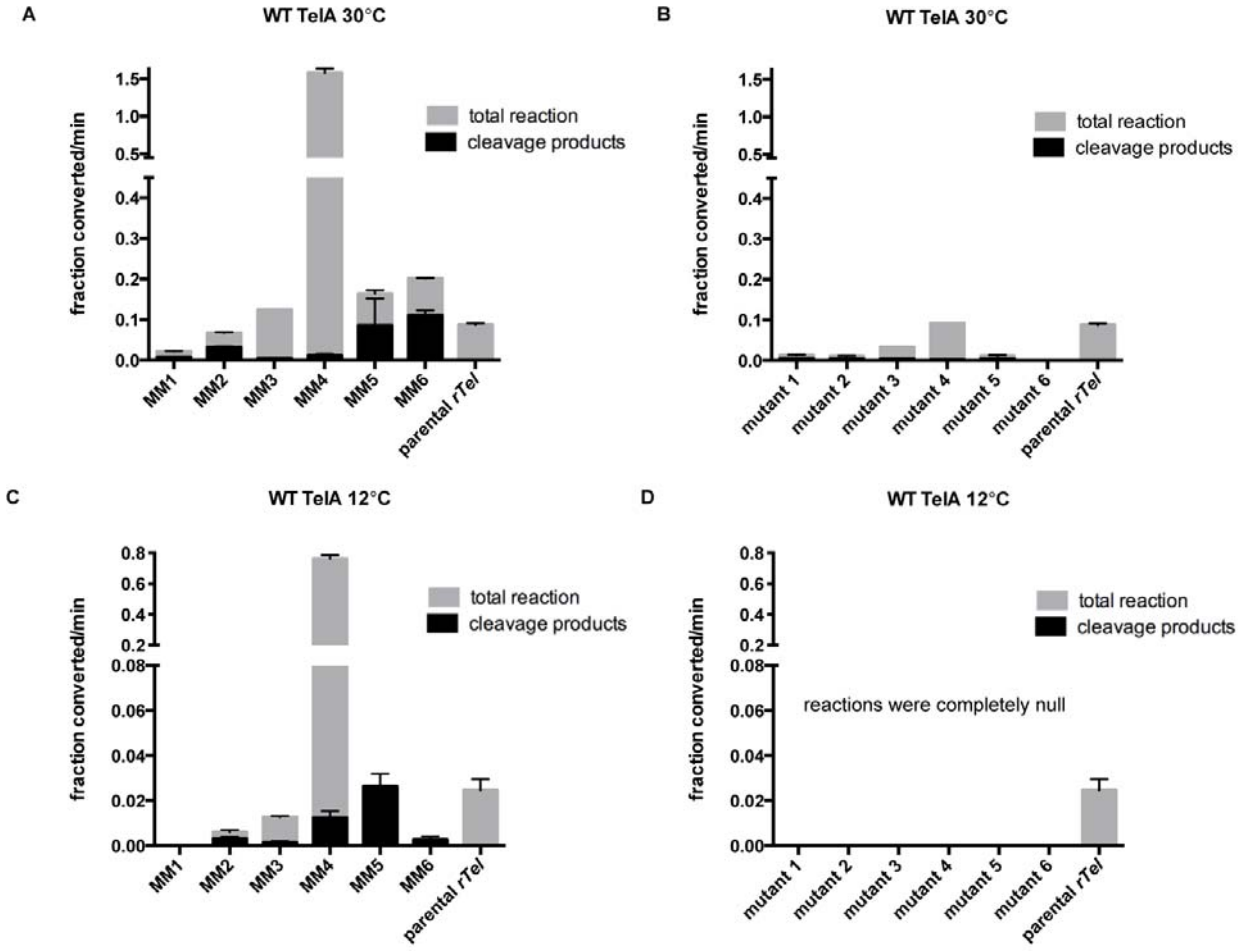

Figure 4.11. The summary of assays performed to rescue the cold-sensitivity of telomere resolution by the use of mismatch substrates. A) Comparison of the initial rates of cleavage product formation and the total reaction of the parental *rTel* and the mismatches substrates with WT TelA at 30°C. **B)** Comparison of the initial rate of control mutant *rTels* at 30°C. **C)** Comparison of the initial rates of cleavage product formation and the total reaction of the parental *rTel* and the mismatches substrates with WT TelA at 12°C. **D)** Comparison of the initial rates of cleavage product formation and the total reaction of the parental *rTel* and the mutant *rTel* substrates with WT TelA at 12°C. The initial rates are demonstrated as the fraction substrate converted/min (1.0 being 100% conversion). The mean and standard deviation of at least three separate replicates are displayed. The gray bars indicate the total reaction and the black bars indicate the cleavage product formation. The discontinuous y-axis emphasizes that activity occurred from MM1 to 6, not only with MM4.

4.3.2. Attempt to rescue the cold-sensitivity of telomere resolution with missing base substrates

Studies on ResT showed that the cold-sensitivity of ResT can be rescued notably with abasic substrates (Lucyshyn et al., 2015). Contrary to previous results with ResT and the marked rescue afforded by the MM4 *rTel*, the cold-sensitivity of TelA was not significantly rescued with any of the abasic substrates (Figure 4.12; (Figure 2, Lucyshyn et al., 2015)). As previously mentioned, in the ResT system, a variety of different sequences between the scissile phosphates need to be accommodated compared to TelA system. It can be inferred that TelA makes more base-specific contacts between the scissile phosphates than ResT which needs to accommodate several different sequences between the scissile phosphates (Shi et al., 2013). Therefore, we inferred that the lesser degree of flexibility for TelA in processing *rTels* with alternate sequences between the scissile phosphates may have caused the difference in cold-sensitivity rescue by removing the bases or introducing mismatches. The lack of rescue of cold-sensitivity with missing bases was in contrast to what was observed with mismatches indicating the breaking of the base pairing between the scissile phosphates at positions 3 and 4 is the main step for unwinding the DNA substrate. The presence of these bases is probably crucial for stabilizing the refolding intermediate. Additionally, the hairpin refolding step may also display cold-sensitivity; disruption of the normal basepairing across the refolding strands may block the reactions at this later step.

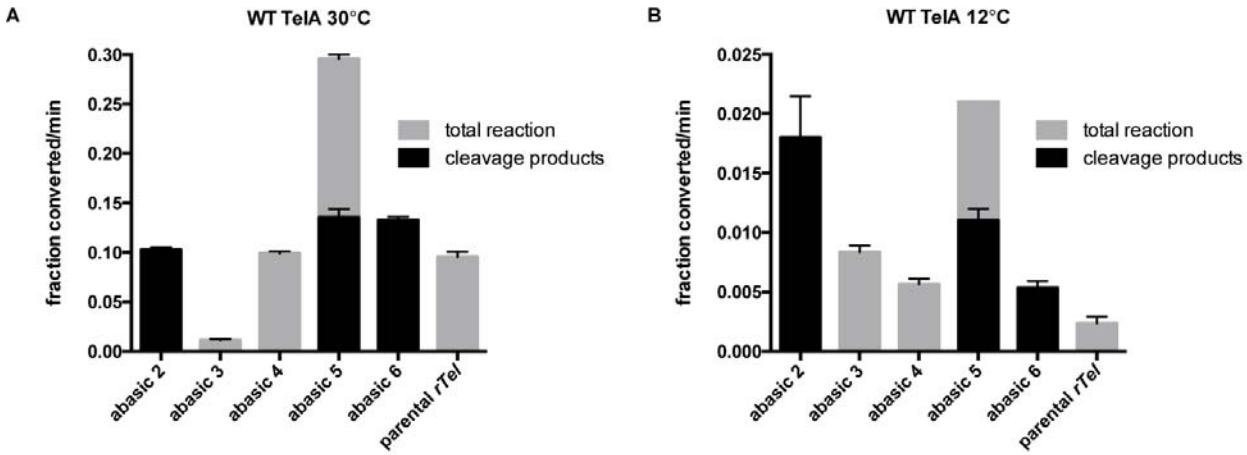

Figure 4.12. The summary of assays performed to rescue the cold-sensitivity of telomere resolution by the use of missing base substrates. A) The comparison of the initial rate of cleavage products and the total reaction of parental *rTel* and abasic substrates with WT TelA at 30°C. **B)** The comparison initial of cleavage products and the total reaction of the parental *rTel* and the missing base substrates with WT TelA at 12°C. Note that the scale of the y-axis is $1/10^{th}$ that used in A). The initial rates are demonstrated as the fraction substrate converted/min (1.0 being 100% conversion). The mean and

standard deviation of at least three separate replicates are displayed. The gray bars indicate the total reaction, and the black bars indicate the cleavage products.

4.4. Results with TelA variants in the hp binding module

4.4.1. TelA (Y201)

TelA (Y201) has been reported to have a crucial role in refolding the cleaved strands into a hairpin conformation by stabilizing the A6 base that is transiently in an extrahelical conformation in the refolding intermediate. TelA (Y201A) variant has been reported to be cleavage competent but unable to form hairpins (Shi et al., 2013). We introduced the Y201A mutation in TelA and purified the protein. Although the folding of TelA (Y201A) was verified by the previous crystallography study, we first checked and verified the folding of our protein preparation with the band shift assay and by assaying the annealing activity of TelA (Y201A) (Figure 4.13).

4.4.1.1. Is TelA (Y201A) properly folded?

We confirmed that TelA (Y201A) can anneal the single-strand TAR oligonucleotide to its complement, and that it binds to its *rTel* substrate with normal affinity (Figure 4.13). We observed that the EMSA assay for TelA (Y201A) resulted in two bands. The upper band of the band shift presumably indicates the gel mobility of the dimer of TelA bound to *rTel* and the lower band indicates the binding of one monomer.

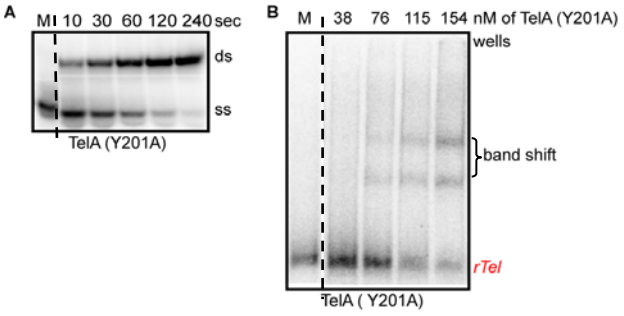

Figure 4.13. Folding of TelA (Y201A) assessed by activity in ssDNA annealing and *rTel* binding assays. A) A representative example of 8% PAGE/ 1X TAE/ 0.1% SDS gel panels of timecourse reactions with TelA (Y201A) and TAR oligonucleotides. The gel mobility of 5'-^{32}P endlabeled TAR oligonucleotide is shown as ss, and the double-strand product is shown as ds. **B)** A representative example of 6% PAGE/ 0.5X TBE gel panel of endpoint reactions of titration of TelA (Y201A) and *rTel* incubated at 0°C for 20 minutes. Band shift indicates gel mobility of the TelA bound to *rTel*; *rTel* in red color indicates the *rTel* substrate; M stands for mock protein-free reaction. Irrelevant samples are removed. Displacement is indicated by dash line.

4.4.1.2. Results with TelA (Y201A)

We continued our investigation of TelA (Y201A) with parental *rTel* and mismatch substrates. We noted that this variant is severely defective with parental *rTel*, however, the reaction was rescued with some mismatch substrates. TelA (Y201A) had an asymmetric pattern

of rescue with MM4, 5, and 6 while the MM1-3 substrates failed to show any rescue over the parental *rTel* (Figure 4.14c). The rescue was from the mismatches rather than the sequence changes as was evident by the fact that TelA (Y201A) was inactive with all control mutant *rTel* substrates (Figure 4.14d). The asymmetric nature of the rescue was unexpected as the MM *rTel*s substrates have inverted repeat symmetry within the telomeric sequence. However, there are two potential reasons. First, the crystallography study captured a slightly asymmetric conformation of TelA dimer bound to hairpin telomeres; the Y201 residue was part of the small difference between the conformation on the two sides of the dimeric product complex (Shi et al., 2013). Additionally, the flanking sequences in the *rTel* used are asymmetric which might affect the results by impacting the conformation of the DNA. DNA flexibility and bending potentially be altered by different DNA sequences.

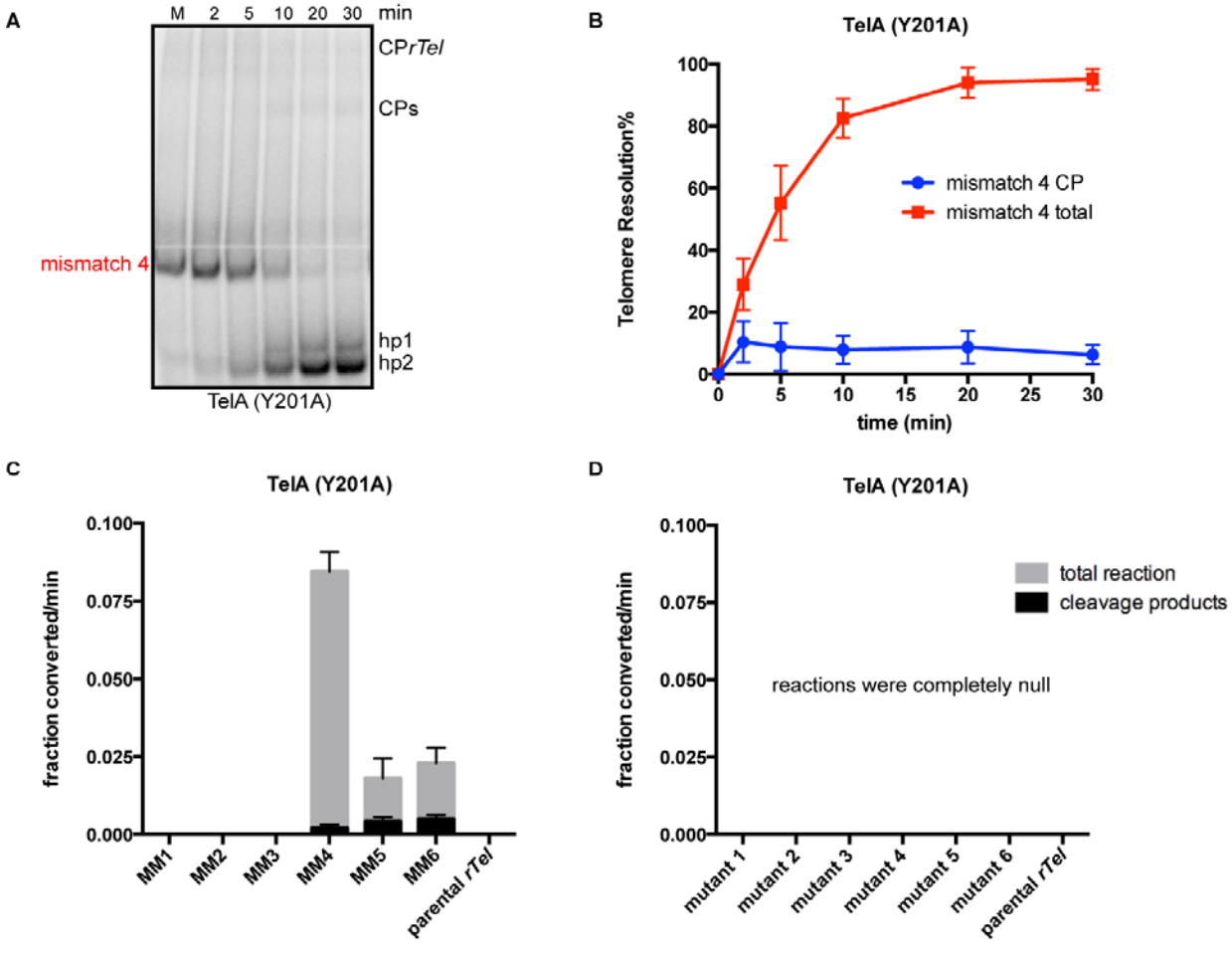

Figure 4.14. Result of the assays with TelA (Y201A) and mismatch substrates. A) A representative example of 8% PAGE, 1X TAE/0.1% SDS gel panel of a timecourse reaction of TelA (Y201A) with MM4 incubated at 30°C. The mobility of the substrate in the gel is represented by mismatch 4; CP*rTel*

marks the migration of a product that TelA has cleaved only one strand; CPs is gel migration of the cleavage products; hp1 and hp2 are the position of the hairpin telomere products on the gel; M stands for mock protein-free reaction. **B)** The % of cleavage products and total reaction *vs*. reaction time plot of telomere resolution reaction with TelA (Y201A) and MM4 at 30°C. **C)** Comparison of the initial rates of cleavage product formation and the rate of the total reaction of the parental *rTel* and the substrates with mismatches. The initial rates are demonstrated as the fraction substrate converted/min (1.0 being 100% conversion). The mean and standard deviation of at least three separate replicates are displayed. The gray bars indicate the total reaction, and the black bars indicate the cleavage products. **D)** The initial rates of mutant control *rTels* with TelA (Y201A).

The next step in the characterization of TelA (Y201A) was to conduct assays with the missing base substrates. A stacking interaction to stabilize a base out of the helix is not necessary if that base is removed. Therefore, a missing base substrate would be expected to partially rescue the reaction with the mutation in the residue with such a stabilizing role. In contrast to what we expected based on the structure, TelA (Y201A) made hairpin telomeres with abasic 5 instead of abasic 6. Structural studies of the refolding intermediate indicated a role for stacking of Y201 with A6 but our results are more consistent with such an interaction with G5 instead. This reaction rescue was without accumulation of CP in contrast to the results with WT TelA (Figure 4.15c). Abasic 4 was a poor substrate for TelA (Y201A) in contrast to mismatch results with MM4.

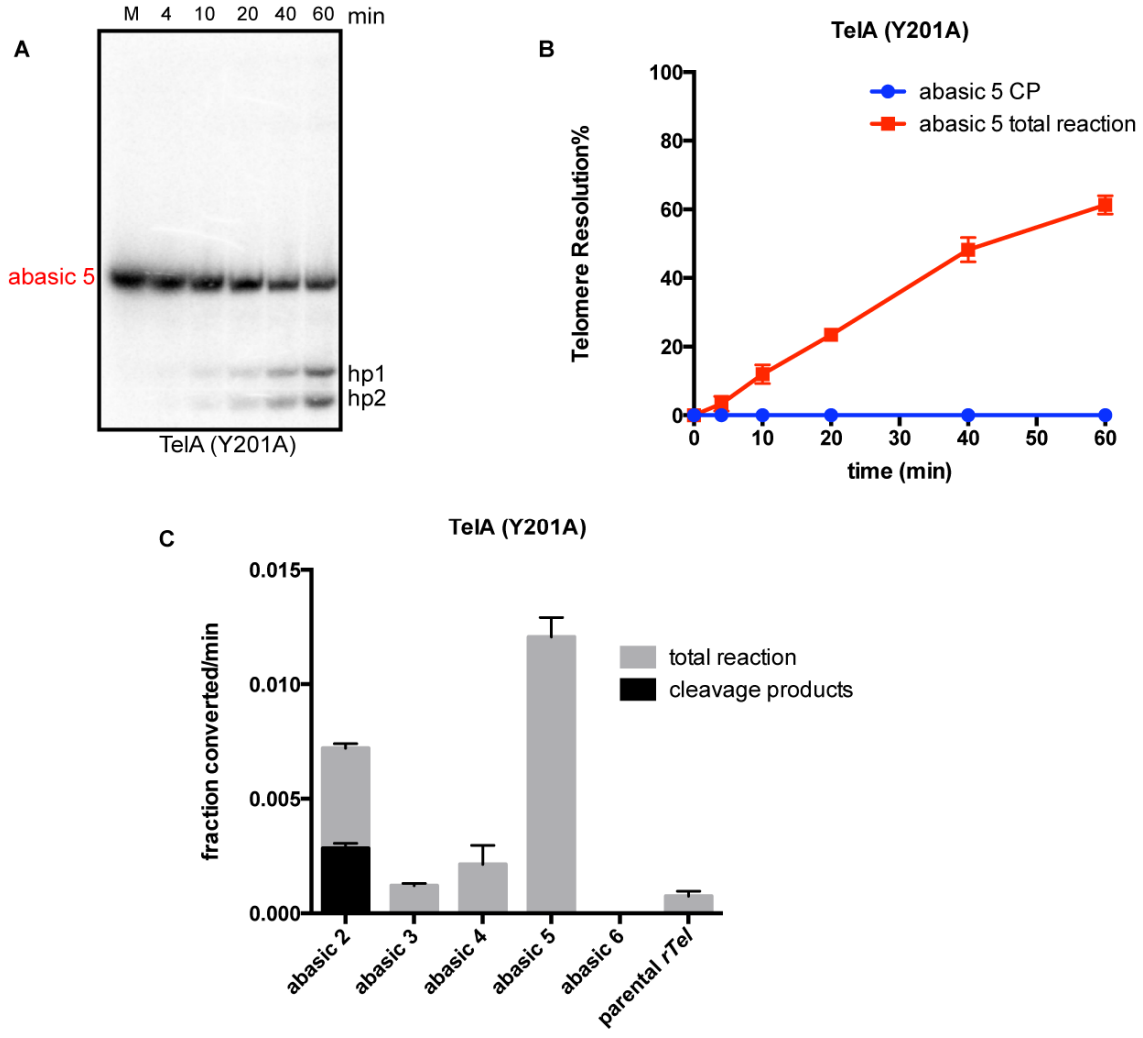

Figure 4.15. Result of the assays with TelA (Y201A) and missing base substrates. A) A representative example of 8% PAGE, 1X TAE/0.1% SDS gel panel of a timecourse reaction of TelA (Y201A) with abasic 5 incubated at 30°C. The mobility of the substrate in the gel is represented by mismatch 4; hp1 and hp2 are the position of the hairpin telomere products on the gel; M stands for mock protein-free reaction. **B)** The % of cleavage products and total reaction *vs*. reaction time plot of telomere resolution reaction with TelA (Y201A) and abasic 5 at 30°C. **C)** Comparison of the initial rates of cleavage product formation and the rate of the total reaction of the parental *rTel* and the substrates with missing substrates with TelA (Y201A). The initial rates are demonstrated as the fraction substrate converted/min (1.0 being 100% conversion). The mean and standard deviation of at least three separate replicates are displayed. The gray bars indicate the total reaction and the black bars indicate the cleavage products.

The last set of modified substrates we used for TelA (Y201A) was nick modifications between the scissile phosphates. These substrates stimulated the reaction to some extent compared to parental *rTel* with the exception of the +1 Nick substrate. TelA (Y201A) showed a strong preference of nick positions, and the rescue was site-specific. The nick +4 was preferred over other nick substrates, and the +1 nick was inactive. Most of the other variants did not show

such a strong preference for the nick position which is discussed in the following sections. This site-specific pattern of rescue might relate to the stacking interaction of Y201 near the position of the +4 nick (Shi et al., 2013). Similar to WT TelA, TelA (Y201A) was unable to make hp1 because of the nick on the top strand (Figure 4.16).

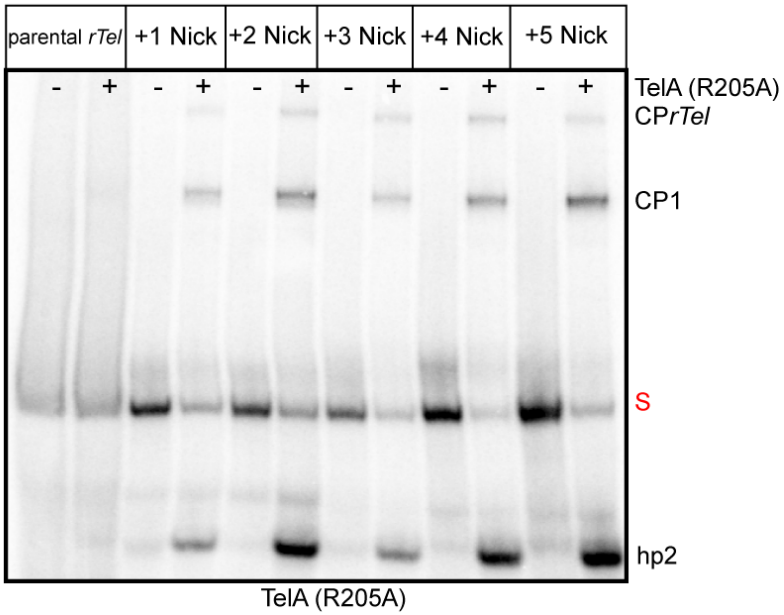

Figure 4.16. Telomere resolution of TelA (Y201A) with nick modified substrates. A representative 8% PAGE/ 1X TAE/0.1% SDS gel panel of the endpoint reactions of TelA (Y201A) and the nick substrates incubated at 30°C for 10 minutes. The mobility of the substrate in the gel is represented by S; CP*rTel* marks the migration of a product that TelA has cleaved only one strand; CP1 is gel migration of the cleavage products; hp2 is the position of the hairpin telomere product on the gel. + indicates the reactions incubated with protein; - indicates protein-free mock reactions.

4.4.2. TelA (R205A)

It was proposed that the positive charge of TelA (R205) promotes strand refolding after the DNA cleavage step. This variant has also been reported to be cleavage competent but unable to form hairpins (Shi et al., 2013). Additionally, the crystal structure of the refolding intermediate and hairpin product complex revealed that TelA (R205) makes contacts with the T4 and A6 in the *rTel* sequence (Shi et al., 2013). We substituted arginine with alanine in TelA at position 205 and purified the resulting TelA (R205A). For the first step, we verified the folding of the protein we purified with band shift assay and annealing activity of TelA (R205A) (Figure 4.17). Additionally, TelA (R205A) displayed proper folding in the structural study of TelA (Shi et al., 2013).

4.4.2.1. Is TelA (R205A) properly folded?

We validated the ssDNA annealing and *rTel* binding activities of TelA (R205A) (Figure 4.17).

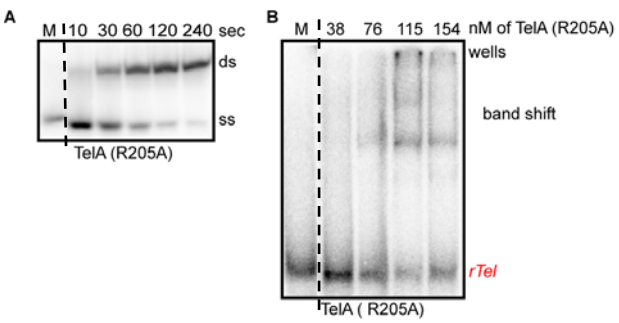

Figure 4.17. Folding of TelA (R205A) assessed by activity in ssDNA annealing and *rTel* binding assays A) A representative example of 8% PAGE/ 1X TAE/ 0.1% SDS gel panels of timecourse reactions with TelA (R205A) and TAR oligonucleotide. The gel mobility of 5'-^{32}P endlabeled TAR oligonucleotide is shown as ss, and the double-strand product is shown as ds. **B)** A representative example of 6% PAGE/ 0.5X TBE gel panel of endpoint reactions of titration of TelA (Y201A) and *rTel* incubated at 0°C for 20 minutes. Band shift indicates gel mobility of the TelA bound to *rTel*, *rTel* in red color indicates the *rTel* substrate; The upper band of the band shift indicates the gel mobility of the dimer of TelA bound to *rTel* and the lower band indicates the binding of one monomer. M stands for mock protein-free reaction. Irrelevant samples are removed. Displacement is indicated by dash line.

4.4.2.2. Results with TelA (R205A)

The analysis of TelA (R205A) was continued with parental *rTel* and mismatch substrates. TelA (R205A) had low activity with parental *rTel* at 30°C. The reaction could be rescued with mismatch substrates. MM4 stimulated the reaction with TelA (R205A) roughly 3-fold. MM3 was the second substrate that stimulated and rescued the reaction (Figure 4.18c). The mutant *rTel* substrates were inactive with TelA (R205A) indicating the rescue was from the broken base pairs between the scissile phosphates rather than the sequence change (Figure 4.14, d).

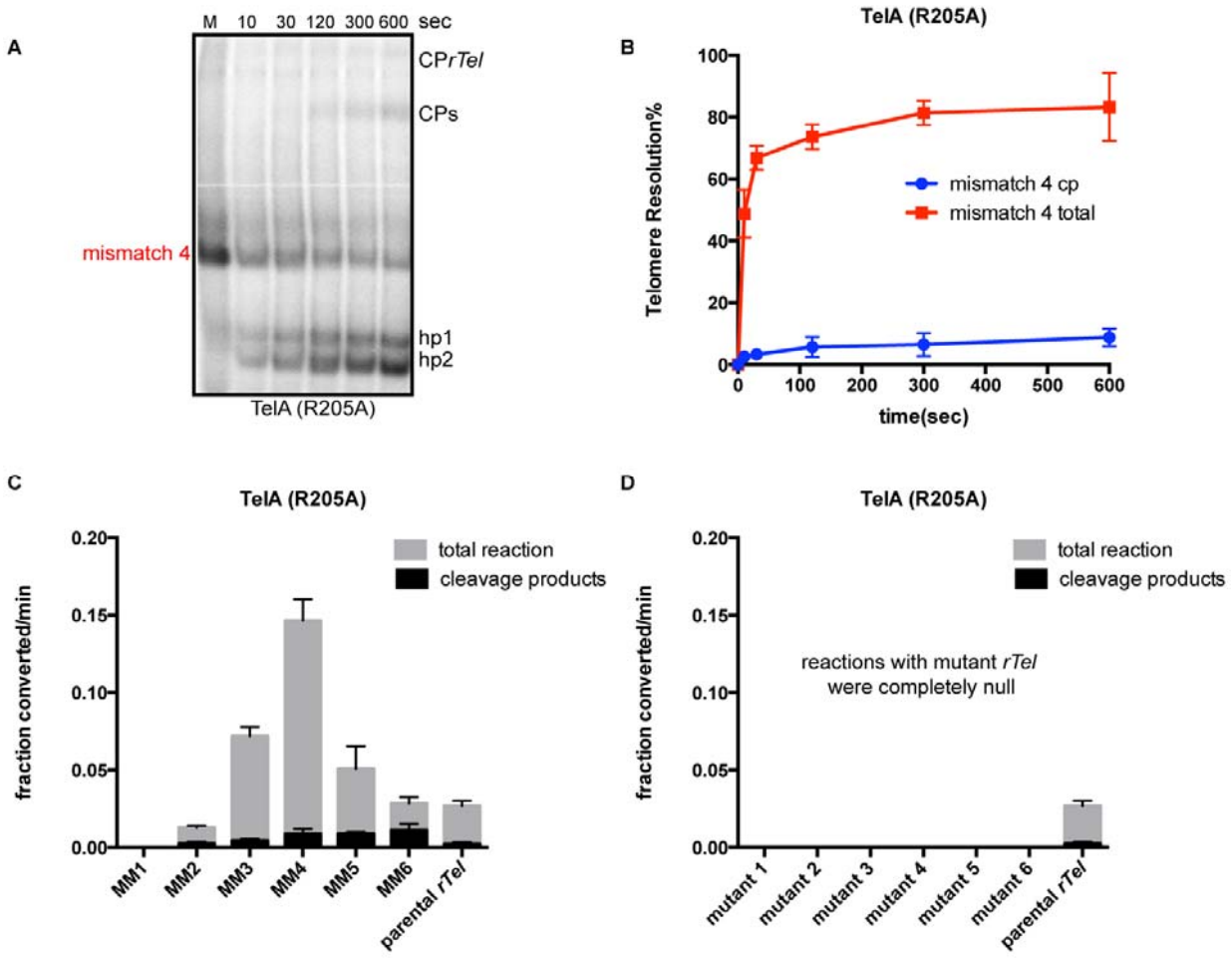

Figure 4.18. Results of assays with TelA (R205A) and *rTel* substrates with mismatches. A) A representative example of 8% PAGE, 1X TAE/0.1% SDS gel panel of a timecourse reaction of TelA (R205A) with MM4 incubated at 30°C. The mobility of the substrate in the gel is represented by mismatch 4; CP*rTel* marks the migration of a product that TelA has cleaved only one strand; CPs is gel migration of the cleavage products; hp1 and hp2 are the position of the hairpin telomere products on the gel; M stands for mock protein-free reaction. **B)** The % of cleavage products and total reaction *vs.* reaction time plot of telomere resolution reaction with TelA (R205A) and MM4 at 30°C. **C)** Comparison of the initial rates of cleavage product formation and the rate of the total reaction of the parental *rTel* and the substrates with mismatches. The initial rates are demonstrated as the fraction substrate converted/min (1.0 being 100% conversion). The mean and standard deviation of at least three separate replicates are displayed. The gray bars indicate the total reaction and the black bars indicate the cleavage products. **D)** The initial rates of mutant control *rTels* with TelA (R205A).

We continued our investigations of TelA (R205A) with the missing base substrates. TelA (R205A) failed to make hairpins with abasic 2 and 6, additionally, abasic 3 and 4 were poor substrates in contrast with the mismatch results. Abasic 5 was the most stimulatory modified substrate but led to the accumulation of a significant proportion of CPs (Figure 4.19c).

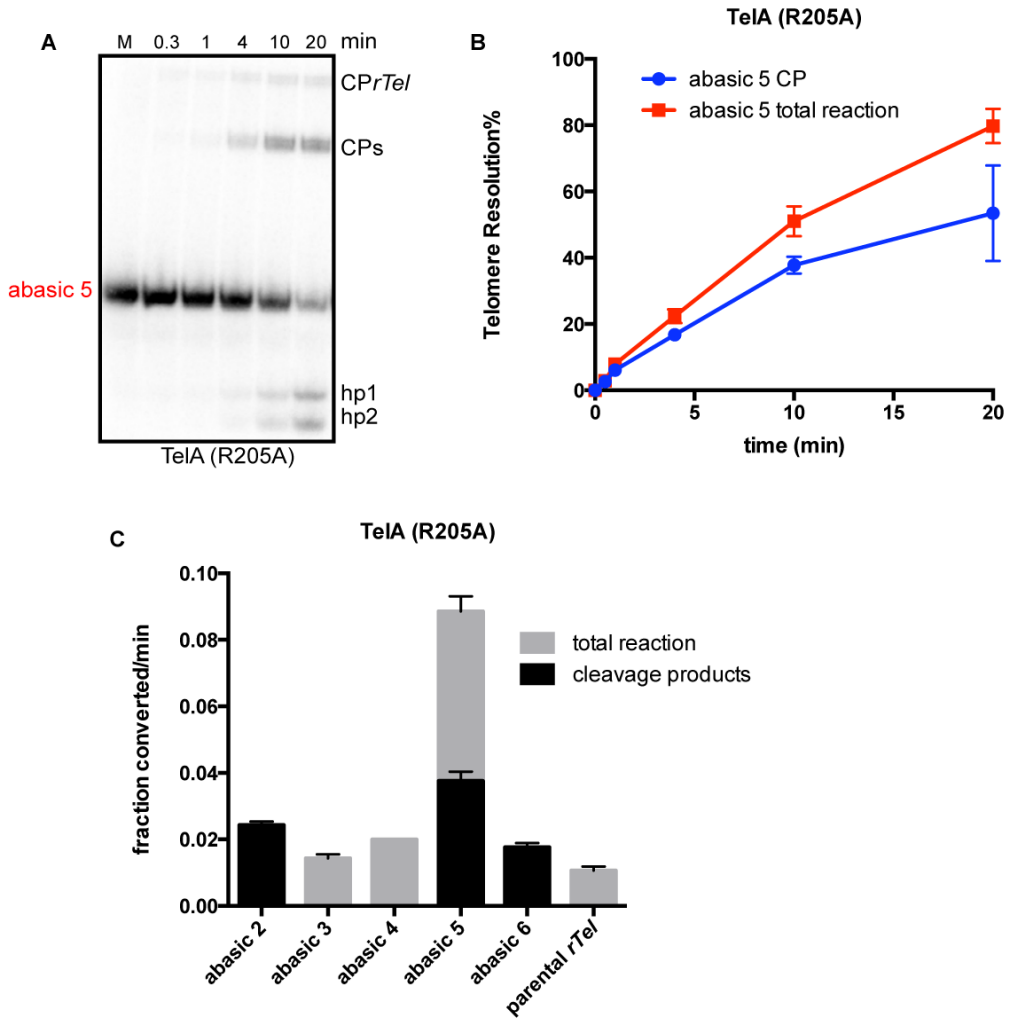

Figure 4.19. Result of the assay with TelA (R205A) and missing base substrates. A) A representative example of 8% PAGE, 1X TAE/0.1% SDS gel panel of a timecourse reaction of TelA (R205A) with abasic 5 incubated at 30°C. The mobility of the substrate in the gel is represented by abasic 5; hp1 and hp2 are the position of the hairpin telomere products on the gel; M stands for mock protein-free reaction. **B)** The % of cleavage products and total reaction *vs*. reaction time plot of telomere resolution reaction with TelA (R205A) and abasic 5 at 30°C. **C)** Comparison of the initial rates of cleavage product formation and the rate of the total reaction of the parental *rTel* and the substrates with missing substrates with TelA (R205A). The initial rates are demonstrated as the fraction substrate converted/min (1.0 being 100% conversion). The mean and standard deviation of at least three separate replicates are displayed. The gray bars indicate the total reaction and the black bars indicate the cleavage products.

TelA (R205A) reacted with nick modifications in a similar manner as WT TelA. The nicked substrates stimulated the reaction to some extent compared to the parental *rTel*, TelA (R205A). TelA (R205A) was unable to make hp1 because of the nick on the top strand (Figure 4.20). Despite being previously reported as unable to form hps, TelA (R205A) successfully forms hp2 with all the nicked *rTels* (Shi et al., 2013).

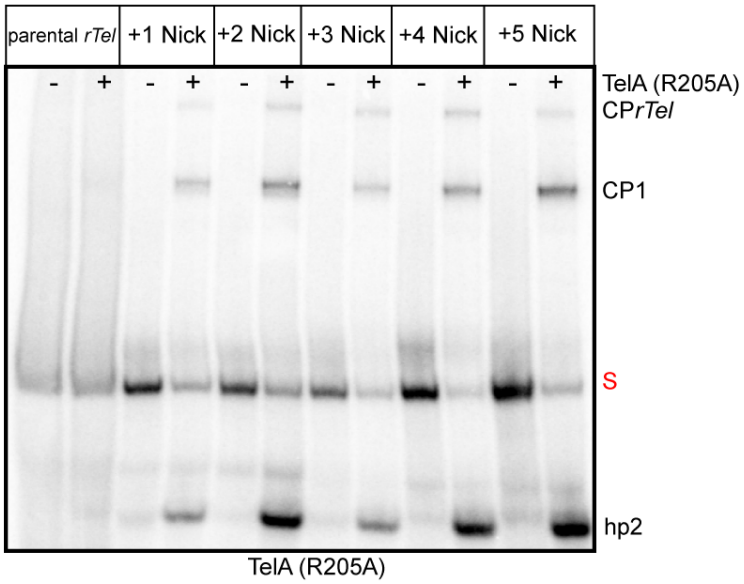

Figure 4.20. Telomere resolution of TelA (R205A) with nick modified substrates. A representative 8% PAGE/ 1X TAE/0.1% SDS gel panel of the endpoint reactions of TelA (R205A) and the nick substrates incubated at 30°C for 10 minutes. The mobility of the substrate in the gel is represented by S; CP*rTel* marks the migration of a product that TelA has cleaved only one strand; CP1 is gel migration of the cleavage products; hp 2 is the position the of the hairpin telomere product on the gel. + indicates the reactions incubated with protein; - indicates protein-free mock reactions.

4.5. Results with TelA variants in the catalytic domain

4.5.1. TelA (K288A)

The proposed model for telomere resolution in the ResT system and the results from the crystal structure of the hp products in the TelA system generated the idea to examine a set of candidate variants in the catalytic domain of TelA. K288 was reported to make direct interactions with T1 and C2 between the scissile phosphates (Figure 4.2; (Shi et al., 2013)). To evaluate the effect of this residue on telomere resolution, we generated and purified TelA (K288A) for functional assays.

4.5.1.1. Is TelA (K288A) properly folded?

We performed circular dichroism (CD) spectroscopy, in addition to EMSA and single-strand annealing assays to check whether the folding of TelA (K288A) is correctly folded. TelA (K288A) showed annealing and binding activity similar to WT TelA (Figure 4.21). The CD spectra of TelA (K288A) and WT TelA were essentially superimposable and showed that they have comparable to α-helical and β-sheets content.

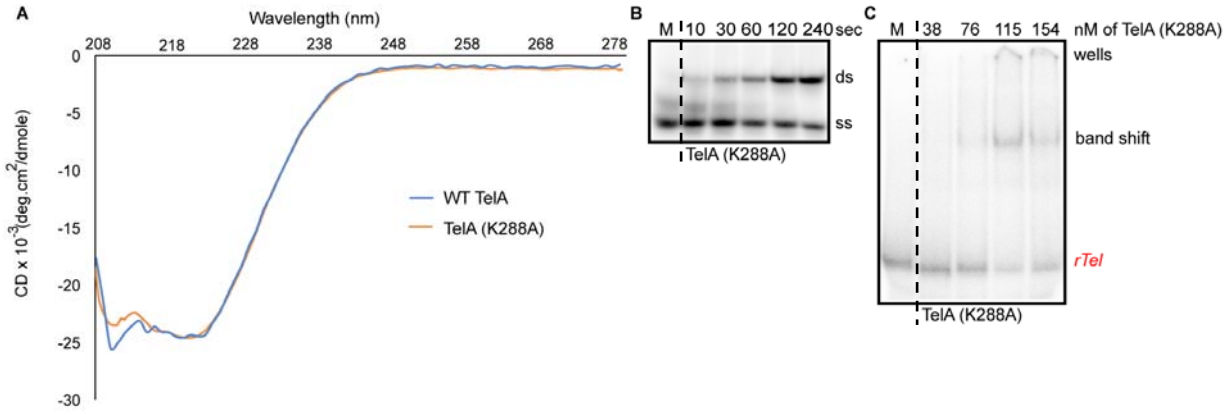

Figure 4.21. Folding of TelA (K288A) assessed by activity in ssDNA annealing and *rTel* binding assays A) The CD spectra of WT TelA and (K288A). The blue line indicates the pattern of α-helix and β-sheet in WT TelA, and the red line indicates the pattern of α-helix and β-sheet in TelA (K288A). **B)** A representative example of 8% PAGE/ 1X TAE/ 0.1% SDS gel panels of timecourse reactions with TelA (K288A) and TAR oligonucleotide. The gel mobility of 5'-^{32}P endlabeled TAR oligonucleotide is shown as ss, and the double-strand product is shown as ds. **C)** A representative example of 6% PAGE/ 0.5X TBE gel panel of endpoint reactions of titration of TelA (K288A) and *rTel* incubated at 0°C for 20 minutes. Band shift indicates gel mobility of the TelA bound to *rTel*, *rTel* in red color indicates the *rTel* substrate; M stands for mock protein-free reaction. The irrelevant samples are cut from the figure and displacement is shown by the dashed line.

4.5.1.2. Results with TelA (K288A)

The telomere resolution activity of TelA (K288A) with a parental *rTel* was found to be disrupted completely as no production of CPs or hps could be detected. However, the reaction could be rescued by mismatch substrates to some extent. TelA (K288A) was inactive with MM 1 and 6, additionally, it failed to make hps with MM2 and 5. TelA (K288A) was well rescued with MM4; however, the reaction with MM4 was accompanied by a marked accumulation of CPs indicating slow hairpin formation (Figure 4.22). Again, the mutant *rTel* substrates were inactive with TelA (K288A) indicating the rescue was from the broken base pairs between the scissile phosphates rather than the sequence change (Figure 4.22).

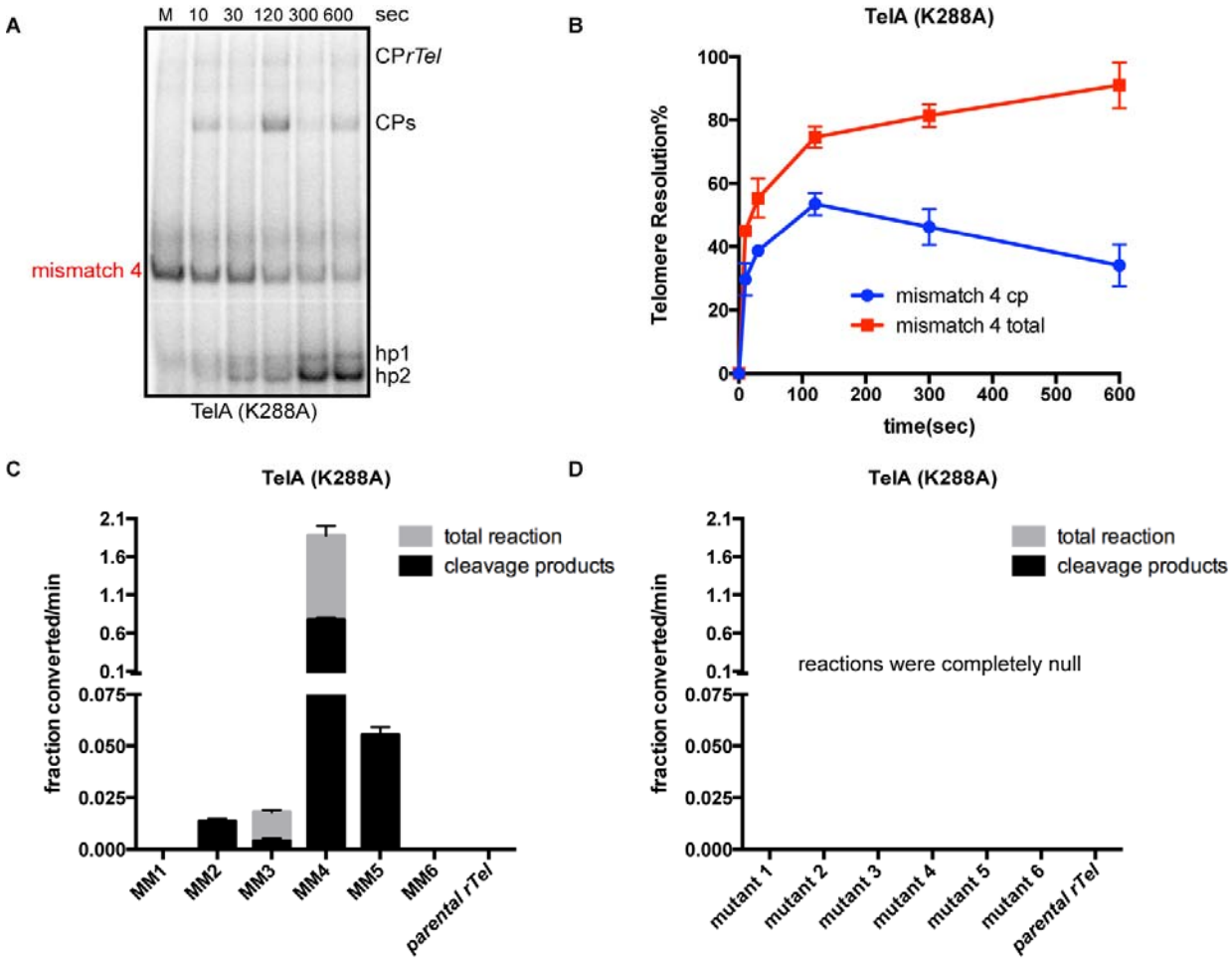

Figure 4.22. Result of the assays with TelA (K288A) and mismatch base substrates. A) A representative example of 8% PAGE, 1X TAE/0.1% SDS gel panel of a timecourse reaction of TelA (K288A) with MM4 incubated at 30°C. The mobility of the substrate in the gel is represented by mismatch 4; CP*rTel* marks the migration of a product that TelA has cleaved only one strand; CPs is gel migration of the cleavage products; hp1 and hp2 are the position of the hairpin telomere products on the gel; M stands for mock protein-free reaction. **B)** The % of cleavage products and total reaction *vs.* reaction time plot of telomere resolution reaction with TelA (K288A) and MM4 at 30°C. **C)** Comparison of the initial rates of cleavage product formation and the rate of the total reaction of the parental *rTel* and the substrates with mismatches. The initial rates are demonstrated as the fraction substrate converted/min (1.0 being 100% conversion). The mean and standard deviation of at least three separate replicates are displayed. The gray bars indicate the total reaction and the black bars indicate the cleavage products. **D)** The initial rates of mutant control *rTels* with TelA (K288A).

The results with the missing base *rTel* substrates and TelA (K288A) were interesting as abasic 4 stimulated the reaction with this variant the most and the reaction with abasic 4 was not accompanied by any accumulation of CPs. Rescue with abasic 6 was almost as good as with abasic 4 accompanied by only cleavage products (since the ability to form the first basepair in the refolding strands is impaired). WT TelA and most other variants were rescued best with

abasic 2 and 5 rather than 4 and 6 like with TelA (K288A). TelA (K288A) was inactive with abasic 3 and it failed to make hps with abasic 2, 5 and 6 (Figure 4.23).

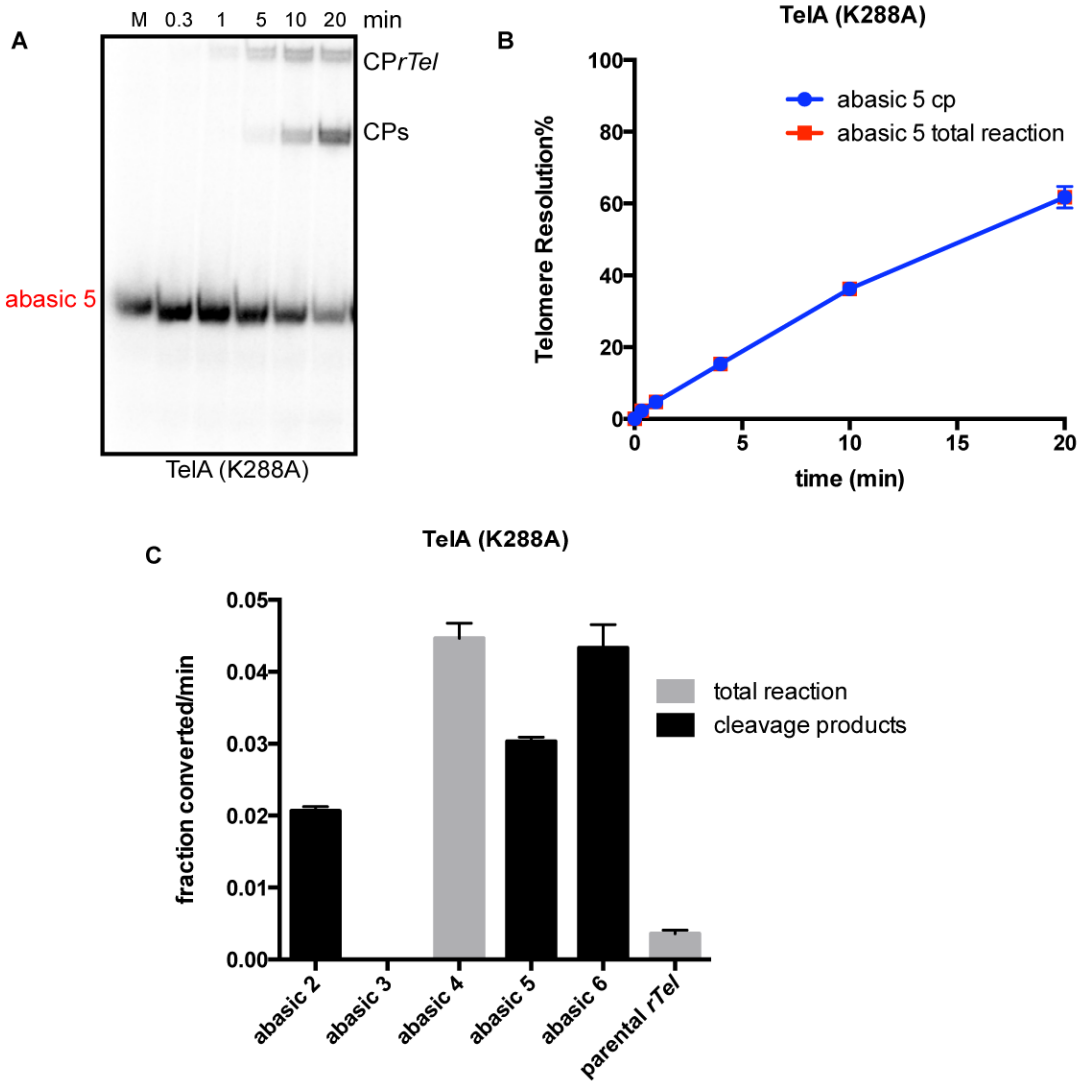

Figure 4.23. Result of the assays with TelA (K288A) and missing base substrates. A) A representative example of 8% PAGE, 1X TAE/0.1% SDS gel panel of a timecourse reaction of TelA (K288A) with abasic 5 incubated at 30°C. The mobility of the substrate in the gel is represented by abasic 5. CP*rTel* marks the migration of a product that TelA has cleaved only one strand; CPs is the gel migration of the cleavage products; M stands for mock protein-free reaction. **B)** The % of cleavage products and total reaction *vs.* reaction time plot of telomere resolution reaction with TelA (K288A) and abasic 5 at 30°C. **C)** Comparison of the initial rates of cleavage product formation and the rate of the total reaction of the parental *rTel* and the substrates with missing substrates with TelA (K288A). The initial rates are demonstrated as the fraction substrate converted/min (1.0 being 100% conversion). The mean and standard deviation of at least three separate replicates are displayed. The gray bars indicate the total reaction and the black bars indicate the cleavage products.

The nick modifications stimulate the reaction to some extent with the +1 nick giving best rescue. In contrast to previous results with other TelA variants, the other nicked *rTels* were relatively poor substrates (Figure 4.24).

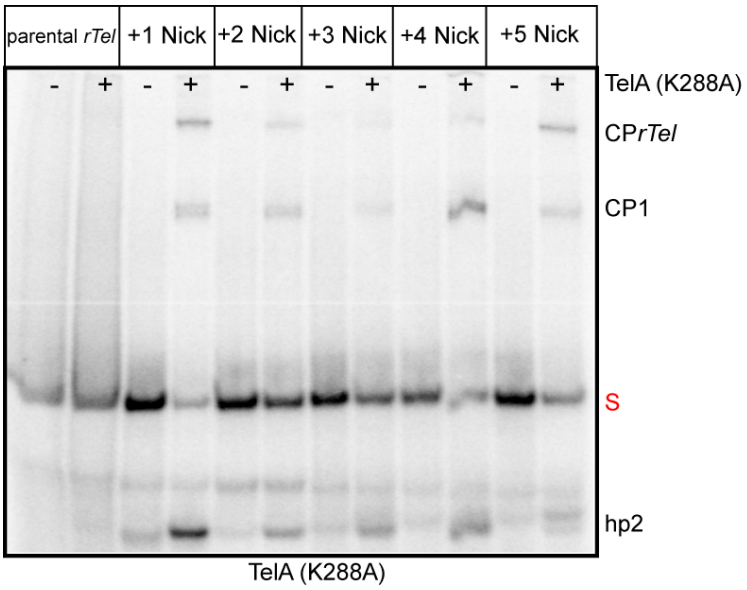

Figure 4.24. Telomere resolution of TelA (K288A) with nick modified substrates. A representative 8% PAGE/ 1X TAE/0.1% SDS gel panel of the endpoint reactions of TelA (K288A) and the nick substrates incubated at 30°C for 10 minutes. The mobility of the substrate in the gel is represented by S; CP*rTel* marks the migration of a product that TelA has cleaved only one strand; CP1 is gel migration of the cleavage products; hp2 is the position of the hairpin telomere product on the gel. + indicates the reactions incubated with protein; - indicates protein-free mock reactions.

4.5.2. TelA (D398A)

4.5.2.1. Is TelA (D398A) properly folded?

The second residue in the catalytic domain that we were interested in was D398. The alignment of TelA and ResT revealed that TelA (D398) aligns with ResT (D328) which is involved in stabilizing the pre-cleavage intermediate in ResT system and in testing the fidelity of basepairing in the developing hp after DNA cleavage (Lucyshyn et al., 2015). Additionally, in the crystal structure of hp product, TelA (D398) was shown to make water-mediated interactions with the backbone of the DNA between T1 and C2. TelA (D398A) is comparable to WT TelA in terms of α-heliceal and β-sheets content as dementrated by CD spectroscopy. To verify that TelA (D398A) is likely in correct conformation, we showed the other known activities of TelA; *rTel* binding, and annealing activity (Figure 4.25).

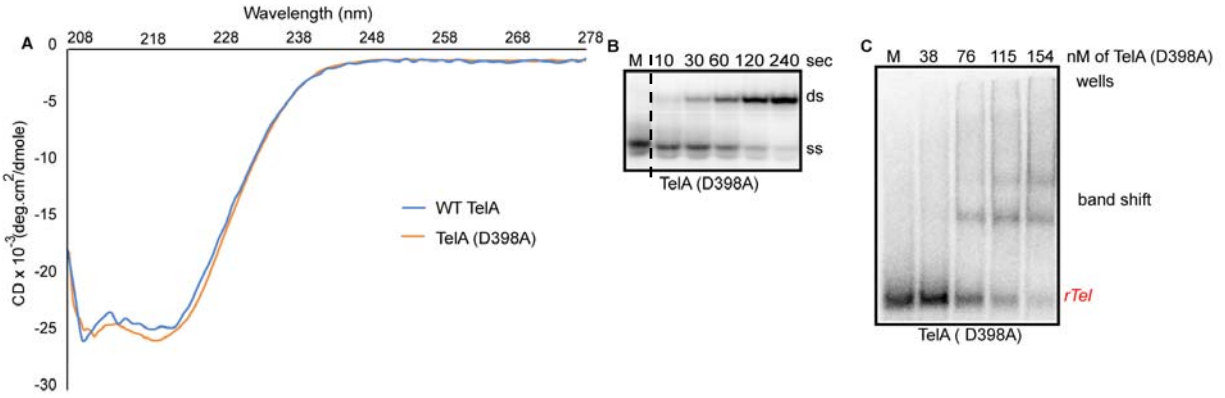

Figure 4.25. Folding of TelA (D398A) assessed by activity in ssDNA annealing, *rTel* binding and CD spectroscopy assays A) The CD spectra of WT TelA and (D398A). The blue line indicates the pattern of α-helix and β-sheet in WT TelA, and the red line indicates the pattern of α-helix and β-sheet in TelA (D398A). **B)** A representative example of 8% PAGE/ 1X TAE/ 0.1% SDS gel panels of timecourse reactions with TelA (D398A) and TAR oligonucleotide. The gel mobility of 5'-^{32}P endlabeled TAR oligonucleotide is shown as ss, and the double-strand product is shown as ds. **C)** A representative example of 6% PAGE/ 0.5X TBE gel panel of endpoint reactions of titration of TelA (D398A) and *rTel* incubated at 0°C for 20 minutes. Band shift indicates gel mobility of the TelA bound to *rTel*, *rTel* in red color indicates the *rTel* substrate; M stands for mock protein-free reaction. The upper band of the band shift indicates the gel mobility of the dimer of TelA bound to *rTel* and the lower band indicates the binding of one monomer. M stands for mock protein-free reaction. Irrelevant samples are removed. Displacement is indicated by dash line.

4.5.2.2. Results with TelA (D398A)

TelA (D398A) was found to be a severely defective variant and it had a low activity with the parental *rTel*. In contrast to the results of assays with other variants, MM3 stimulated the reaction the most in the reaction with TelA (D398A) accompanied by accumulation of a slight amount of CPs (Figure 4.26). Although, MM4 was also stimulatory for reaction with TelA (D398A); it was much less so than that observed with WT TelA and the other variants tested. Additionally, the control mutant 4 showed a small degree of reaction rescue indicating that the majority, but not all, of the stimulation afforded by MM4 was due to the mismatch. All other mutant control *rTels* were inactive with TelA (D398A).

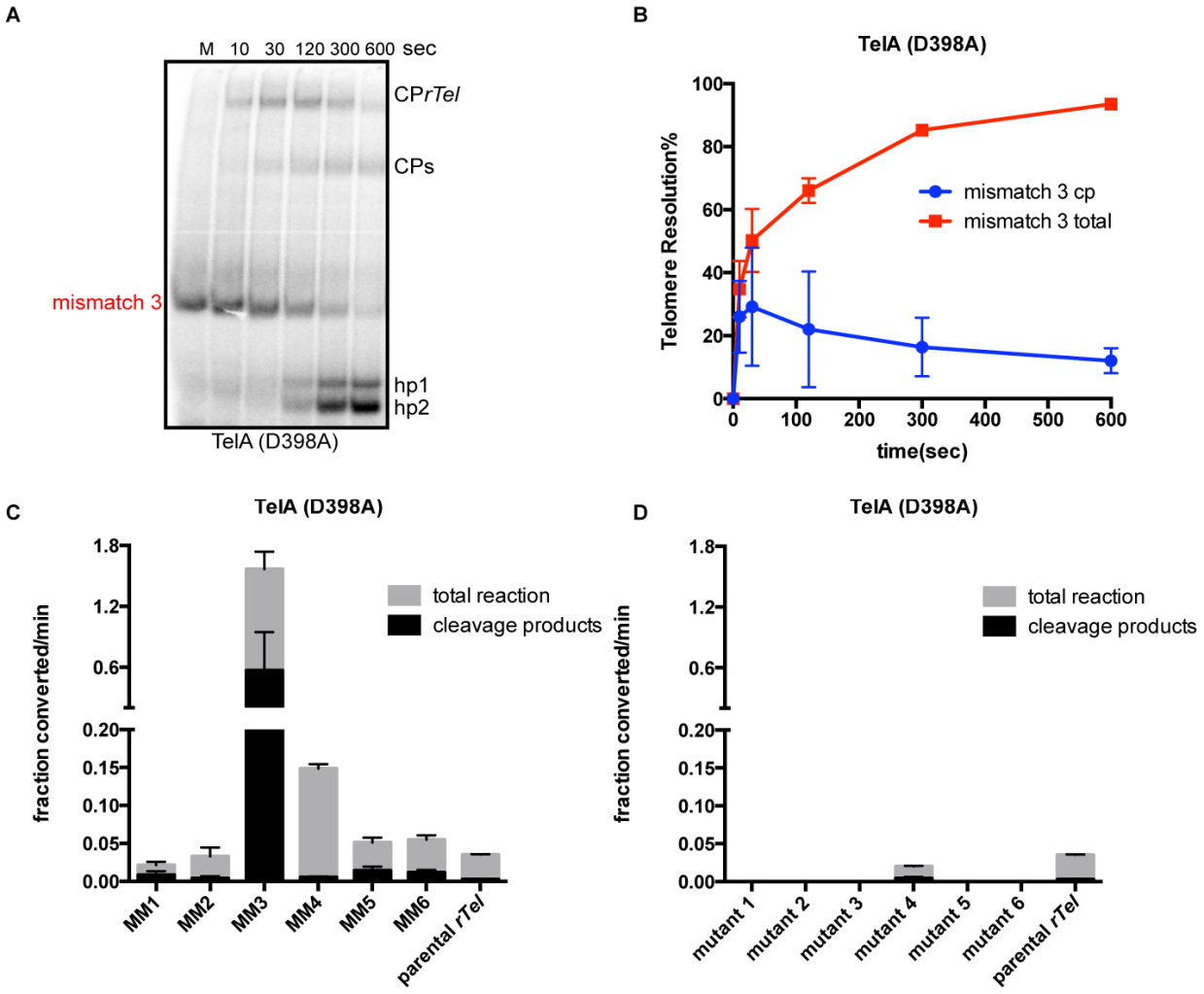

Figure 4.26. Result of the assays with TelA (D398A) and mismatch substrates. A) A representative example of an 8% PAGE, 1X TAE/0.1% SDS gel panel of a timecourse reaction of TelA (D398A) with MM3 incubated at 30°C. The mobility of the substrate in the gel is represented by mismatch 3; CP*rTel* marks the migration of a product that TelA has cleaved only one strand; CPs is gel migration of the cleavage products; hp1 and hp2s are the position of the hairpin telomere products on the gel; M stands for mock protein-free reaction. **B)** The % of cleavage products and total reaction *vs*. reaction time plot of telomere resolution reaction with TelA (D398A) and MM3 at 30°C. **C)** Comparison of the initial rates of cleavage product formation and the rate of the total reaction of the parental *rTel* and the substrates with mismatches. The initial rates are demonstrated as the fraction substrate converted/min (1.0 being 100% conversion). The mean and standard deviation of at least three separate replicates are displayed. The gray bars indicate the total reaction, and the black bars indicate the cleavage products. **D)** The initial rates of mutant control *rTels* with TelA (D398A).

The results with the missing base substrates demonstrated that all of these substrates were stimulatory to some extent. As seen with WT TelA, abasic 2 and 5 rescued the reaction the most; this rescue was accompanied by accumulation of CPs (Figure 4.27).

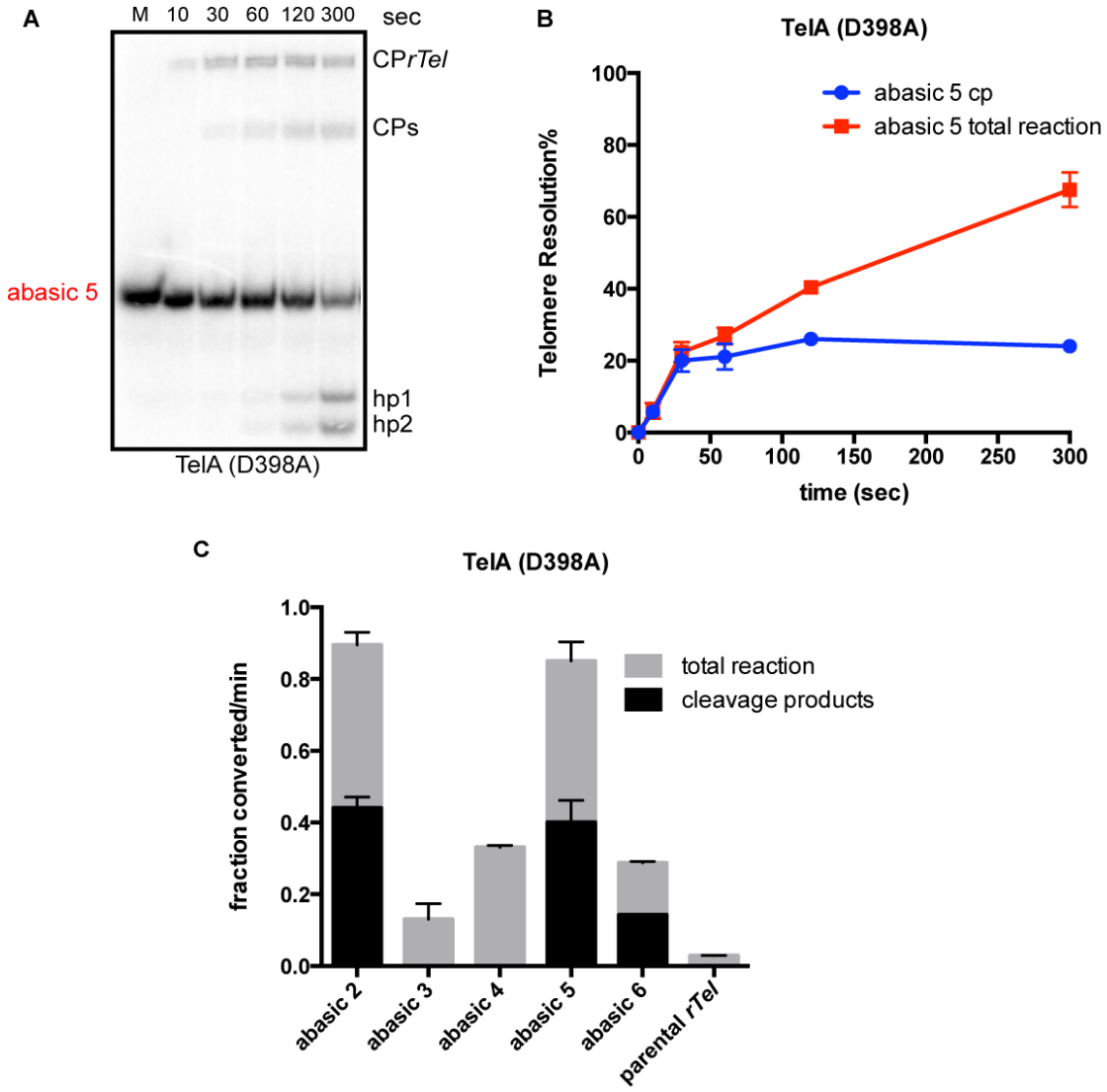

Figure 4.27. Results of assays with TelA (D398A) and missing base substrates. A) A representative example of an 8% PAGE, 1X TAE/0.1% SDS gel panel of a timecourse reaction of TelA (D398A) with abasic 5 incubated at 30°C. The mobility of the substrate in the gel is represented by abasic 5. CP*rTel* marks the migration of a product that TelA has cleaved only one strand; CPs is the gel migration of the cleavage products; M stands for mock protein-free reaction. **B)** The % of cleavage products and total reaction *vs.* reaction time plot of telomere resolution reaction with TelA (D398A) and abasic 5 at 30°C. **C)** Comparison of the initial rates of cleavage product formation and the rate of the total reaction of the parental *rTel* and the substrates with missing substrates with TelA (D398A). The initial rates are demonstrated as the fraction substrate converted/min (1.0 being 100% conversion). The mean and standard deviation of at least three separate replicates are displayed. The gray bars indicate the total reaction, and the black bars indicate the cleavage products.

The previous study on ResT revealed that ResT (D328A) can make hps out of overhangs that are shorter than the standard 6-nt length, therefore, do not have self-complementarity to aid hairpin formation (Lucyshyn et al., 2015). It was inferred that ResT (D328A) may have reduced fidelity at the hairpin formation/DNA strand rejoining steps of

telomere resolution (Lucyshyn et al., 2015). We were expecting the same behavior for TelA (D398A), however, the formation of hps from short overhangs was not detected in assays with nicked *rTels* (Figure 4.28). We concluded that although the nick substrates increased the flexibility of the substrate resulting in the robust rescue of the reaction with TelA (D398A), the fidelity of the hairpin formation/DNA strand rejoining step of the reaction was unaffected by the D398A mutation when used with nicked *rTel* substrates. However, the results with TelA (D398A) when assayed with mismatches and missing base modifications near the scissile phosphate suggest a modest decrease in the fidelity of hairpin formation (see Figures. 4.11 and 4.12 for the activity of WT TelA with these modifications).

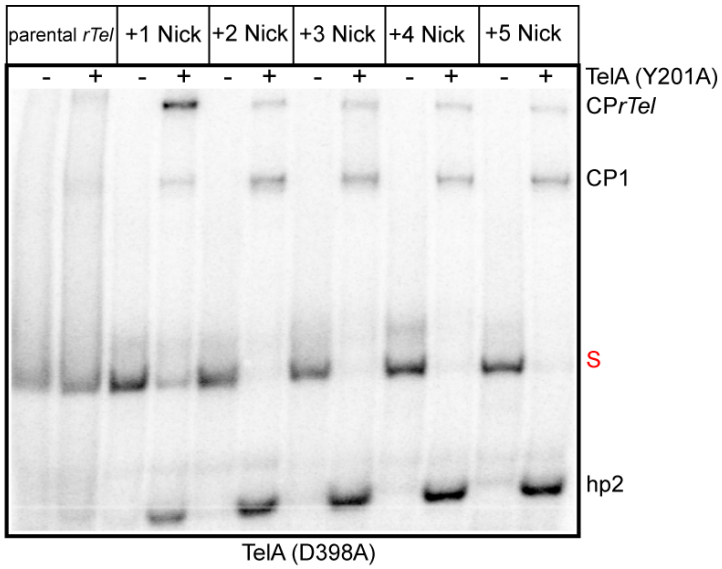

Figure 4.28. Telomere resolution of TelA (D398A) with nick modified substrates. A representative 8% PAGE/ 1X TAE/0.1% SDS gel panel of the endpoint reactions of TelA (D398A) and the nick substrates incubated at 30°C for 10 minutes. The mobility of the substrate in the gel is represented by S; CP*rTel* marks the migration of a product that TelA has cleaved only one strand; CP1 is gel migration of the cleavage products; hp2 is the position the of the hairpin telomere product on the gel. + indicates the reactions incubated with protein; - indicates protein-free mock reactions.

4.6. Results with TelA variants with a cold-sensitive phenotype

The activity of a group of TelA variants was comparable to WT TelA at 30°C, however, at lower incubation temperatures these variants had reduced activity compared to WT TelA reacted with parental *rTel* substrates. We named this group of variants as 'cold-sensitive variants'. Most of these variants were selected by the homology with the residues in ResT found to be involved in stabilizing the pre-cleavage intermediate (Bankhead and Chaconas, 2004; Lucyshyn et al., 2015). We inferred that these residues might make indirect interactions, such as water-mediated interactions, with nucleotides between the scissile phosphates or alternatively to the sugar-phosphate backbone.

4.6.1. Are the cold-sensitive variants properly folded?

The refolding of the cold-sensitive variants was checked with single-stranded DNA annealing and *rTel* binding assays (Figure 4.29). They were mostly properly folded, although a markedly impaired annealing reaction with TelA (T401A) was observed and a lower affinity for the *rTel* substrate. As the telomere resolution activity of TelA (T401A) is normal at 30ºC and its activity at 12ºC could be rescued by the mismatch substrates (shown in the following section), we were confident that the deficiency in telomere resolution activity was not from improper folding. In addition, TelA (T401A) telomere resolution activity was comparable to WT TelA at 30°C but different at lower temperatures.

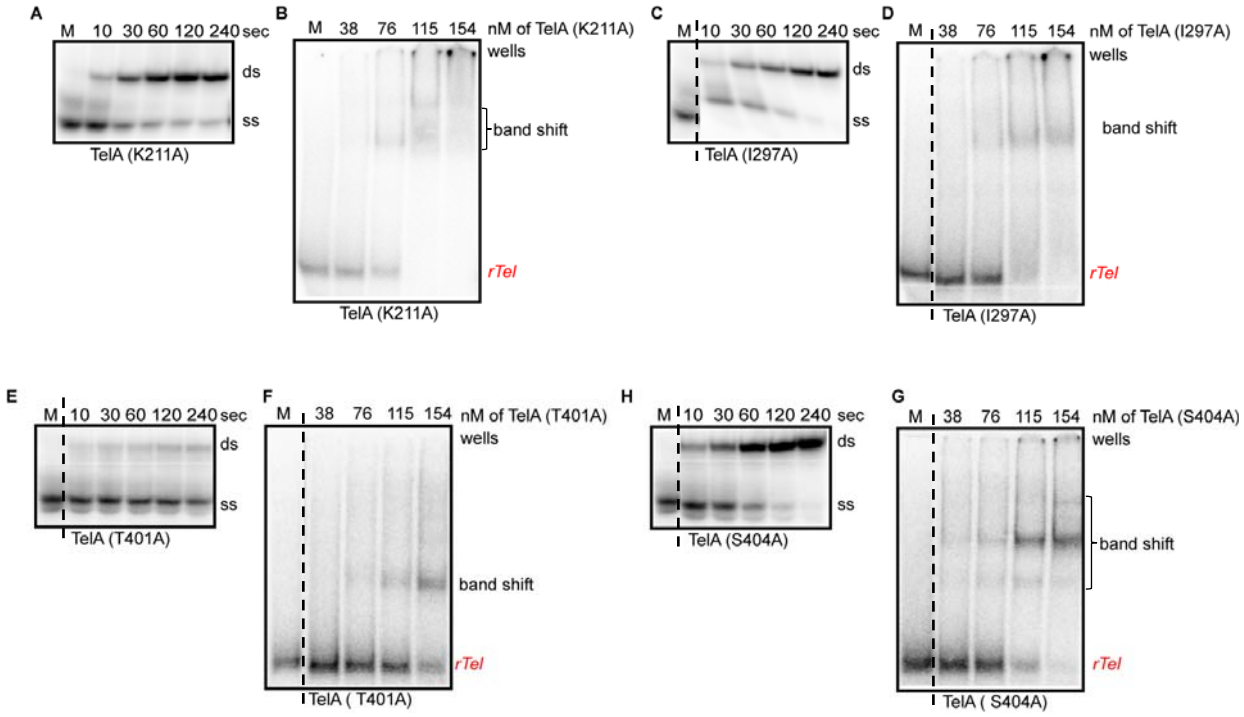

Figure 4.29. Folding of cold-sensitive TelA variants assessed by activity in ssDNA annealing and *rTel* binding assays A) A representative example of 8% PAGE/ 1X TAE/ 0.1% SDS gel panels of timecourse reactions with TelA (K211A) and TAR oligonucleotide. The gel mobility of 5'-^{32}P endlabeled TAR oligonucleotide is shown as ss, and the double-strand product is shown as ds. **B)** A representative example of 6% PAGE/ 0.5X TBE gel panel of endpoint reactions of a titration of TelA (K211A) and *rTel* incubated at 0°C for 20 minutes. Band shift indicates gel mobility of the TelA bound to *rTel*, *rTel* in red color indicates the *rTel* substrate; The upper band of the band shift indicates the gel mobility of the dimer of TelA bound to *rTel* and the lower band indicates the binding of one monomer. The other gel panels followed the same labeling convention. M stands for mock protein-free reaction. Irrelevant samples are removed. Displacement is indicated by dash line.

4.6.2. Results with the cold-sensitive variants

The assays with mismatch substrates were performed with the cold-sensitive variants at 12°C. The results showed that the reaction with each variant can be rescued to some extent. Similar to the results obtained with most of the severely defective variants, MM4 was the most stimulatory substrate for each cold-sensitive variant (Figure 4.30). TelA (K211A) and TelA (I297A) showed a more severe phenotype than the other cold-sensitive variants. Rescue of TelA (S404A) by the MM3 and MM4 *rTels* was much more marked than for the other variants, though no rescue was apparent with any other mismatch substrates. It should be noted that the control mutant *rTel*s were all inactive at 12°C (results not shown). As the cold-sensitivity of WT TelA was not significantly rescued by the abasic substrates, the cold-sensitive variants were not examined with the missing base substrates.

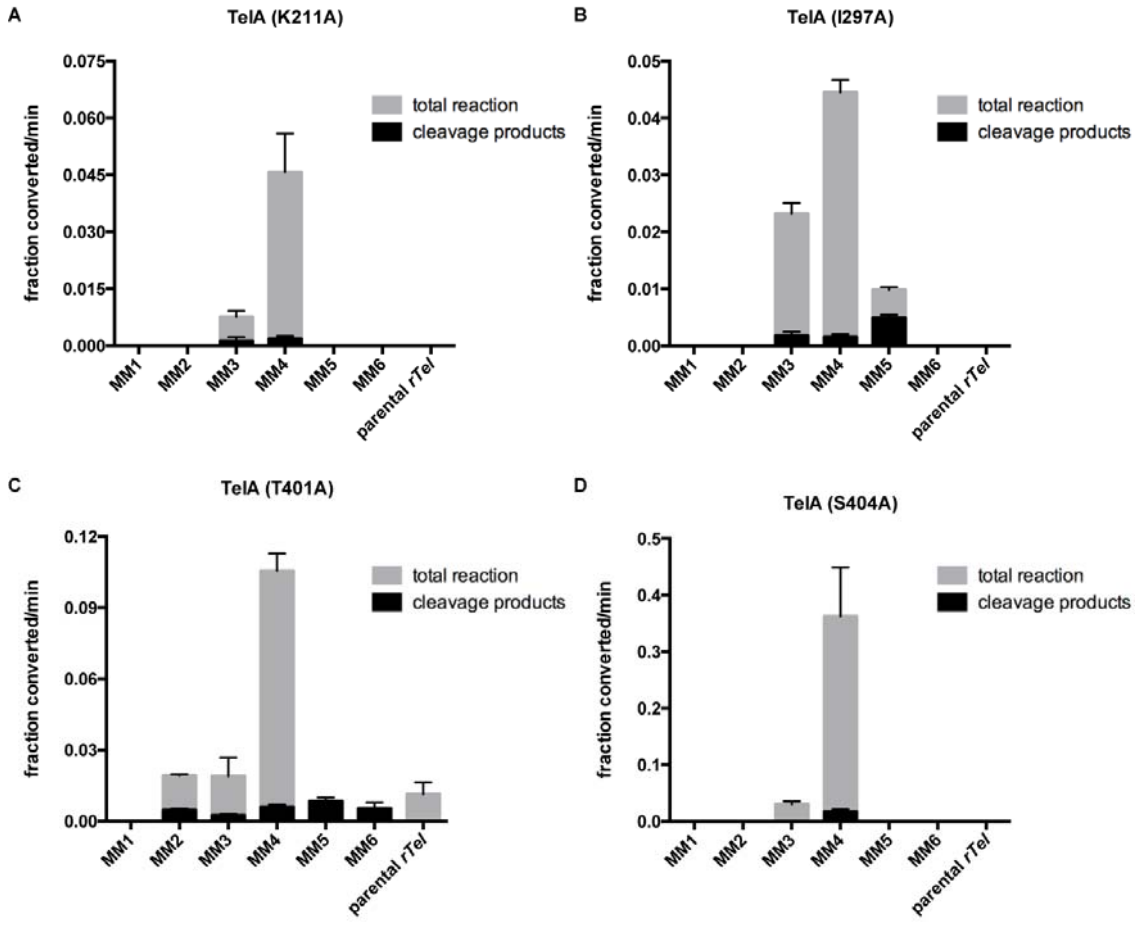

Figure 4.30. The results of the assays with the cold-sensitive variants and mismatch substrates. Comparison of the initial rates of cleavage product formation and the rate of the total reaction of the parental *rTel* and the substrates with mismatches. The initial rates are demonstrated as the fraction substrate converted/min (1.0 being 100% conversion). The mean and standard deviation of at least three

separate replicates are displayed. The gray bars indicate the total reaction, and the black bars indicate the cleavage products.

4.7. Results with alternative mismatch 4

4.7.1. Results with WT TelA

By changing the T to C at position 4 of the *rTel*, to introduce a mismatch, TelA was significantly activated by the presence of this mismatch but not by the corresponding control mutation that restored basepairing to the *rTel*. Since the activation of the reaction with MM4 was so dramatic the impact of a different change at position 4 of the *rTel* was tested with an alternative mismatch at this position. We changed the T to G (pyrimidine to purine) and called the substrate MM4G while the original MM4 was now referred to as MM4C. The control mutants in which basepairing is restored now became mutant 4C and mutant 4G. MM4G activated the reaction almost as well as MM4C but reaction stimulation was also accompanied by a visible accumulation of CPs not apparent with MM4C. Interestingly, 45% of the reaction stimulation of the MM4G *rTel* seems to have been the result of the sequence change rather than the mismatch since mutant 4G was much preferred over the parental *rTel* sequence (Figure 4.31). This property makes the MM4G substrate less useful than the original MM4C *rTel*; nonetheless, the severe TelA variant were assayed with MM4G and its corresponding control mutant (mutant 4G).

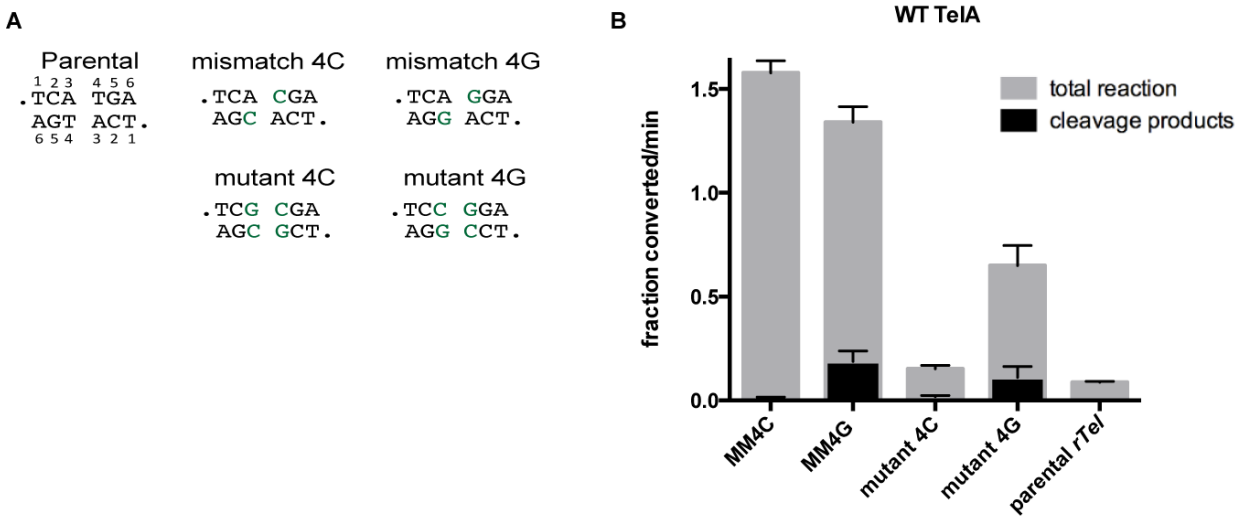

Figure 4.31. The results of the assays with mismatch4G. A) The representation of the MM4G modification between the scissile phosphates of the *rTel*. The green letters represent the mismatch modification, and the dots represent the position of scissile phosphates. **B)** Comparison of the initial rates of cleavage product formation and the rate of the total reaction of the parental *rTel* and the MM4 modifications and control mutant substrates with WT TelA at 30°C. The initial rates are demonstrated as

the fraction substrate converted/min (1.0 being 100% conversion). The mean and standard deviation of at least three separate replicates are displayed. The gray bars indicate the total reaction, and the black bars indicate the cleavage products.

4.7.2. Results with severely defective TelA variants assayed with MM4C *vs.* MM4G.

The results showed all the severe variants, except TelA (D398A), were more active with MM4C compared to MM4G (Figure 2.31). Studies on mismatches in DNA have proposed that the formation of a tautomeric form, such as A-C base pair, causes slight changes in double helix conformation as it is stereochemically similar to standard Watson-Crick base pairs (Watson and Crick, 1953). In addition, the formation of purine-purine base pairs was proposed to be possible through syn orientation for at least one of the purines, otherwise, it will be too large to fit into the double helix (Brown et al., 1986). Although MM4G rescued the reaction considerably, however, due to the mentioned reasons, MM4G was not a better substrate than MM4C. Additionally, as for WT TelA, some of the reaction rescue of the severe TelA variants seen with MM4G was due to the sequence change rather than the mismatch. As mentioned above, TelA (D398A) preferred MM4G *rTel* over MM4C. Some influence of the base identity at position 4 with this variant may indicate a direct contact with position 4 by this residue (the direct contact is discussed in detail in section 5.1)

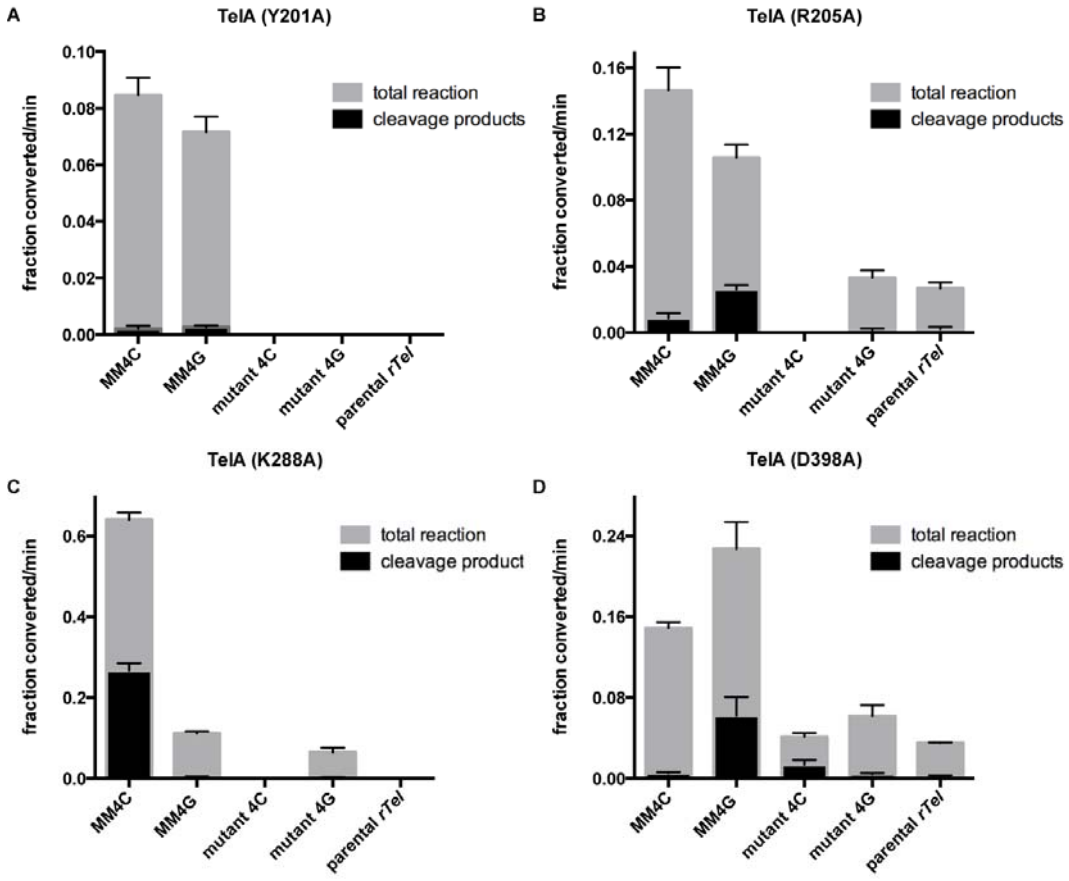

Figure 4.32. The results of assays with the severely defective TelA variants and alternative mismatch 4 *rTels*. Comparison of the initial rates of cleavage product formation and the rate of the total reaction of the parental *rTel* and the mismatch 4 modifications substrates with severely defective variants at 30°C. The initial rates are demonstrated as the fraction substrate converted/min (1.0 being 100% conversion). The mean and standard deviation of at least three separate replicates are displayed. The gray bars indicate the total reaction, and the black bars indicate the cleavage products. The scale of Y-axes is different for each protein as their activity of them are different from each other.

4.8. Results with half-site substrates

4.8.1. Results with parental and mismatch 1C half-site substrates

The severely defective TelA variants could appear inactive on parental *rTel* substrates if the enzyme goes through abortive cycles of DNA strand cleavage and rejoining to reform the substrate DNA. Reactions producing such abortive cycles would look the same as reactions where DNA cleavage never occurred; therefore, we would not be able to differentiate between the variants that are cleavage defective (unable to initiate the reaction) from the cleavage competent variants that were blocked at a later reaction stage. To classify our variants as either cleavage competent or incompetent, we used a class of suicide substrate called a half-site (Figure 4.33). The half-site substrate removed the complication of potentially needing to melt

and/or unwind the DNA to activate DNA cleavage. Additionally, resealing half-site substrates is not possible for TelA as the nucleotide on the other side of the scissile phosphates diffuses away, trapping TelA in a phosphotyrosine linkage with the cleaved DNA. We designed half-sites with parental and MM1C sequences. In addition to blocking the resealing of the substrate, MM1C hinders hairpin formation as the very first base pair that would form in the refolding strand is disrupted; therefore, the reaction, if initiated, would be trapped at the cleavage step (Figure 4.33a). We also needed to use a different gel system called denaturing gels containing urea in addition to other components of SDS PAGE gels. In these gels, the basepairing in double DNA helix is broken by the heating the samples which helps us to differentiate the hairpin products and the substrate. The urea in the gel system would help to keep the basepairing broken in the hairpin products.

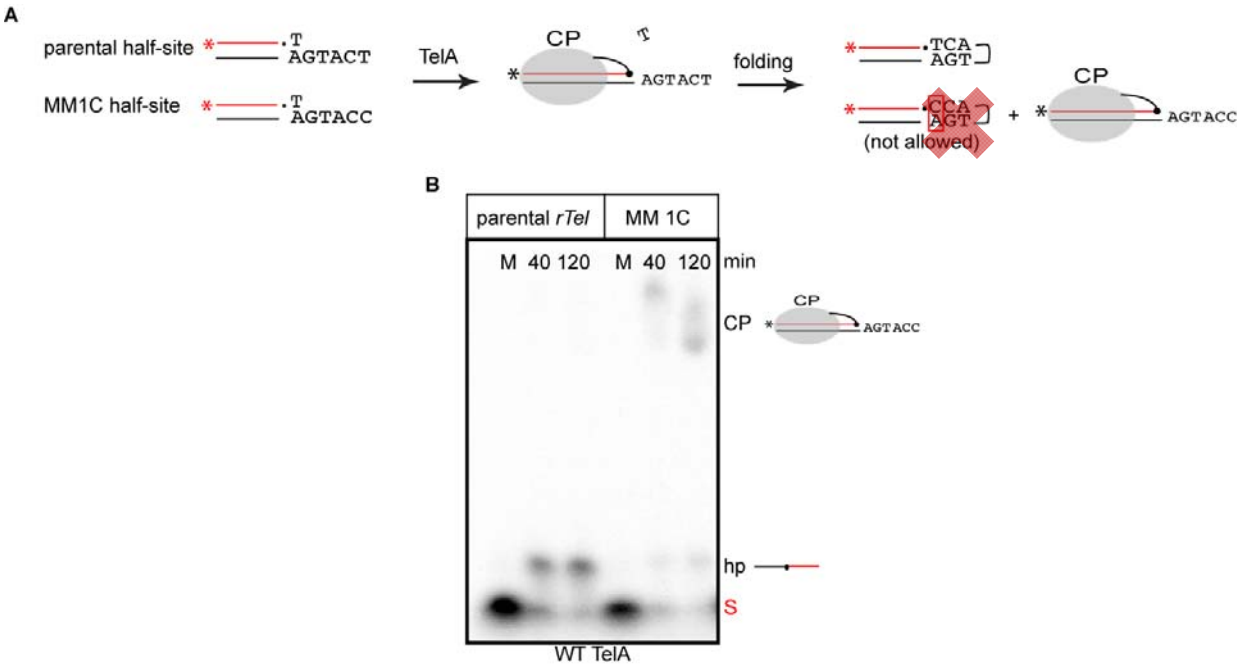

Figure 4.33. The results of assays with half-site substrates and WT TelA. A) The representation of the half-site substrates and the reaction pathway with WT TelA. The 5'-^{32}P endlabeled top strand is represented by the red color line, the red asterisk indicates the 5'-^{32}P endlabeling, and the scissile phosphates are represented by dots. The diagonal T indicates the other side of scissile phosphate that diffuses away after cleavage. The semi-transparent red X indicates the disallowance of hairpin formation with the MM1C half-site. **B)** The representation of 8% PAGE, 1X TBE, 6M Urea, and 0.1% SDS gel panel of a timecourse reaction with WT TelA and half-site substrate incubated at 30°C. This gel system is denaturing for both DNA and protein. S represents the gel mobility of the heated substrate; hp is the hairpin product after heating at 95°C and snapped cooled; CP represents the cleavage products; M stands for mock protein-free reaction.

4.8.1.1. The results with severely defective TelA variants assayed with half-site substrates

Our in-depth biochemical analysis is in poor agreement with structural model proposed by (Shi et. al., 2013). The assessment of the severely defective TelA variants with the half-site substrates showed that TelA (Y201A) and (R205A) were cleavage defective. TelA (D398A) was also established as being defective for DNA cleavage. There was no activity with this set of substrates (Figure 4.34, a, b and d). On the other hand, TelA (K288A) was found be to cleavage competent which means that TelA (K288A) cleaves and rejoins the parental *rTel* in abortive cycles. Similar to WT TelA, reactions with TelA (K288A) made hairpins with the parental half-site and made CPs with half-site MM1C (Figure 4.34c). Since TelA (K288A) is cleavage competent, CP accumulations in the reactions with TelA (K288A), might indicate that mismatch and missing base *rTel*s partially prevent regeneration of the substrate *rTel* and trapping the reaction when hp formation is blocked.

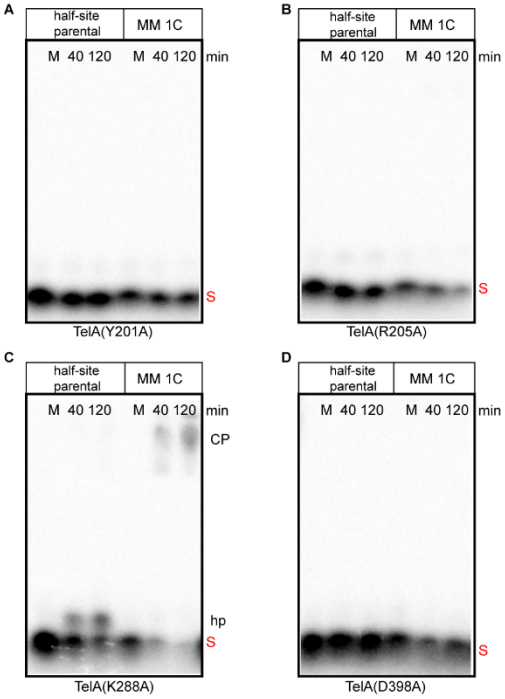

Figure 4.34. The results of assays with severely defective TelA variants reacted with half-site substrates. 8% PAGE, 1X TBE, 6M Urea, and 0.1% SDS gel panels of timecourses with severely defective variants incubated at 30 °C. S represents the gel mobility of the heated substrate; hp is the hairpin product after heating at 95°C and snapped cooled; CP represents the cleavage products; M stands for mock protein-free reaction.

4.8.1.2. The results of assays with the cold-sensitive TelA variants and the half-site substrates

In contrast to the results with the severely telomere resolution defective TelA variants, all of the cold-sensitive variants were found to be cleavage competent at 12ºC (Figure 4.35).

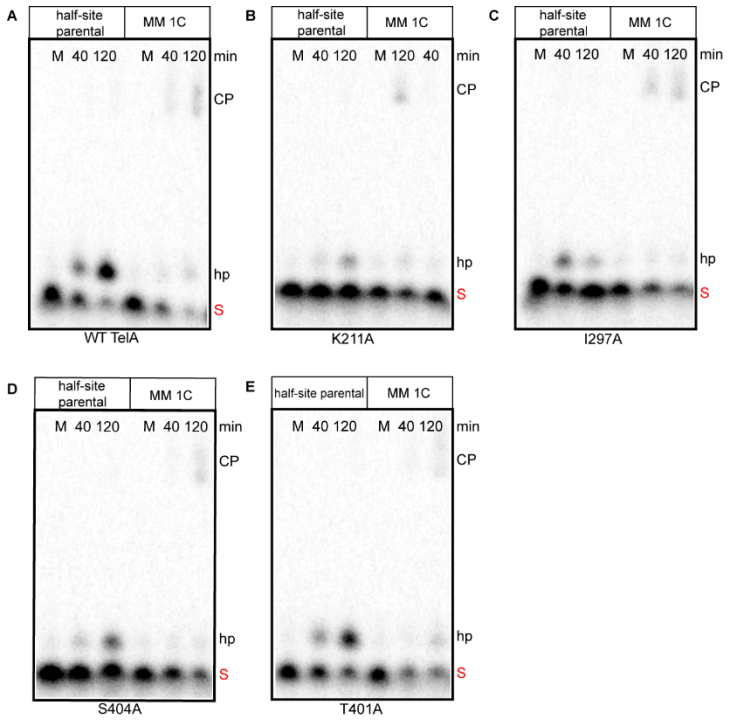

Figure 4.35. The result of assays with cold-sensitive TelA variants tested with the half-site substrates. 8% PAGE, 1X TBE, 6M Urea, and 0.1% SDS gel panels of timecourse with cold-sensitive variants incubated at 12 °C. These variants were able to make hairpins with parental half-site substrates. S represents the gel mobility of the heated substrate; hp is the hairpin product after heating at 95°C and snapped cooled; CP represents the cleavage products; M stands for mock protein-free reaction.

4.8.2. Results with parental and abasic half-site substrates

The results with the mismatch and abasic substrates generated the idea to test abasic 5 and 6 half-site substrates with our variants, especially with TelA (Y201A) (Figure 4.36). The proposed model based on crystallography data, suggeted that Y201 is stacked against A6 which has an out-of-helix conformation. In contrast, our biochemical data indicates the base at position 5, rather than position 6, might flip out and Y201 stabilizes it as the abasic 5 rescued the reaction with TelA (Y201A). We believe that the details of the structural model are not correct. Our biochemical model suggests a one-nucleotide shift in the refolding structure (the model is discussed in detail in section 5.2). However, we could not directly test either model since TelA (Y201A) was found to be cleavage defective, in contrast data reported by Shi et. al. (Figure 4.37). We believed the reaction conditions used in the crystallography study might be the reason for the difference in results. The absence of divalent metal ions from the reaction buffer and the use of a ~100-fold higher concentration of TelA in the Shi et. al., study (6.7 μM *vs*. 76 nM) likely accounts for the different results between the two studies. It was reported that with divalent metal ion in the reaction buffer, much less TelA is required to drive complete reactions (McGrath et al., 2022). Additionally, as the result of the cleavage assays in Shi et. al. not being shown, making any judgment on the percentage of cleavage is not possible. Our use

of the identical substrate but with nM concentrations of enzyme and the presence of divalent metal ions probably constitutes more physiologically relevant conditions. Perhaps the addition of viscogens such as PEG, glycerol or sucrose, to our reactions, would produce crowding effects mimicking 100-fold more enzyme/substrate concentration used in the Shi et. al., study. This could, conceivably, harmonize our results with theirs.

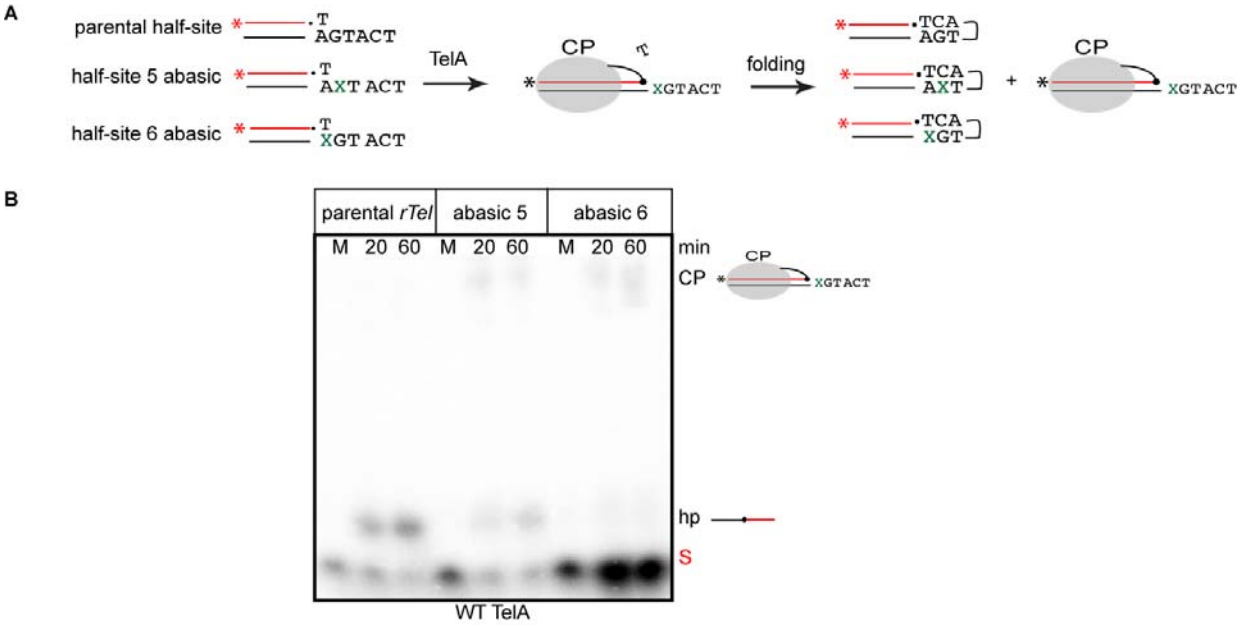

Figure 4.36. The result of the assay with WT TelA and abasic half-site substrates. A) The schematic representation of parental and abasic half-site substrates and the reaction pathway with WT TelA. The 5'-32P endlabeled top strand is represented by a red color line, the red asterisk indicates the 5'-^{32}P endlabelling, and the scissile phosphates are represented by dots. The diagonal T indicate the other side of scissile phosphate that diffuses away after cleavage. **B)** 8% PAGE, 1X TBE, 6M Urea, and 0.1% SDS gels of timecourse reactions with WT TelA and parental and abasic half-site substrates incubated at 30°C. S represents the gel mobility of heated substrate; hp is the hairpin product after heating at 95°C and snapped cooling; CP represents the cleavage products; M stands for mock protein-free reaction.

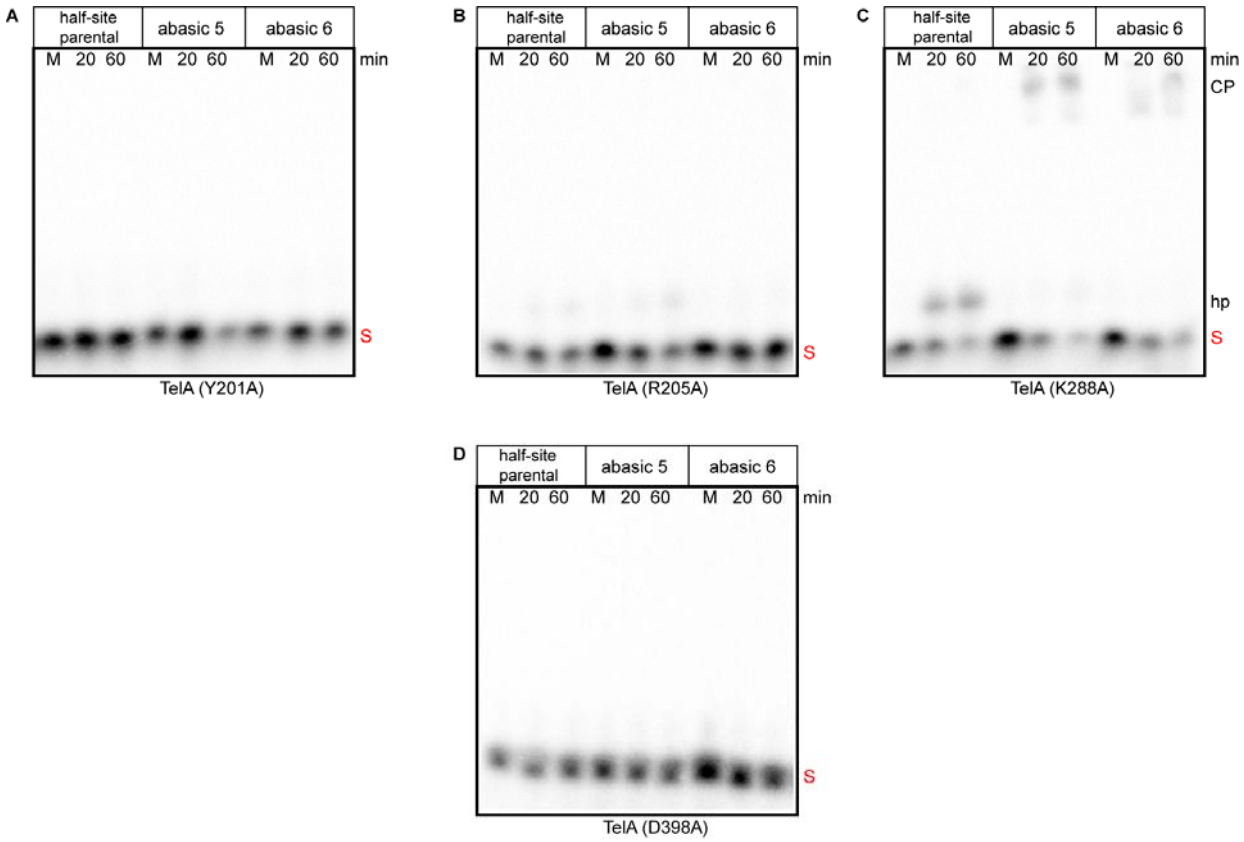

Figure 4.37. The result of assays with severely defective variants with half-site substrates. 8% PAGE, 1X TBE, 6M Urea, and 0.1% SDS gels of timecourse with cold sensitive variants incubated at 30°C. These variants were able to make hairpins with parental half-site substrates. S represents the gel mobility of heated substrate; hp is the hairpin product after heating at 95°C and snapped cooled; CP represents the cleavage products; M stands for mock protein-free reaction.

4.9. Results with plasmid substrates

The use of substrate modifications like mismatches and missing bases were only possible using *rTels* made from synthetic DNAs. However, when using the half-site substrates, we were concerned that the results may not accurately reflect the behavior of TelA on a full site. We addressed this potential problem with half-site substrates by cloning the parental *rTel* and a version of the mutant 1C *rTel* (5'-CCATGA-3') which blocks hairpin formation in a similar way as in the MM1C half-site, into pUC19. We first assessed the reaction of WT TelA and TelA variants with linearized parental *rTel* (Figure 4.38a). To verify the products of our proteins, contain hairpin telomeres, we used alkaline agarose gels which denature the double stranded DNAs (Figure 4.38b). The base pairing between the products with hairpin ends is broken in the denaturing alkaline agarose gel; therefore, they migrate at twice the size they do

in the native gel system. Unexpectedly, TelA (R205A) and (D398A) had low activity with plasmid substrates in contrast to their complete inactivity documented with oligonucleotide *rTels*. In the plasmid-based telomere resolution assay, TelA (Y201A) and TelA (K288A) were found to display the most defective phenotype.

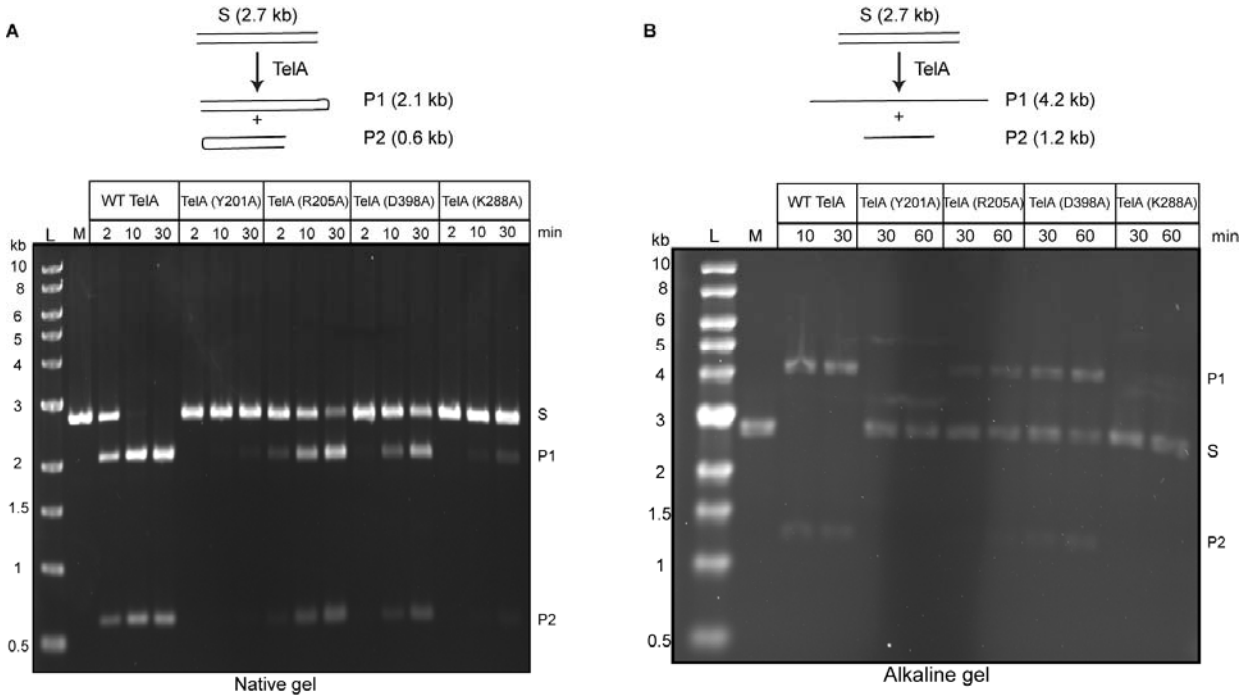

Figure 4.38. The result of assays with parental *rTel* on linearized plasmid. A) The representation of a native 0.8% agarose 1X TAE gel of timecourse reactions with WT and TelA variants incubated at 30°C. S represents the gel mobility of the plasmid substrate; the P1 and P2 represent the gel mobility of hairpin products; M stands for mock protein-free reaction. **B)** The representation of a denaturing 0.8% alkaline agarose gel of timecourse reactions with WT and TelA variants incubated at 30°C. S represents the gel mobility of the plasmid substrate; the P1 and P2 represent the gel mobility of hairpin products; M stands for mock protein-free reaction.

4.10. *rTel* plasmid relaxation assay

As mentioned before, TelA activity is topoisomerase IB-like regarding the mode of DNA strand cleavage and rejoining. The topology of DNA is controlled by DNA topoisomerases by this reversible DNA cleavage and rejoining mechanism. After binding to the DNA, topoisomerase IB cleaves one of the strands. The intact strand is free to rotate around the other strand. The result, after strand resealing is relaxation/removal of a DNA supercoil from the DNA. For the final step, the topoisomerase reseals the DNA backbone and detaches from it (Figure 4.39; (Nitiss et al., 2021)).

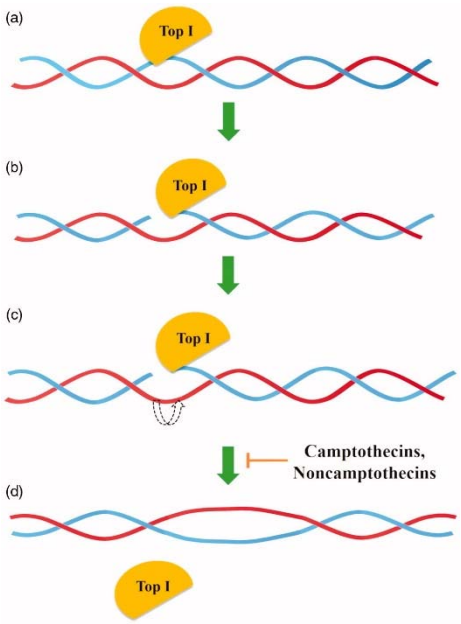

Figure 4.39. The schematic representation of topoisomerase activity of a type I DNA topoisomerase. Topoisomerase (TopI) binds to backbone of DNA. TopI cleaves one strand (blue) by attacking the phosphorus group. The other strand (red) can rotate around the DNA strand. TopI relegates the cleaved DNA strand results in more relax supercoiled DNA (Buzun et al, 2020).

As the mutant 1C *rTel* blocks hairpin formation TelA was expected to reseal the cleaved strand quickly when hairpin formation was blocked in any variant of TelA that was cleavage competent. This activity of TelA can be related to topoisomerase activity rather than telomere resolution. With the mutant 1C *rTel* on a supercoiled plasmid, WT TelA relaxed the substrate by cleavage and resealing each time which results in a ladder of topoisomer bands in an agarose gel, indicating different stages of plasmid relaxation. In contrast to the results with half-site MM1C, TelA (R205A) and (D398A) were found to be cleavage competent as the ladder of topoisomers was readily detected. TelA (D398A) showed an unexpected additional character of forming plasmid multimers, probably reflecting activation of a latent site-specific recombination activity between parental *rTels* also characterized for ResT (Kobryn et al., 2009). The basis of this altered reactivity will require more investigation. Nonetheless, TelA (D398A) also produces topoisomers with the mutant 1C *rTel* indicating that it is cleavage competent in this context (Figure 4.40). Even though TelA (R205A) and (D398A) were more active with the plasmid substrates, TelA (Y201A) was still a severely defective variant showing no telomere resolution or DNA cleavage activity. TelA (K288A) was also defective for telomere resolution, but it was cleavage competent.

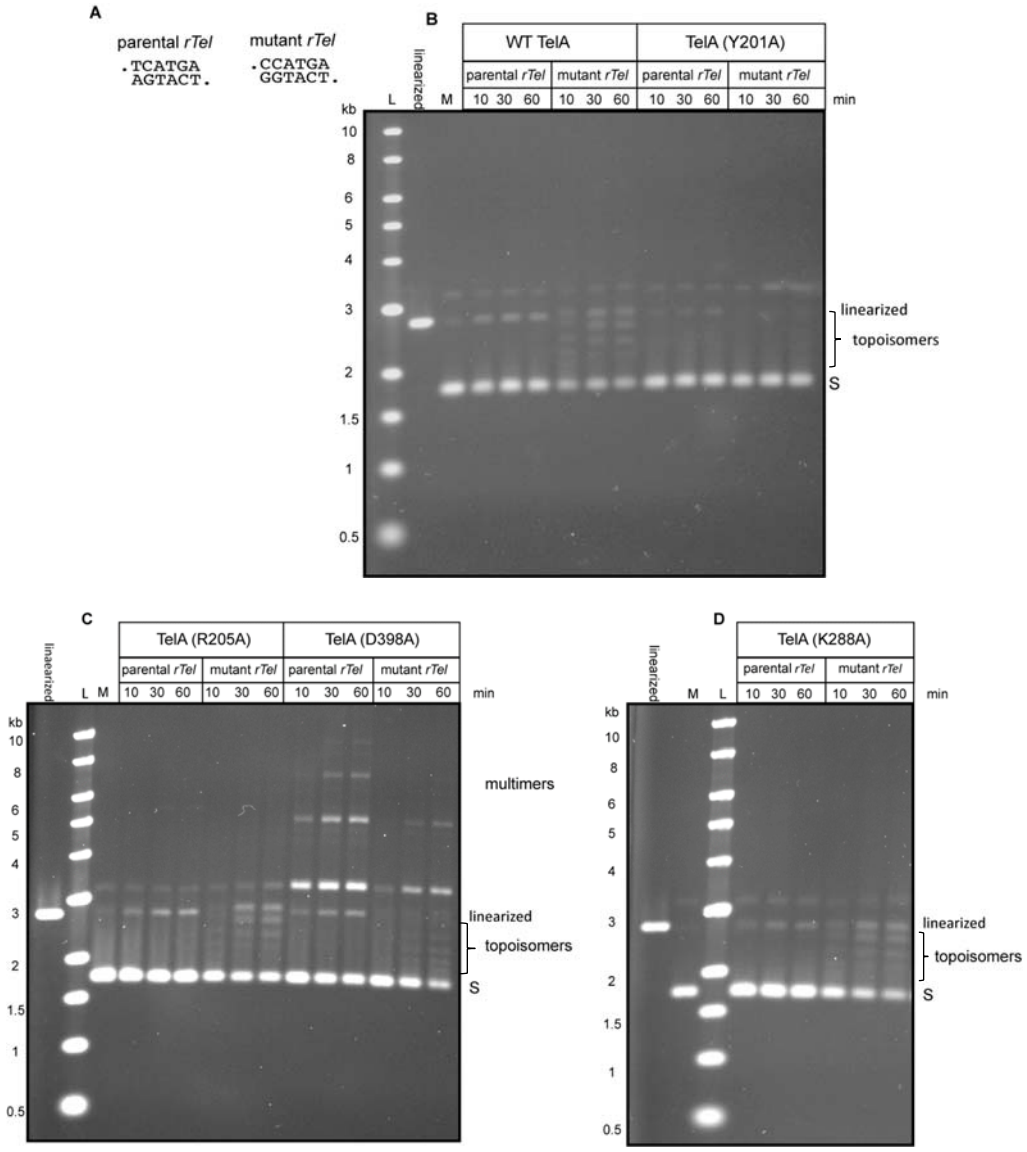

Figure 4.40. Assaying for topoisomerase activity of severely defective TelA variants with supercoiled substrates. The representation of 0.8% agarose gel of timecourse reaction with WT and variants TelA incubated at 30°C. S represents the gel mobility of the plasmid substrate. The migration of products are labeled accordingly.

4.11. Summary of results

Table 4.1. The comparison of results of TelA and ResT in pre-cleavage intermediate studies

TelA	Result with MM	Result with abasic	ResT	Result with MM	Result with abasic
Y201A	Rescued with MM4,5 and 6	Made hp with abasic 5	Y145A	Not investigated	Not investigated
R205A	Rescued with MM4	Rescued with abasic 5	H147A	Not investigated	Not investigated
K211A	Cold sensitive, rescued with MM3 and 4	Not investigated	K150A	Not investigated	Not investigated
K288A	Rescued with MM4	Made hp with abasic 4	K225A	Not investigated	Not investigated
I297A	Cold sensitive, rescued with MM3 and 4	Not investigated	V231A	Cold sensitive, rescued with MM1 and 2	Rescued with abasic 2
D398A	Rescued with MM3	Rescued with abasic 2 and 5	D328A	Made hp with MM1 and 2	Rescued with abasic 2
T401A	Cold sensitive, rescued with MM3 and 4	Not investigated	T301A	Not investigated	Not investigated
S404A	Cold sensitive, rescued with MM3 and 4	Not investigated	H334A	Made hp with MM1	Rescued with abasic 6

Table 4.2. The comparison of results of biochemical and structural studies on TelA

Results / Residues	Biochemical	Structural
Y201A	Stacks against G5	Stacks against A6
R205A	Interacts with T4, ejection of refolding strand with its positive charge	Interacts with T4, ejection of refolding strand with its positive charge
K211A	Interacts with A3 and T4 by water-mediated interaction or with backbone	Interacts with DNA backbone between T-2 and A-3 near scissile phosphates
K288A	Interacts with T1, C2 and A6	Interacts with T1 and C2
I297A	Interacts with A3 and T4 by water-mediated interaction or with backbone	On a loop near hp turnaround but not in contact with DNA
D398A	Interacts with T4 and possibly G5	Interacts with back bone of DNA between T1 and C2
T401A	Interacts with A3 and T4 by water-mediated interaction or with backbone	Positioned near scissile phosphates
S404A	Interacts with A3 and T4 by water-mediated interaction or with backbone	Interacts, via water, with backbone between A-1 and T-2 near scissile phosphates

5. Discussion

Among telomere resolvases that have been characterized, most biochemical analyses were performed on borrelial telomere resolvase, ResT. ResT was found to possess ssDNA annealing and an ATP-dependent, 3’-5’ unwinding activity, in addition to its primary telomere

resolution activity (Mir et al., 2013; Huang et al., 2017). The biochemical studies conducted in the Kobryn lab on the agrobacterial telomere resolvase, TelA, were initiated by characterizing TelA's telomere resolution activity and determining whether TelA is also multifunctional (McGrath 2021., McGrath 2022). Previously, a structural study captured the refolding intermediate and TelA complex bound to its hp telomere products. The structures provided model of the TelA interactions with these different DNA structures (Shi et al., 2013). Half-site substrates, suicide half-site substrates, and TelA variants were used in the crystallography study. Excellent data, therefore, are available for TelA in the last two steps of telomere resolution.

On the other hand, the 'spring-loading model' was proposed for the telomere resolution pathway in the ResT system and focused on the early steps of telomere resolution (Lucyshyn et al., 2015). This model suggests that the hairpin-binding module and the catalytic domain of ResT are involved in stabilizing an underwound conformation of the DNA between the scissile phosphates at a stage before DNA cleavage has occurred. The underwound conformation is thought to promote telomere resolution. This underwound intermediate ensures the strand ejection to prevent the regeneration of substrate. These available data and comparability of size and sequence homology of TelA to ResT led the hypothesis that TelA and ResT share a similar telomere resolution pathway. If TelA uses the pre-cleavage spring-loaded reaction mechanism like ResT, an almost complete pathway would be defined for telomere resolution promoted by TelA. We studied the phenotypes of TelA with mutations in the residues that have homology with the ones in ResT with crucial roles in 'spring-loading' telomere resolution, in addition to the residues that had been reported to make interactions with the sequence between the scissile phosphates in the telomere resolution process from structural studies (Figure 5.1; (Shi et al., 2013; Lucyshyn et al., 2015)).

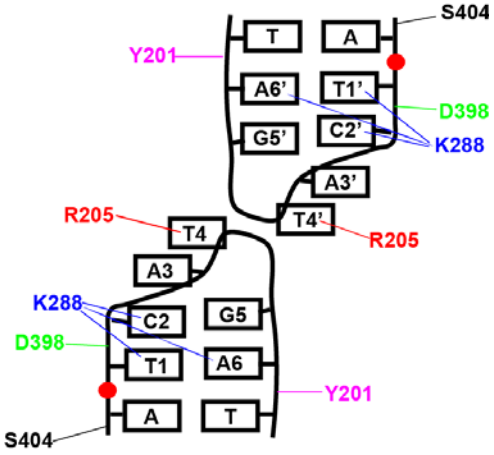

Figure 5.1. The summary of the interactions of key residues in TelA with the hairpin products. The interactions of the TelA residues with the sequence between the scissile phosphates are shown by direct lines to the bases or the backbone of the DNA. The scissile phosphates are represented by red dots. The *rTel* sequence is numbered and the top and bottom strands are divided by apostrophes. The model is derived from the 4e0g (pdb) (Shi et al., 2013).

5.1. The pre-cleavage intermediate

The initial results with parental *rTel* and the TelA variants showed a deficiency in telomere resolution either at 30°C for TelA (Y201A), (R205A), (K288A) and (D398A). However, the reactions can be rescued with substrates that mimic the melting of the DNA between the scissile phosphates. We inferred from results with mismatches and missing base substrates that the basepairing of the four central basepairs between the scissile phosphates are broken, likely prior to the initiation of DNA cleavage. A pre-cleavage intermediate is probably formed where the A3 and T4 are in the helix. G5 flips out of the helix and C2 remains in the helix without a partner (Figure 5.2). As the abasic 3 and 4 *rTels* were poor substrates generally, we concluded that the presence of these two bases may be crucial for the later strand refolding step and the stabilizing of the base across the dimer axis in a basepair between the refolding strands. When a specific MM *rTel* activates a variant, it is likely that the direct contact of the residue is with the unchanged base. For instance, MM3 activates the reaction with TelA (D398A) which is otherwise profoundly deficient for telomere resolution on a parental substrate. Therefore, D398 can be inferred to make direct contact with base 4 (T4), with the broken basepair between positions 3 and 4 activating the reaction. The reverse case is also possible as well where changing the base with another base was acceptable to activate the reaction.

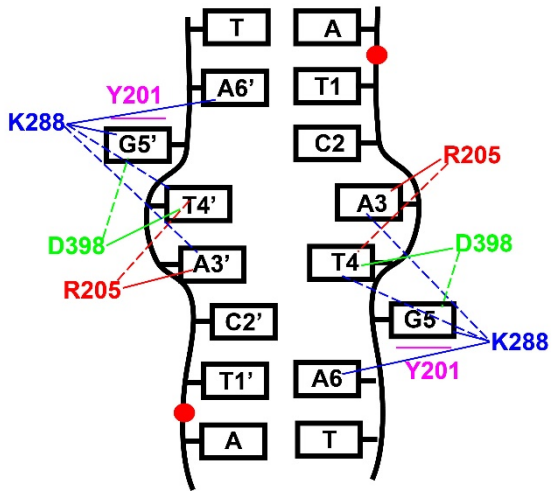

Figure 5.2. The model of a pre-cleavage intermediate in the TelA system. The underwound basepairs are shown as a bubble. The flipped-out base is shown by facing outside of helix. The scissile phosphates are shown by red dots. The direct interactions are shown by solid lines. The alternative/possible interactions are shown by dashed lines. The magenta line over/under the G5 base models a stacking interaction with the aromatic ring of the Y201 residue and the base.

5.2. The strand refolding intermediate

We proposed a new model for the refolding intermediate in TelA that takes into account the functional/biochemical results shown here. We proposed that the stabilization across the dimer axis happens between A3 and T4 with canonical basepairing, instead of T4 and G5 with non-canonical basepairing. Our results, especially with TelA (Y201A) and (R205A), did not agree with previous results from the structural study (Shi et al., 2013). In the structural model, Y201 stacks against A6. We were expecting abasic 6 to partially rescue the reaction with TelA (Y201A). However, abasic 5 activated hairpin formation without the accumulation of CPs, and abasic 6 was completely inactive. Considering the structural model showed Y201 stacking with A6 we expected the 6 abasic substrate to at least activate the TelA (Y201A) mutant for DNA cleavage. In the refolding intermediate we suggested, if there is any stacking interaction, it happens with G5 (Figure 5.3). However, we were not able to test our hypothesized model as a second discrepancy with the reported data was found. TelA (Y201A) and (R205A) were reported as cleavage competent with half-site substrates. Our data showed that these two variants were cleavage defective with this type of substrate under the reaction conditions we employed. Our data, collected under more physiologically relevent conditions than Shi et. al might explain to the differences between the two studies (Shi et al., 2013). However, our findings are in good agreement with Shi et. al data in that TelA (R205) is inferred to interact with T4, and the positive charge of its sidechain would help the strand ejection and prevent the reformation of the substrate.

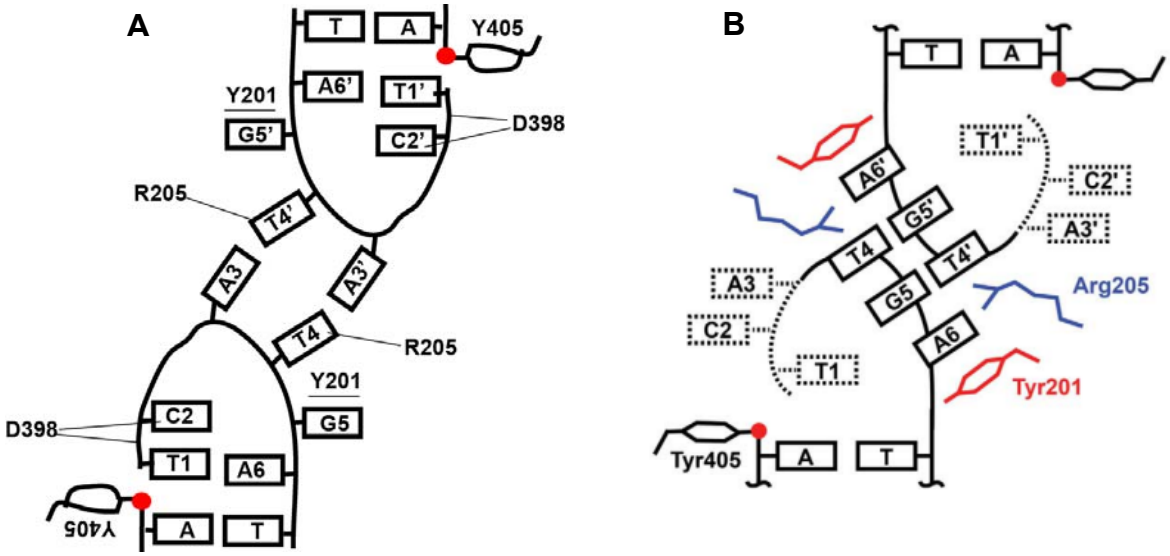

Figure 5.3. The comparison of our strand refolding intermediate model and the reported structure. A) The proposed model of the refolding strand intermediate based on our data. The canonical basepairing to promote the strand refolding happens between A3 and T4. TelA (Y201) stacks against G5 to stabilize it as it flips out of the helix. The positive charge of TelA (R205A) ejects the strand to prevent the reformation of the substrate. **B)** The crystallized structure of refolding strand intermediate. The non-canonical basepairing is formed between T4 and G5. A6 is stabilized by Y201. The difference between our model and structure is a shift of one nucleotide. The scissile phosphates are shown by red dots. The catalytic residue, TelA Y405, is still bound to the scissile phosphate in the strand refolding intermediate. This figure is modofied from (Shi et al., 2013). Part B was shown in figure 1.11, previously.

We attempted to find out if the TelA variants act before or after DNA cleavage (or both) by classifying them as cleavage defective or competent. We determined that TelA (Y201A) likely acts on steps before DNA cleavage as it was inactive for the cleavage step on both half-site and plasmid substrates. TelA (K288A) probably has a role at the steps after cleavage as this variant was found to be cleavage competent on all tested substrates. However, we faced contradictory results for TelA (R205A) and (D398A). These variants showed topoisomerase activity but inactive with half-site substrates. Therefore, predicting the step these residues act on requires more investigation as discussed in the following chapter.

6. Conclusions and future directions

6.1. Conclusions

We conclude that for TelA there is likely an underwound pre-cleavage intermediate during telomere resolution similar to the one found in ResT where the sequence between the scissile phosphates is largely unwound. We propose a model that shows the contacts of TelA

residues with bases between the scissile phosphates that contribute to formation/stabilization of a pre-cleavage intermediate. Up to four basepairs are broken in this underwound intermediate. We also propose a new biochemical model of the refolding intermediate. Our findings indicate that there are stabilizing basepairs formed across the refolding strands is probably true. However, there are difference between our biochemical model and the structural model reported in previous study. Our biochemical model indicates a canonical basepairing between T's and A's *vs.* the T's and G's proposed in the crystal structure model which is a non-canonical basepair (Shi et al., 2013).

We also conclude that there are some differences between the phenotypes of telomere resolution promoted by TelA and ResT. First, TelA shows less cold-sensitivity in telomere resolution than what was observed in ResT. ResT was mostly inactive at 20°C whereas TelA inactivate for telomere resolution at 8°C. The cold-sensitivity in TelA was not rescued significantly by many of the modified substrates with disrupted basepairs between the scissile phosphates, with the exception of strong rescue afforded by MM4. It is possible that breaking the basepairing in the pre-cleavage intermediate is less crucial in telomere resolution by TelA. Another possible reason could be the fact that TelA makes more base-specific contacts between the scissile phosphates than ResT. ResT needs to recognize several different sequence variants between the scissile phosphates. The refolding intermediate in TelA might also contribute to the cold-sensitivity of telomere resolution of TelA. It is still unknown whether such an intermediate exists for telomere resolution ResT. The second difference in telomere resolution between ResT and TelA can be the detection of proper hairpin formation. It was demonstrated that a couple of residues in the catalytic domain of ResT are involved in detecting whether the basepairs are formed properly in the refolding hp. In case of formation of improper basepairs, these residues push the reaction to go backwards to regenerate substrate. These residues are also involved in the stabilization/formation of the pre-cleavage intermediate (Lucyshyn et al., 2015). Substitution of these residues to alanine resulted in ResT variants that could make hairpins without proper basepairing and even improper strand lengths. Our data did not support the same phenotype for the analogous residues in TelA (Figure 4.27).

There are some ambiguities in our model that need to be resolved. Because of the difference for cleavage competency, it is still unresolved whether our TelA variants act before,

after or both the cleavage step. Previous results with ResT showed that ResT always acts like a dimer *in vitro;* when half-site substrates are used the half-sites must assemble into a dimer arrangement that mimics the *rTel* (Briffotaux and Kobryn, 2010). However, under our conditions, it is entirely possible that TelA might work as a monomer on half-sites without the need to bring half-sites together into a mimic of the *rTel* (data not shown). A monomer of TelA might act on a half-site substrate rather than a dimer acting on half-sites brought together into an *rTel* mimic despite the fact that the structures that show a dimer of TelA bound to two hp's and that this was assembled from half-site substrates. It is not known if this possibility would yield different results than with a real *rTel* that must be processed by a dimer. To verify the result with half-site substrates would be the same as full site *rTel*s, we cloned a variant of the mutant 1C *rTel* into (mutant *rTel*) into a supercoiled plasmid. WT TelA and the cleavage competent TelA variants are able to cleave and rejoin one strand of the mutant *rTel* but are unable to make hairpins with this substrate. After cleavage, the supercoiled plasmid is free to swivel around the opposite strand and TelA rejoins the cleaved strand at the next step. This activity of TelA is more related to topoisomerase IB activity rather than to telomere resolution. It was expected that cleavage defective TelA variants show inactivity with this class of substrate, however, we observed topoisomerase activity with some variants that showed a cleavage defect with the half-site substrates. It was also noted that the reaction is generally much better with a WT (parental) plasmid substrate both with WT TelA and most of the tested TelA variants than for synthetic oligonucleotide substrates. Additionally, it is still formally possible that the topoisomerase activity noted with the mutant *rTel* plasmid could be due to TelA monomer action.

6.2. Future directions

Because of these potential complications the best follow-up substrate to classify our variants as cleavage competent or not would be a synthetic *rTel* with 5'-bridging phosphorothiolate modifications of the scissile phosphates. 5'-bridging phosphorothiolate substrates have been used in structural and mechanistic studies of enzymes such as vaccinia virus topoisomerase I, lambda integrase, and *Borrelia* telomere resolvase, ResT (Burgin, 2001; Burgin et al., 1995; Lucyshyn et al., 2015; Stivers et al., 1994; Woodfield et al., 2000). The result of cleaving this substrate would be 5'-SH instead of 5'-OH. The rate of the second

transesterification is extremely low as the 5'-SH is a poor nucleophile at phosphorous and the ligation of DNAs with this modification is significantly impaired (Eckstein, 1985; Pearson, 1997). Additionally, the thio-anion is a better leaving group than the oxy-anion; this accelerates the rate of DNA cleavage. These properties make this class of substrate an ideal substrate to classify TelA variants as cleavage competent or cleavage defective (Burgin, 2001; Milstien and Fife, 1967). It has been difficult to source such modifications during my studies.

Another potential approach to address the presence of pre-cleavage intermediate in the TelA pathway is the chemical probing with chemical compounds such as potassium permanganate ($KMnO_4$) (Benn et al., 1960; Chatamra and Jones, 1963; Smooker and Cotton, 1993). Chemical probing would be physical evidence of an underwound pre-cleavage intermediate. In principle, we might be able to detect the unpaired Ts in the pre-cleavage intermediate during telomere resolution. However, it might also be the case that TelA may protect the accessibility of such unpaired bases. Detection of unpaired T's between the scissile phosphates under conditions that inhibit DNA cleavage would be strong support for the model of an underwound pre-cleavage intermediate being present. A wide range of applications have been developed based on permanganate oxidizing DNA, including sequencing methods, footprinting assays, DNA interference assays, thymine-dimer assays, and the chemical cleavage of mismatches method, etc. Under alkaline conditions, $KMnO_4$ is highly active with thymine double bonds base of thymine without disturbing the sugar or phosphate in denatured DNAs (Sasse-Dwight and Gralla, 1989). $KMnO_4$ is relatively inactive with the fully complementary double-strand DNA. The underwound or melted DNA resulting from a biological process like DNA replication induces exposure of nucleotide bases to $KMnO_4$. The sugar phosphate backbone of modified Ts can be cleaved by various reagents such as piperidine (Bloch, 1999). A DNA fragment would be the result of piperidine cleavage which is detectable by denaturing gel electrophoresis or primer extension analysis (Sasse-Dwight and Gralla, 1989).

TelA (D398) was shown to have an active role in the formation of a stabilized underwound intermediate in telomere resolution. Surprisingly, TelA (D398A) also promoted site-specific recombination on a supercoiled plasmid containing an *rTel* sequence. More investigation is needed to understand why suppressing the unwinding DNA between the scissile phosphates would promote recombination. We speculate that TelA (D398A) might be biased

for cleaving one strand instead of two and exchanging the cleaved strand rather than resealing it. Reactions with TelA (D398A) resulted in an unusual amount of the CP*rTel* cleavage product in which TelA has cleaved only one strand of the *rTel*. This may indicate a bias for TelA (D398A) to cleave only one strand. This could help explain why it readily recombines *rTel*s into a HJ. The likely way that could happen is that for some reason TelA (D398A) can assemble tetramer easily that synapses two *rTels* together, similar to how tyrosine recombinases like Cre synapse their reaction sites (*loxP*) for recombination. Regarding the telomere resolution activity, TelA (D398A) is quite defective but in the context of plasmid substrate, it is cleavage competent promoting the cleavage of one strand and exchanging the cleaved strand to make a HJ (KK personal communication). Assays that check the tetramerization of proteins might shed more light on the tetramerization of this variant (Kobryn et al., 2009). We can attempt to capture the synapses between *rTel*s by crosslinking and running agarose gels; or checking for crosslinked tetramers using TelA (D398A) with protein gels in the contexts of telomere resolution *vs.* recombination.

We are close to defining a complete TelA telomere resolution pathway. However, there are ambiguities about whether some of interesting residues act before or after the DNA cleavage step. Once these future works are done, we will have a more complete picture of the TelA reaction pathway.

7. References

Aguero-Rosenfeld, M.E., Wang, G., Schwartz, I., and Wormser, G.P. (2005). Diagnosis of lyme borreliosis. Clin. Microbiol. Rev. *18*, 484–509.

Aihara, H., Huang, W.M., and Ellenberger, T. (2007). An Interlocked Dimer of the Protelomerase TelK Distorts DNA Structure for the Formation of Hairpin Telomeres. Mol. Cell *27*, 901–913.

Anguita, J., Samanta, S., Revilla, B., Suk, K., Das, S., Barthold, S.W., and Fikrig, E. (2000). Borrelia burgdorferi gene expression in vivo and spirochete pathogenicity. Infect. Immun. *68*, 1222–1230.

Ason, B., and Reznikoff, W.S. (2002). Mutational analysis of the base flipping event found in Tn5 transposition. J. Biol. Chem. *277*, 11284–11291.

Bandy, N.J., Salman-Dilgimen, A., and Chaconas, G. (2014). Construction and Characterization of a Borrelia burgdorferi Strain with Conditional Expression of the Essential Telomere Resolvase, ResT. J. Bacteriol. *196*, 2396–2404.

Bankhead, T., and Chaconas, G. (2004). Mixing active-site components: A recipe for the

unique enzymatic activity of a telomere resolvase. Proc. Natl. Acad. Sci. U. S. A. *101*, 13768–13773.

Bankhead, T., Kobryn, K., and Chaconas, G. (2006). Unexpected twist: Harnessing the energy in positive supercoils to control telomere resolution. Mol. Microbiol. *62*, 895–905.

Bao, K., and Cohen, S.N. (2003). Recruitment of terminal protein to the ends of Streptomyces linear plasmids and chromosomes by a novel telomere-binding protein essential for linear DNA replication. Genes Dev. *17*, 774–785.

Barbour, A.G., and Garon, C.F. (1987). Linear plasmids of the bacterium Borrelia burgdorferi have covalently closed ends. Science (80-.). *237*, 409–411.

Barre, F.X., Aroyo, M., Colloms, S.D., Helfrich, A., Cornet, F., and Sherratt, D.J. (2000). FtsK functions in the processing of a Holliday junction intermediate during bacterial chromosome segregation. Genes Dev. *14*, 2976–2988.

Benn, M.H., Chatamra, B., and Jones, A.S. (1960). The permanganate oxidation of thymine and some 1-substituted thymines. J. Chem. Soc. *46*, 1014–1020.

Bhasin, A., Goryshin, I.Y., and Reznikoff, W.S. (1999). Hairpin formation in Tn5 transposition. J. Biol. Chem. *274*, 37021–37029.

Bischerour, J., and Chalmers, R. (2007). Base-flipping dynamics in a DNA hairpin processing reaction. Nucleic Acids Res. *35*, 2584–2595.

Blanco, L., Bernad, A., Esteban, J.A., and Salas, M. (1992). DNA-independent deoxynucleotidylation of the φ29 terminal protein by the φ29 DNA polymerase. J. Biol. Chem. *267*, 1225–1230.

Bloch, W. (1999). Improved detection of mutations in nucleic acids by chemical cleavage.

Briffotaux, J., and Kobryn, K. (2010). Preventing broken Borrelia telomeres: ResT couples dual hairpin telomere formation with product release. J. Biol. Chem. *285*, 41010–41018.

Brown, T., Hunter, W.N., Kneale, G., and Kennard, O. (1986). Molecular structure of the G·A base pair in DNA and its implications for the mechanism of transversion mutations. Proc. Natl. Acad. Sci. U. S. A. *83*, 2402–2406.

Burgin, A.. (2001). Synthesis and Use of DNA Containing a 5′-Bridging Phosphorothioate as a Suicide Substrate for Type I DNA Topoisomerases. (Methods in Molecular Biology).

Burgin, A.B., Huizenga, B.N., and Nash, H.A. (1995). A novel suicide substrate for DNA topoisomerases and site-specific recombinases. Nucleic Acids Res. *23*, 2973–2979.

Byram, R., Stewart, P.E., and Rosa, P. (2004). The essential nature of the ubiquitous 26-kilobase circular replicon of Borrelia burgdorferi. J. Bacteriol. *186*, 3561–3569.

Casjens, S. (1999). Evolution of the linear DNA replicons of the Borrelia spirochetes. Curr. Opin. Microbiol. *2*, 529–534.

Casjens, S., Murphy, M., DeLange, M., Sampson, L., Van Vugt, R., and Huang, W.M. (1997). Telomeres of the linear chromosomes of Lyme disease spirochaetes: Nucleotide sequence and

possible exchange with linear plasmid telomeres. Mol. Microbiol. *26*, 581–596.

Casjens, S., Palmer, N., Van Vugt, R., Huang, W.M., Stevenson, B., Rosa, P., Lathigra, R., Sutton, G., Peterson, J., Dodson, R.J., et al. (2000). A bacterial genome in flux: The twelve linear and nine circular extrachromosomal DNAs in an infectious isolate of the Lyme disease spirochete Borrelia burgdorferi. Mol. Microbiol. *35*, 490–516.

Casjens, S.R., Gilcrease, E.B., Huang, W.M., Bunny, K.L., Pedulla, M.L., Ford, M.E., Houtz, J.M., Hatfull, G.F., and Hendrix, R.W. (2004). The pKO2 Linear Plasmid Prophage of Klebsiella oxytoca. J. Bacteriol. *186*, 1818–1832.

Casjens, S.R., Mongodin, E.F., Qiu, W.G., Luft, B.J., Schutzer, S.E., Gilcrease, E.B., Huang, W.M., Vujadinovic, M., Aron, J.K., Vargas, L.C., et al. (2012). Genome stability of lyme disease spirochetes: Comparative genomics of borrelia burgdorferi plasmids. PLoS One *7*.

Chaconas, G. (2005). Hairpin telomeres and genome plasticity in Borrelia: All mixed up in the end. Mol. Microbiol. *58*, 625–635.

Chaconas, G., Stewart, P.E., Tilly, K., Bono, J.L., and Rosa, P. (2001). Telomere resolution in the Lyme disease spirochete. EMBO J. *20*, 3229–3237.

Chang, P.C., and Cohen, S.N. (1994). Bidirectional replication from an internal origin in a linear streptomyces plasmid. Science (80-.). *265*, 952–954.

Chatamra, B., and Jones, A.S. (1963). The permanganate oxidation of uracil and cytosine and their 1-substituted derivatives. J. Chem. Soc. 811–815.

Chen, Y., and Rice, P.A. (2003). The role of the conserved Trp330 in Flp-mediated recombination: Functional and structural analysis. J. Biol. Chem. *278*, 24800–24807.

Cui, T., Moro-oka, N., Ohsumi, K., Kodama, K., Ohshima, T., Ogasawara, N., Mori, H., Wanner, B., Niki, H., and Horiuchi, T. (2007). Escherichia coli with a linear genome. EMBO Rep. *8*, 181–187.

Davies, D.R., Goryshin, I.Y., Reznikoff, W.S., and Rayment, I. (2000). Three-dimensional structure of the tn5 synaptic complex transposition intermediate. Science (80-.). *289*, 77–85.

Deneke, J., Ziegelin, G., Lurz, R., and Lanka, E. (2000). The protelomerase of temperate Escherichia coli phage N15 has cleaving-joining activity. Proc. Natl. Acad. Sci. U. S. A. *97*, 7721–7726.

Deneke, J., Burgin, A.B., Wilson, S.L., and Chaconas, G. (2004). Catalytic residues of the telomere resolvase ResT: A pattern similar to, but distinct from, tyrosine recombinases and type IB topoisomerases. J. Biol. Chem. *279*, 53699–53706.

Draper, G.C., McLennan, N., Begg, K., Masters, M., and Donachie, W.D. (1998). Only the N-terminal domain of FtsK functions in cell division. J. Bacteriol. *180*, 4621–4627.

Eckstein, F. (1985). Nucleoside Phosphorothioates. J. Am. Chem. Soc. *88*, 4292–4294.

Erdel, F., Kratz, K., Willcox, S., Griffith, J.D., Greene, E.C., and de Lange, T. (2017). Telomere Recognition and Assembly Mechanism of Mammalian Shelterin. Cell Rep. *18*, 41–53.

Fraser, C.M., Casjens, S., Huang, W.M., Sutton, G.G., Clayton, R., Lathigra, R., White, O., Ketchum, K.A., Dodson, R., Hickey, E.K., et al. (1997). Genomic sequence of a Lyme disease spirochaete, Borrelia burgdorferi. Nature *390*, 580–586.

Ghosh, K., Lau, C.K., Gupta, K., and Van Duyne, G.D. (2005). Preferential Synapsis of Loxp Sites Drives Ordered Strand Exchange in Cre-Loxp Site-Specific Recombination. Nat. Chem. Biol. *1*, 275–282.

Godiska, R., Mead, D., Dhodda, V., Wu, C., Hochstein, R., Karsi, A., Usdin, K., Entezam, A., and Ravin, N. (2009). Linear plasmid vector for cloning of repetitive or unstable sequences in Escherichia coli. Nucleic Acids Res. *38*, 1–9.

Goodner, B., Hinkle, G., Gattung, S., Miller, N., Qurollo, B., Goldman, B.S., Cao, Y., Askenazi, M., Mullin, L., Houmiel, K., et al. (2001). Linked references are available on JSTOR for this article : Genome Genome Sequence Sequence of of the the Plant Plant Pathogen Pathogen and and Biotechnology Biotechnology Agent Agent Agrobacterium Agrobacterium tumefaciens C58.

Goodner, B.W., Markelz, B.P., Flanagan, M.C., Crowell, C.B., Racette, J.L., Schilling, B.A., Halfon, L.M., Mellors, J.S., and Grabowski, G. (1999). Combined genetic and physical map of the complex genome of Agrobacterium tumefaciens. J. Bacteriol. *181*, 5160–5166.

Greenfield, N.J. (2007). Using circular dichroism spectra to estimate protein secondary structure. Nat. Protoc. *1*, 2876–2890.

Grindley, N.D.F., Whiteson, K.L., and Rice, P.A. (2006). Mechanisms of site-specific recombination. Annu. Rev. Biochem. *75*, 567–605.

Gu, H., Ho, P.L., Tong, E., Wang, L., and Xu, B. (2003). Presenting vancomycin on nanoparticles to enhance antimicrobial activities. Nano Lett. *3*, 1261–1263.

Hermoso, J.M., Méndez, E., Soriano, F., and Salas, M. (1985). Location of the serine residue involved in the linkage between the terminal protein and the DNA of phage φ29. Nucleic Acids Res. *13*, 7715–7728.

Hertwig, S., Klein, I., Lurz, R., Lanka, E., and Appel, B. (2003). PY54, a linear plasmid prophage of Yersinia enterocolitica with covalently closed ends. Mol. Microbiol. *48*, 989–1003.

Hoess, R.H., Wierzbicld, A., Abremski, K., and Station, E. (1986). The role of the loxP spacer region in PI site-specific recombination. Nucleic Acids Res *14*, 5417–5430.

Huang, S.H., and Kobryn, K. (2016). The Borrelia burgdorferi telomere resolvase, ResT, anneals ssDNA complexed with its cognate ssDNA-binding protein. Nucleic Acids Res. *44*, 5288–5298.

Huang, S.H., Cozart, M.R., Hart, M.A., and Kobryn, K. (2017). The Borrelia burgdorferitelomere resolvase, ResT, possesses ATP-dependent DNA unwinding activity. Nucleic Acids Res. *45*, 1319–1329.

Huang, W.M., Joss, L., Hsieh, T., and Casjens, S. (2004a). Protelomerase Uses a Topoisomerase IB/Y-Recombinase Type Mechanism to Generate DNA Hairpin Ends. J. Mol. Biol. *337*, 77–92.

Huang, W.M., Robertson, M., Aron, J., and Casjens, S. (2004b). Telomere Exchange between Linear Replicons of Borrelia burgdorferi. *186*, 4134–4141.

Huang, W.M., DaGloria, J., Fox, H., Ruan, Q., Tillou, J., Shi, K., Aihara, H., Aron, J., and Casjens, S. (2012). Linear chromosome-generating system of agrobacterium tumefaciens C58: Protelomerase generates and protects hairpin ends. J. Biol. Chem. *287*, 25551–25563.

Hunfeld, K.-P., and Brade, V. (2006). Antimicrobial susceptibility of Borrelia burgdorferi sensu lato: What we know, what we don't know, and what we need to know. Wien Klin Wochenschr 659–668.

J.D watson F.H C. Crick (1953). Molecular Structure of Nucleic Acids: A Structure for Deoxyribose Nucleic Acid. Nature *171*, 737–738.

Kantake, N., Madiraju, M.V.V.M., Sugiyama, T., and Kowalczykowski, S.C. (2002). Escherichia coli RecO protein anneals ssDNA complexed with its cognate ssDNA-binding protein: A common step in genetic recombination. Proc. Natl. Acad. Sci. U. S. A. *99*, 15327–15332.

Kennedy, A.K., Guhathakurta, A., Kleckner, N., and Haniford, D.B. (1998). Tn10 transposition via a DNA hairpin intermediate. Cell *95*, 125–134.

Kobryn, K. (2021). Replication of the Borrelia burgdorferi Genome. In Lyme Disease and Relapsing Fever Spirochetes: Genomics, Molecular Biology, Host Interactions and Disease Pathogenesis, (Caister Academic Press), pp. 73–86.

Kobryn, K., and Chaconas, G. (2002). ResT, a telomere resolvase encoded by the Lyme disease spirochete. Mol. Cell *9*, 195–201.

Kobryn, K., and Chaconas, G. (2005). Fusion of hairpin telomeres by the B. burgdorferi telomere resolvase ResT: Implications for shaping a genome in flux. Mol. Cell *17*, 783–791.

Kobryn, K., and Chaconas, G. (2014). Hairpin Telomere Resolvases. Microbiol. Spectr. *2*.

Kobryn, K., Naigamwalla, D.Z., and Chaconas, G. (2000). Site-specific DNA binding and bending by the Borrelia burgdorferi Hbb protein. Mol. Microbiol. *37*, 145–155.

Kobryn, K., Briffotaux, J., and Karpov, V. (2009). Holliday junction formation by the Borrelia burgdorferi telomere resolvase, ResT: Implications for the origin of genome linearity. Mol. Microbiol. *71*, 1117–1130.

Koudelka, G.B., Harbury, P., Harrison, S.C., and Ptashne, M. (1988). DNA twisting and the affinity of bacteriophage 434 operator for bacteriophage 434 repressor. Proc. Natl. Acad. Sci. U. S. A. *85*, 4633–4637.

Kuzminov, A. (1999). Recombinational Repair of DNA Damage in Escherichia coli and Bacteriophage λ . Microbiol. Mol. Biol. Rev. *63*, 751–813.

De Lange, T. (2005). Shelterin: The protein complex that shapes and safeguards human telomeres. Genes Dev. *19*, 2100–2110.

Lapadat-tapolsky, M., Pernelle, C., Borie, C., and Darlix, J. luc (1995). Analysis of the nucleic acid annealing activites of nucleocapsid protein from HIV-1. Nucleic Acids Res. *23*, 2434–

2441.

Leach, D., and Lindsey, J. (1986). In vivo loss of supercoiled DNA carrying a palindromic sequence. MGG Mol. Gen. Genet. *204*, 322–327.

Lee, S.Y., and Landy, A. (2004). The efficiency of mispaired ligations by λ integrase is extremely sensitive to context. J. Mol. Biol. *342*, 1647–1658.

Lee, J., Tonozuka, T., and Jayaram, M. (1997). Mechanism of active site exclusion in a site-specific recombinase: Role of the DNA substrate in conferring half-of-the-sites activity. Genes Dev. *11*, 3061–3071.

Lee, L., Chu, L.C.H., and Sadowski, P.D. (2003). Cre induces an asymmetric DNA bend in its target loxP site. J. Biol. Chem. *278*, 23118–23129.

Lefas, G., and Chaconas, G. (2009). High-throughput screening identifies three inhibitor classes of the telomere resolvase from the lyme disease spirochete. Antimicrob. Agents Chemother. *53*, 4441–4449.

Li, X.Y., and McClure, W.R. (1998). Stimulation of open complex formation by nicks and apurinic sites suggests a role for nucleation of DNA melting in Escherichia coli promoter function. J. Biol. Chem. *273*, 23558–23566.

Lin, Y. -S, M-Kieser, H., Hopwood, D.A., and Chen, C.W. (1993). The chromosomal DNA of Streptomyces lividans 66 is linear. Mol. Microbiol. *14*, 1103–1103.

Lingner, J., Cooper, J.P., and Cech, T.R. (1995). Telomerase and DNA end replication: No longer a lagging strand problem? Science (80-.). *269*, 1533–1534.

Lucyshyn, D., Huang, S.H., and Kobryn, K. (2015). Spring loading a pre-cleavage intermediate for hairpin telomere formation. Nucleic Acids Res. *43*, 6062–6074.

Mardanov, A. V., and Ravin, N. V. (2006). Functional characterization of the repA replication gene of linear plasmid prophage N15. Res. Microbiol. *157*, 176–183.

Mardanov, A. V., and Ravin, N. V. (2009). Conversion of Linear DNA with Hairpin Telomeres into a Circular Molecule in the Course of Phage N15 Lytic Replication. J. Mol. Biol. *391*, 261–268.

McGrath, S.L., Huang, S.H., and Kobryn, K. (2021). Single stranded DNA annealing is a conserved activity of telomere resolvases. PLoS One *16*, 1–23.

McGrath, S.L., Huang, S.H., and Kobryn, K. (2022). The N-terminal domain of the Agrobacterium tumefaciens telomere resolvase, TelA, regulates its DNA cleavage and rejoining activities. J. Biol. Chem. *298*, 101951.

Mendez, J., Blanco, L., Esteban, J.A., Bernad, A., and Salas, M. (1992). Initiation of φ29 DNA replication occurs at the second 3’ nucleotide of the linear template: A sliding-back mechanism for protein-primed DNA replication. Proc. Natl. Acad. Sci. U. S. A. *89*, 9579–9583.

Milstien, S., and Fife, T.H. (1967). The Hydrolysis of S-Aryl Phosphorothioates. J. Am. Chem. Soc. *89*.

Mir, T., Huang, S.H., and Kobryn, K. (2013). The telomere resolvase of the Lyme disease spirochete, Borrelia burgdorferi, promotes DNA single-strand annealing and strand exchange. Nucleic Acids Res. *41*, 10438–10448.

Moriarty, T.J., and Chaconas, G. (2009). Identification of the Determinant Conferring Permissive Substrate Usage in the Telomere Resolvase , ResT * □. J. Biol. Chem. *284*, 23293–23301.

Mouw, K.W., and Rice, P.A. (2007). Shaping the Borrelia burgdorferi genome: Crystal structure and binding properties of the DNA-bending protein Hbb. Mol. Microbiol. *63*, 1319–1330.

Nash, H.A., and Robertson, C.A. (1989). Heteroduplex substrates for bacteriophage lambda site-specific recombination: Cleavage and strand transfer products. EMBO J. *8*, 3523–3533.

Newell, C.A. (2000). Plant Transformation Technology Developments and Applications. Mol. Biotechnol *part B*.

Nitiss, J.L., Kiianitsa, K., Sun, Y., Nitiss, K.C., and Maizels, N. (2021). Topoisomerase Assays. Curr. Protoc. *1*, e250.

Nunes-Düby, S.E., Kwon, H.J., Tirumalai, R.S., Ellenberger, T., and Landy, A. (1998). Similarities and differences among 105 members of the Int family of site-specific recombinases. Nucleic Acids Res. *26*, 391–406.

Olovnikov, A.M. (1973). A theory of marginotomy. The incomplete copying of template margin in enzymic synthesis of polynucleotides and biological significance of the phenomenon. J. Theor. Biol. *41*, 181–190.

Pâques, F., and Haber, J.E. (1999). Multiple Pathways of Recombination Induced by Double-Strand Breaks in Saccharomyces cerevisiae . Microbiol. Mol. Biol. Rev. *63*, 349–404.

Pearson, R.G. (1997). Acids and Bases. Science (80-.). *151*, 1–22.

Picardeau, M., Lobry, J.R., and Hinnebusch, B.J. (1999). Physical mapping of an origin of bidirectional replication at the centre of the Borrelia burgdorferi linear chromosome. Mol. Microbiol. *32*, 437–445.

Pribil, P.A., and Haniford, D.B. (2000). Substrate recognition and induced DNA deformation by transposase at the target-capture stage of Tn10 transposition. J. Mol. Biol. *303*, 145–159.

Ravin, N. V. (2011). N15: The linear phage-plasmid. Plasmid *65*, 102–109.

Ravin, N. V. (2015). Replication and Maintenance of Linear Phage-Plasmid N15. Microbiol. Spectr. *3*, 1–12.

Ravin, N. V., Kuprianov, V. V., Gilcrease, E.B., and Casjens, S.R. (2003). Bidirectional replication from an internal ori site of the linear N15 plasmid prophage. Nucleic Acids Res. *31*, 6552–6560.

Ravin, V., Ravin, N., Casjens, S., Ford, M.E., Hatfull, G.F., and Hendrix, R.W. (2000). Genomic sequence and analysis of the atypical temperate bacteriophage N15. J. Mol. Biol. *299*, 53–73.

Rice, P.A., and Baker, T.A. (2001). Nsb0401_302. *8*, 6–11.

Rossetti, G., Dans, P.D., Gomez-Pinto, I., Ivani, I., Gonzalez, C., and Orozco, M. (2015). The structural impact of DNA mismatches. Nucleic Acids Res. *43*, 4309–4321.

Rybchin, V.N., and Svarchevsky, A.N. (1999). The plasmid prophage N15: A linear DNA with covalently closed ends. Mol. Microbiol. *33*, 895–903.

Sasse-Dwight, S., and Gralla, J.D. (1989). KMnO4 as a probe for lac promoter DNA melting and mechanism in vivo. J. Biol. Chem. *264*, 8074–8081.

Senecoff, J.F., and Cox, M.M. (1986). Directionality in FLP protein-promoted site-specific recombination is mediated by DNA-DNA pairing. J. Biol. Chem. *261*, 7380–7386.

Shi, K., Huang, W.M., and Aihara, H. (2013). An Enzyme-Catalyzed Multistep DNA Refolding Mechanism in Hairpin Telomere Formation. PLoS Biol. *11*.

Smith, E.F., and Townsend, C.O. (1907). A Plant-Tumor of Bacterial Origin. Science (80-.). 671–673.

Smooker, P.M., and Cotton, R.G.H. (1993). The use of chemical reagents in the detection of DNA mutations. Mutat. Res. *288*, 65.

Steere, A.C., Coburn, J., and Glickstein, L. (2004). The emergence of Lyme disease. J. Clin. Invest. *113*, 1093–1101.

Stivers, J.T., Shuman, S., and Mildvan, A.S. (1994). DNA Topoisomerase I: Kinetic Evidence for General Acid-Base Catalysis and a Conformational Step1". Biochemistry *33*, 15449–15458.

Stoppel, R.D., Meyer, M., and Schlegel, H.G. (1995). The nickel resistance determinant cloned from the enterobacterium Klebsiella oxytoca: conjugational transfer, expression, regulation and DNA homologies to various nickel-resistant bacteria. Biometals *8*, 70–79.

Tilly, K., Fuhrman, J., Campbell, J., and Samuels, D.S. (1996). Isolation of Borvelia burgdorferi genes encoding homologues of DNA-binding protein HU and ribosomal protein S20. Microbiology *142*, 2471–2479.

Tourand, Y., Kobryn, K., and Chaconas, G. (2003). Sequence-specific recognition but position-dependent cleavage of two distinct telomeres by the Borrelia burgdorferi telomere resolvase, ResT. Mol. Microbiol. *48*, 901–911.

Tourand, Y., Lee, L., and Chaconas, G. (2007). Telomere resolution by Borrelia burgdorferi ResT through the collaborative efforts of tethered DNA binding domains. Mol. Microbiol. *64*, 580–590.

Tourand, Y., Deneka, J., Moriarty, T.J., and Chaconas, G. (2009). Characterization and in vitro reaction properties of 19 unique hairpin telomeres from the linear plasmids of the lyme disease spirochete. J. Biol. Chem. *284*, 7264–7272.

Tsai, H.-H., Huang, C.-H., Lin, A.M., and Chen, C.W. (2008). Terminal proteins of Streptomyces chromosome can target DNA into eukaryotic nuclei. Nucleic Acids Res. *36*, 62.

Vesnaver, G., Chang, C.N., Eisenberg, M., Grollman, A.P., and Breslauer, K.J. (1989).

Influence of abasic and anucleosidic sites on the stability, conformation, and melting behavior of a DNA duplex: correlations of thermodynamic and structural data. Proc. Natl. Acad. Sci. U. S. A. *86*, 3614–3618.

Volff, J.N., and Altenbuchner, J. (2000). A new beginning with new ends: Linearisation of circular chromosomes during bacterial evolution. FEMS Microbiol. Lett. *186*, 143–150.

Volff, J.N., Viell, P., and Altenbuchner, J. (1997). Artificial circularization of the chromosome with concomitant deletion of its terminal inverted repeats enhances genetic instability and genome rearrangement in Streptomyces lividans. Mol. Gen. Genet. *253*, 753–760.

Wang, L., and Lutkenhaus, J. (1998). FtsK is an essential cell division protein that is localized to the septum and induced as part of the SOS response. Mol. Microbiol. *29*, 731–740.

Wang, S.J., Chang, H.M., Lin, Y.S., Huang, C.H., and Chen, C.W. (1999). Streptomyces genomes: Circular genetic maps from the linear chromosomes. Microbiology *145*, 2209–2220.

Whiteson, K.L., Chen, Y., Chopra, N., Raymond, A.C., and Rice, P.A. (2007). Identification of a Potential General Acid/Base in the Reversible Phosphoryl Transfer Reactions Catalyzed by Tyrosine Recombinases: Flp H305. Chem. Biol. *14*, 121–129.

Woodfield, G., Cheng, C., Shuman, S., and Burgin, A.B. (2000). Vaccinia topoisomeras and Cre recombinase catalyze direct ligation of activated DNA substrates containing a 3'-para-nitrophenyl phosphate ester. Nucleic Acids Res. *28*, 3323–3331.

Wormser, G.P., Nadelman, R.B., Dattwyler, R.J., Dennis, D.T., Shapiro, E.D., Steere, A.C., Rush, T.J., Rahn, D.W., Coyle, P.K., Persing, D.H., et al. (2000). Practice guidelines for the treatment of Lyme disease. Clin. Infect. Dis. *31*, S1–S14.

Wynford-Thomas, D., and Kipling, D. (1997). Cancer and the knockout mouse. Nature *389*, 551–552.

Yang, C.C., Tseng, S.M., and Chen, C.W. (2015). Telomere-associated proteins add deoxynucleotides to terminal proteins during replication of the telomeres of linear chromosomes and plasmids in Streptomyces. Nucleic Acids Res. *43*, 6373–6383.

Yang, C.C., Tseng, S.M., Pan, H.Y., Huang, C.H., and Chen, C.W. (2017). Telomere associated primase Tap repairs truncated telomeres of Streptomyces. Nucleic Acids Res. *45*, 5838–5849.

Zhang, J.R., Hardham, J.M., Barbour, A.G., and Norris, S.J. (1997). Antigenic variation in Lyme disease borreliae by promiscuous recombination of VMP-like sequence cassettes. Cell *89*, 275–285.

Ziegelin, G., Scherzinger, E., Lurz, R., and Lanka, E. (1993). Phage P4 α protein is multifunctional with origin recognition, helicase and primase activities. EMBO J. *12*, 3703–3708.

8. Appendix

Permissions from publishers are available in the following link:

https://drive.google.com/drive/folders/1zA3D8tj4J1le5B4EvMAaC7IdY2X5Pio_?usp=share_link